Exploring pearl millet root system and its outcome for drought tolerance

Sixtine Passot

Collège Doctoral du Languedoc-Roussillon

THÈSE

Pour obtenir le grade de

Docteur

Délivré par **l'Université de Montpellier**

Préparée au sein de l'école doctorale GAIA
Et de l'unité de recherche DIADE

Spécialité : **Biologie, Interactions, Diversité Adaptative des Plantes**
CNU : Physiologie

Présentée par **Sixtine PASSOT**

Exploration du système racinaire du mil et ses conséquences pour la tolérance à la sécheresse

-

Exploring pearl millet root system and its outcome for drought tolerance

Soutenue le 30 septembre 2016 devant le jury composé de

M. Tom BEECKMAN, Professeur, Ghent University	Rapporteur
M. Teva VERNOUX, Directeur de recherche, CNRS	Rapporteur
M. Claude DOUSSAN, Chargé de recherche, INRA	Examinateur
M. Xavier DRAYE, Professeur, UCL	Examinateur
M. Philippe NACRY, Chargé de recherche, INRA	Président du jury
M. Laurent LAPLAZE, Directeur de recherche, IRD	Directeur de thèse
M. Yann GUEDON, Chercheur, CIRAD	Co-encadrant

This PhD was prepared in the DIADE research unit

DIversité - **A**daptation - **DE**veloppement des plantes

Centre IRD de Montpellier
911 Avenue Agropolis
34394 Montpellier Cedex 5
France

Résumé

Le mil est une céréale d'importance majeure pour la sécurité alimentaire dans les régions arides d'Afrique et d'Inde. Pourtant, elle a fait l'objet de relativement peu d'efforts d'amélioration variétale par rapport à d'autres céréales. En particulier, l'amélioration de son système racinaire pourrait permettre une amélioration de la tolérance de cette plantes aux contraintes physiques qu'elle subit (sécheresse et faible disponibilité en nutriments) et ainsi un accroissement substantiel de la production. L'objectif de ce travail est de caractériser ce système racinaire, en vue de produire des connaissances nécessaires à l'amélioration variétale, axée principalement sur la tolérance à la sécheresse en début de cycle.

Dans un premier temps, nous avons décrit précisément la morphologie du système racinaire dans les premiers stades de développement, la dynamique de mise en place des axes racinaires ainsi que l'anatomie des différents types de racines. Ce travail a mis en évidence l'existence de trois types anatomiques distincts pour les racines latérales. Nous avons également mis en évidence l'existence de variabilité dans la dynamique de mise en place précoce du système racinaire au sein d'un panel de diversité issu de variétés cultivées. Notre étude a aussi révélé une grande variabilité des profils de croissance des racines latérales.

Pour analyser plus avant cette diversité, la croissance d'un grand nombre de racines latérales a été mesurée quotidiennement et un modèle statistique a été conçu pour classer ces racines en trois grandes tendances selon leurs profils de croissance. Ces trois catégories distinguent les racines en fonction de leur taux de croissance et de leur durée de croissance. Ces différents types racinaires sont répartis aléatoirement le long de la racine primaire et il ne semble pas y avoir d'influence des types sur les intervalles entre racines latérales successives. Les trois types cinétiques correspondent, imparfaitement cependant, aux trois types anatomiques mis en évidence dans le premier chapitre. Un travail similaire a été effectué sur le maïs, ce qui a permis de comparer ces deux céréales phylogénétiquement proches.

Enfin, nous avons débuté la recherche de marqueurs génétiques associés à la croissance de la racine primaire, un trait supposément impliqué dans la tolérance à la sécheresse précoce. Ce travail a nécessité le phénotypage de ce trait sur un panel de lignées de mil fixées, qui a confirmé la présence d'une grande variabilité existante pour ce trait. Ces lignées ont ensuite été génotypées par séquençage. Les analyses d'association génotype/phénotype sont en cours.

Ce travail de thèse a permis de caractériser plus précisément le système racinaire du mil, relativement mal connu jusqu'à ce jour. Il a fourni des données utiles pour la paramétrisation et le test de modèles fonctionnels de croissance et de transport d'eau. La caractérisation cinétique précise des types de racines latérales est une approche originale et pourra être utilisée chez d'autres céréales. Enfin, les données acquises par génétique d'association devraient pouvoir servir à une meilleure compréhension de la mise en place de ce système racinaire et ouvrent la voie à l'amélioration assistée par marqueurs génétiques pour des traits racinaires chez le mil.

Mots clés : système racinaire, anatomie, modélisation

Summary

Pearl millet plays an important role for food security in arid regions of Africa and India. Nevertheless, it lags far behind other cereals in terms of genetic improvement. Improving its root system could improve pearl millet tolerance to abiotic constraints (drought and low nutrient availability) and lead to a significant increase in production. The objective of this work is to characterize pearl system root system development in order to produce knowledge for breeding, mainly targeted on tolerance to drought stress occurring at the early growth stages.

First, we described the dynamics of early pearl millet root system development and the anatomy of the different root types. This work revealed the existence of three anatomically distinct types for lateral roots. We also showed the existence of variability in primary root growth and lateral root density in a diversity panel derived from cultivated varieties. Our study also revealed a large variability among the growth profiles of lateral roots.

To further analyze this diversity, the growth rates of a large number of lateral roots were measured daily and a statistical model was developed to classify these lateral roots into three main trends, according to their growth profiles. These three categories distinguish roots according to their growth rate and their growth duration. These different lateral root types are randomly distributed along the primary root and there seem to be no influence of root types on the intervals between successive lateral roots. The three growth types correspond, though imperfectly, to the three anatomical types evidenced in the first chapter. A similar work has been performed on maize, which was used to compare these two phylogenetically close cereals.

Finally, we initiated the search for genetic markers associated to primary root growth, a trait potentially involved in early drought stress tolerance. A large panel of genetically fixed pearl millet inbred lines was phenotyped, confirming the presence of a large variability existing for this trait. These lines were then genotyped by sequencing. Analyses of association between phenotype and genotype are underway.

This work provides a precise description of pearl millet root system that was little studied to date. Our data were used for parameterization and testing of functional structural plant models simulating root growth and water transport. The statistical tool developed for the characterization of the different lateral root growth types is an original approach that can be used on other cereals. Finally, results from our association study will reveal new information on the genetic control of root growth and open the way to marker assisted selection for root traits in pearl millet.

Keywords: root system, anatomy, modeling

Acknowledgments

Je tiens à remercier toutes les personnes qui ont contribué, chacune à leur façon, à ce travail de thèse.

Un immense merci tout d'abord à Laurent Laplaze, mon directeur de thèse. Je crois à la magie des rencontres et celle-là fut, de mon point de vue, particulièrement réussie. J'ai beaucoup apprécié ton dynamisme scientifique, une qualité précieuse et que tu incarnes d'une façon que j'ai rarement rencontrée. Tu associes cela à l'optimisme et à beaucoup de bienveillance. Merci pour tes conseils et ton aide en toutes circonstances.

Merci à Yann Guédon, mon co-encadrant, pour l'aide et le soutien que tu m'as apportés à toutes les étapes de ma thèse, en particulier pour le modèle statistique. Tu m'as donné l'occasion d'expérimenter la recherche en collaboration, ce qui est particulièrement formateur dans l'apprentissage scientifique. La vision tu as de la recherche m'a également beaucoup appris. C'est par ton intermédiaire que j'ai pu trouver mon sujet de thèse et je me souviens très clairement de notre premier contact au téléphone, alors que j'étais encore en M2, assise dans une rotonde de la fac de Jussieu.

Merci aux membres de mon jury qui ont accepté d'évaluer mon travail de thèse en assistant à ma soutenance. Merci à mes deux rapporteurs, Tom Beeckman et Teva Vernoux, qui ont en plus accepté d'évaluer mon manuscrit de thèse, et merci à Claude Doussan, Xavier Draye et Philippe Nacry qui ont accepté de venir juger ma soutenance de thèse avec eux.

Merci aux membres de l'équipe CERES qui m'ont accompagnée et soutenue pendant ces 3 années, scientifiquement et personnellement. Merci à Soazig pour ton aide sur les rhizotrons et l'histologie, ainsi que le soutien et l'inspiration que tu m'as apportés en termes d'équilibre personnel. Merci à Mikaël pour ton aide dans les manips, la rédaction et l'illustration. Même si je n'ai pas gagné le concours, j'ai grâce à toi un super beau poster! Merci à Daniel pour ton soutien technique et ta vision sur l'IRD et la recherche. Merci à Isabelle pour ton aide en serre. Merci à Pascal pour ton aide scientifique, en particulier sur la génétique du riz, et administrative avec l'unité et l'école doctorale. Merci Antony pour ta présence à l'IRD et merci d'être venu me chercher à l'aéroport pour mon premier séjour à Dakar!

Merci à tous les étudiants, doctorants, stagiaires, post-docs, bref, les « jeunes chercheurs » passés et présent de l'équipe CERES pour leur présence, leur aide technique et le plaisir de partager les déjeuners : Mélanie, qui a été ma première stagiaire, Fatoumata, avec qui j'ai partagé de longs moments en manip à Nottingham et qui a beaucoup contribué aux études d'anatomie, Adama, grâce à qui mes résultats sont réutilisés dans un modèle, Marilyne, qui m'a sauvée de la biologie moléculaire, Marie-Thérèse et Awa, qui reprennent le flambeau de la recherche sur le mil dans l'équipe au Sénégal, Khanh, Jérémy, Mathieu, Khadidiatou, Khadija, Dylan et Sarah (elle est loin mais je ne l'oublie pas!). Une petite pensée également pour Hermann et Julien, anciens doctorants de l'équipe Rhizo et qui ont partagé mon bureau dans les premiers mois de ma thèse.

Merci aux membres de l'équipe Virtual Plants qui m'a accueillie en co-encadrement. Merci à Christophe Godin pour son accueil au sein de son équipe, merci à Frédéric Boudon pour sa contribution au calcul des volumes explorés, merci à Jonathan pour son aide sur le clustering et merci aussi à tous les membres de l'équipe avec qui j'ai passé de bons moments à la Galéra, au bâtiment 5 ou au Hameau de l'Etoile.

Merci aux membres de l'équipe DYNADIV pour leur aide sur le mil, la biologie moléculaire et la génétique. Merci à Yves Vigouroux pour sa participation à l'encadrement de ma thèse et grâce à qui j'ai pu avoir accès à mes premières graines de mil. Merci à Leïla Zekraoui, Marie Couderc et Cédric Mariac pour leur aide et leurs conseils pour les manips de biologie moléculaire.

Merci à Harold qui a bichonné mes plantes en serre pour la production de graines.

Merci à tous les doctorants IRD qui ont cheminé sur la voie de la thèse en même temps que moi : Emilie, Hélène, Cécile, Mathilde, Lucile, Rémi, Fabien, Céline, Mathilde, Chloé... J'ai apprécié l'ambiance sympathique qui régnait au sein de cette petite communauté, que ce soit aux réunions de doctorants, au café ou au goûter, mais aussi à la plage, au ski, au karting, au lasergame, à l'escape room, au paintball…

Je remercie les membres du LEPSE de l'INRA qui m'ont aidée lors de ma thèse. Merci Bertrand Muller pour tous tes conseils et ton aide pour les rhizotrons, en comité de thèse ou encore en congrès. Merci Beatriz pour tous les moments que nous avons passés ensemble à discuter, maniper, rédiger. Et merci à Crispulo pour son aide sur les rhizotrons et ses histoires de mécanique et de science.

I also thank all the people from Nottingham University who welcomed me in their lab, helped me with the phenotyping experiments and advised me for my PhD. Thank you Jonathan Atkinson for allowing me to use your phenotyping system on my tropical cereal, for all the hours spent in the growth room transferring seeds or taking pictures in friendly company and for your help with Sutton Bonington's life. Thank you Darren Wells for your availability, all your tips and your kindness. Thank you Malcolm Bennett for your warm welcome, your advises and your enthusiasm. Thank you Anthony Bishopp for your help with tissue fixation and for our shared climbing sessions, in the UK and in France. Thank you Craig Sturrock for allowing me using the X-ray CT and thank Brian Atkinson for helping me in that task. Thank you Jennifer Dewick for all your practical help with housing, transport and so on, that rendered my stays in Sutton Bonington so smooth. I also thank Marcus, Ute, and many other members of the CPIB with whom I shared nice moments, the yoga and pilates teachers and all my climbing partners, for the moments they allowed me to spend, rendering these stays in a lost countryside less lonely.

Merci à Jean-Luc Verdeil pour son aide très précieuse sur l'anatomie et sa contribution à la rédaction de mon premier article.

Merci à Tom Hash pour son aide dans l'approvisionnement des graines et ses connaissances sur le mil qu'il a partagées avec moi.

Merci aux membres, passés ou présents, de l'Université Catholique de Louvain-la-Neuve qui m'ont accueillie dans leur laboratoire et m'ont permis de découvrir le fameux

système d'aéroponie. Je remercie tout particulièrement Xavier Draye qui m'a aidée à de nombreuses étapes de ma thèse. Merci à Benjamin Lobet qui m'a aidée pour la manip et m'a fait découvrir Louvain-la-Neuve et merci à Mathieu qui m'a accueillie chez lui. Même s'il n'est plus à Louvain, je remercie également Guillaume Lobet, un des pères de SmartRoot, pour avoir créé ce logiciel et surtout pour m'avoir énormément aidée dans sa prise en main et avoir toujours été très disponible pour la résolution des problèmes, quelle qu'ait été leur nature.

Merci également à ceux qui m'ont permis de transmettre ma passion de la biologie par l'enseignement : Bruno Touraine, Jean-Luc Regnard et tous les enseignants avec qui j'ai interagi au département Bio-MV dans le cadre du monitorat. Merci également à Muriel Tapiau qui m'a donné l'occasion d'animer un atelier à la fête de la science et merci à Genopolys pour son accueil. Je remercie au passage tous les étudiants à qui j'ai donné des cours, des TP ou des TD pour leur investissement, leur motivation (parfois) et leur tolérance (toujours!), au cas où certains liraient cette thèse! J'espère que mes enseignements leur auront été profitables, j'ai en tous cas beaucoup appris de ces dizaines d'heures passées en salle de classe.

Merci à tous ceux qui ont géré les aspects matériels, financiers ou administratifs de ma thèse : Clothilde, Virginie, Bruno, Carole, Laurence et Valérie.

Merci au personnel de la cantine de l'IRD pour tous ces desserts (souvent chocolatés) qui m'ont nourrie pendant ma thèse !

Parce que ces 3 ans n'ont pas été passés qu'au laboratoire, je souhaiterai aussi remercier tous ceux qui ont partagé ma vie lors de cette thèse. Il s'agit en premier lieu de mes colocataires : Anne-Sophie, Nina, David, Thomas, Samuel, Gaëlle, Gaetan et Sammy.

Merci à mes amis parisiens : Stéphane, Florian, Frédéric et tous les membres du B6.

Merci à mes partenaires d'escalade : Elodie, Nicolas, Pacôme, Fred, Nans, Kassem, Petra, Pierre, Elsa, Guillaume...

Merci à ceux qui se sont occupé de mon cheval: Laura, Julie, Christophe, Gabrielle, Franck, Marie ainsi qu'à ceux qui ont pris le relai lors de mes absences.

Merci au groupe rando, récemment baptisé « les mathématiciens » : Sylvain, Juline, Marion, Gautier, Thomas, Rémi.

Merci également à certains qui m'ont aidée à leur façon: Manon, Guillaume, Mélanie, Nicolas et les autres.

Je remercie également ma famille, mes parents et mes sœurs, qui m'ont vue partir loin de Paris et ont suivi de plus ou moins loin mes péripéties montpelliéraines.

Je remercie enfin les organismes qui ont financé pendant ces 3 ans de thèse ma bourse de thèse, mon environnement de travail, mes manips et mes déplacements à l'étranger : le MESR et l'ENS, l'IRD, le CIRAD, l'INRIA, l'UMR DIADE, les fondations Agropolis et Cariplo, l'EPPN, l'école doctorale GAIA et la SEB.

Frequently used acronyms

bp: base pair

CT: computed tomography

DAG: days after germination

DNA: deoxyribonucleic acid

FAO: Food and Agriculture Organization

Gb: Gigabase

GBS: genotyping by sequencing

ICRISAT: International Crops Research Institute for the Semi-Arid Tropics

MRI: magnetic resonance imaging

QTL : quantitative trait locus

RNA: ribonucleic acid

sd: standard deviation

SMSLM: semi-markov switching linear model

SNP: single nucleotide polymorphism

SOM: soil organic matter

SWC: soil water content

XTE: xylem tracheary element

Table of content

General introduction

Food security is a major challenge for agronomic research in the 21st century. According to the Food and Agriculture Organization of the United Nations (FAO, FIDA and PAM, 2015) hunger concerned 795 million people in 2015, including 780 million in developing countries. Although hunger regressed in some regions of the world, Sub-Saharan Africa remains the region with the highest prevalence of undernourishment, with nearly 25% people affected by chronic hunger. There is a need to increase food production for small farmers in sub-Saharan Africa in a context of global changes that poses new threats to agriculture.

Pearl millet is the 6th cereal grown in the world with over 33 million hectares harvested in 2013, and it is a crop of major importance in arid and semi-arid regions such as the Sahel. Pearl millet is the cereal with the largest cultivated area in West Africa, with over 13 million hectares in 2013. However, it is only the 4th in terms of total production. Pearl millet is especially tolerant to harsh conditions (high temperature, low rainfall, low fertility soils) and is therefore preferably grown in areas where other cereals would fail. On the contrary, as soon as the growth conditions improve (potential irrigation for example), pearl millet is abandoned to the benefit of more demanding crops (sorghum, maize; National Research Council, 1997). Pearl millet is therefore preferably cultivated in arid and low fertility regions, where it is often the only viable cereal. Increasing yield in these areas would produce a substantial improvement of food security, but agronomic practices are often constrained and the deployment of irrigation or the enhanced use of fertilizers is difficult in some areas. Research efforts could therefore concentrate on selection and breeding in order to release varieties that produce more in usual pearl millet culture conditions. Pearl millet has a good nutritional profile among cereals, and this advantage should be kept and, if possible, improved in newly released varieties.

Breeding efforts in pearl millet only targeted physiological or architectural characters observed on the aerial part such as grain yield, shoot height or resistance to bioagressors (Bilquez, 1974; Vadez et al., 2012). A novel idea would be to target root traits for breeding (Vadez et al., 2012). The root system is the interface between the plant and the soil, which constitutes the water and nutrient pool for the plant. In some cultivated plants, selection has led to a reduction of the size of the root system (Schmidt et al., 2016; Waines and Ehdaie, 2007). Indeed, since cereal domestication, farmers have focused on the maximization of the production of edible grains and, during the Green Revolution, this objective was pursued by developing varieties with a high harvest index and plant architecture adapted to a massive input of fertilizers. However, this strategy requires the use of fertilizers unaffordable for poor farmers and typically African crops such as millet were left aside this breeding effort (Bishopp and Lynch, 2015). Target root system breeding may lead to varieties with higher water and nutrient capture efficiency. This opportunity is even more interesting with poor soils and under a dry climate, giving that yield improvement cannot be mediated by irrigation or by a substantial increase in fertilization.

Introduction

1. Pearl millet

1.1 Botanical description

Pearl millet [*Pennisetum glaucum* (L.) R. Br.] is an annual cereal. It belongs to the PACMAD clade (for Panicoideae, Arundinoideae, Chloridoideae, Micrairoideae, Aristidoideae and Danthonioideae) and is a Panicoideae. It has a C_4 metabolism like sorghum, maize or sugarcane (Edwards, 2012). The wide variability existing amongst the pearl millet species led to the early classification of different forms in different species. It is now well known that all these forms belong to a single species, in the sense of interfecundity, but history left a few names by which the pearl species was designated in old publications. The most common are *Pennisetum typhoides*, *Pennisteum americanum* and *Pennisetum glaucum*, the later being the actual binomial name of the species.

The plant height varies from 0.5 to 3 meters at maturity and can even reach 4 meters in wetlands (Guigaz, 2002). Wild relative have many tillers and tillering is still frequent in domesticated millet. The leaves are lance-like and are 20 to 100 cm long and 5 to 50 mm wide. Millet seeds are held on a spike, often called panicle, measuring 10 to over 100 cm long. Seed size is generally around 2 to 5 mm, with a large existing variability (Brunken et al., 1977). Seed shape varies from globular to lanceolate and its weight goes from 5 to 20 mg (Andrew and Kumar, 1992). **Figure In-1** presents pictures of pearl millet plants in a field and pearl millet seeds after harvest. The plant is mainly cross-pollinated, with an allofecundation level around 80 to 90%. Cycle length ranges from 60 days for varieties in the desert margin areas in northwestern India to up to 180 days in the northern Guinea zone of West Africa (Bidinger and Hash, 2004).

Figure In-1: Picture of a millet field in Niger (left) and focus on mature seeds after harvest (right).
Pictures: C. Tom Hash

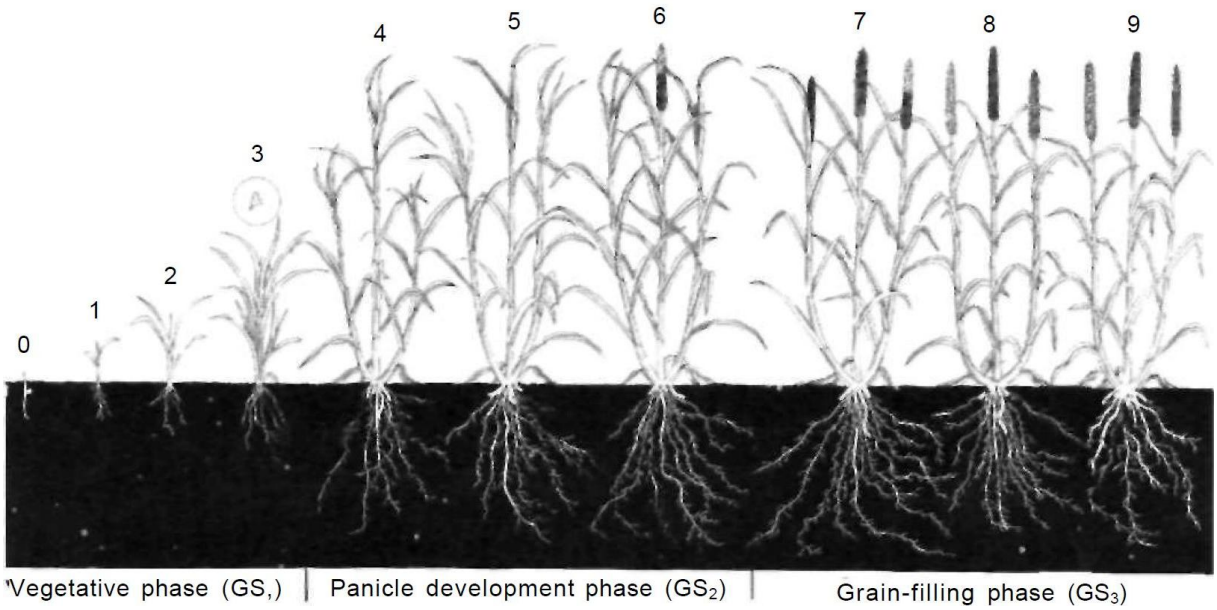

Figure In-2: Schematic diagram of the major developmental phases of pearl millet: GS1, GS2, GS3. The numbers 0 to 9 illustrate the detailed stages of development described in the text. The encircled enlargement of stage 3 shows the dome-like shape of the apex and the constriction at its base that may be observed at this stage of change from the vegetative to the reproductive phase.
(Maiti and Bidinger, 1981)

Pearl millet development can be divided in 3 developmental phases (Maiti and Bidinger, 1981). The **vegetative phase** (GS_1) goes from emergence to panicle initiation, the **panicle development phase** (GS_2) goes from panicle initiation to flowering and the **grain-filling phase** (GS_3) goes from flowering to the end of the grain-filling period. If several shoots are present, the GS_1 and GS_2 phases are defined upon the developmental stage of the main stem. The relative lengths of these phases depend on the variety, but represent generally about one third of the whole cycle each. These phases are further divided into 10 developmental stages, represented in **Figure In-2**:

S0: Emergence of the coleoptiles from the soil surface. This event happens 2 to 3 days after germination, which itself starts with seed imbibition and ends with radicle emergence less than 24 hours later.

S1: Three-leaf stage. The third leaf starts to appear approximately 5 days after coleoptiles emergence. The first leaf is fully expanded, but not the second one. The primary root grows quickly and develops ramifications and crown roots start to appear.

S2: Five-leaf stage. The fifth leaf appears about 15 days after emergence. Tiller leaf start to emerge from inside the sheaths of the basal leaves. The root system development carries on with primary root ramification and crown root growth.

S3: Panicle initiation. This stage determines the end of the vegetative phase and the beginning of the reproductive phase. All leaf primordia have been initiated, though only six to seven are fully expanded, and the apical meristem switches to the generation of spikelet primordia. This change is noticeable by the dome-like shape taken by the apex, with a constriction at its base. The growing point, which was under or at soil surface level up to this point, is now above this level as the first two or three internodes begin to elongate. The emerged tillers undergo the same development as the main shoot with some delay. The primary root system is well developed and crown roots grow rapidly.

S4: Flag leaf stage. The last leaf becomes visible, rolled in the lamina of the preceding leaf. The internodes follow on their elongation sequentially, from the base to the top, raising the young panicle.

S5: Boot stage. The panicle is enclosed in the sheath of the flag leaf, now fully expanded. Its development is nearly full and it rapidly increases in length and width.

S6: 50% flowering (half bloom). Pearl millet is protogynous, which means that stigmas appear before anthers. This stage is attained when half of the panicle has emerged stigmas. The stigmas can stay fresh if they are unpollinated, and shrivel few hours after pollination. The anthers appear at or just before anther emergence completion.

S7: Milk stage. The grains become visible 6-7 days after fertilization. They are filled with a watery and later milky liquid. This stage marks the beginning of starch deposition in the endosperm. The seed dry weight increases quickly.

S8: Dough stage. This stage corresponds to the starch filling of the seed. It is a gradual stage and not a distinct stage, corresponding to the change of content in the seed, from liquid to solid. The grain consistency changes from soft to hard.

S9: Physiological maturity. This stage corresponds to the cessation of movement of materials into the grain, and thus the cessation of grain growth. It is characterized by the

formation of a small black layer in the hilar region of the seed. The grain has attained its maximum dry weight but has only partly dried. The remaining drying occurs after maturity.

1.2 Domestication

In West Africa, three forms of pearl millet species are found: the wild progenitor, the cultivated form and an intermediate form called shibra (Brunken et al., 1977). All these forms can hybridize and produce fertile offspring. The wild progenitor does not need any human intervention to survive and reproduce. Its size is generally around 1 meter. It has very small spike (less than 15 cm) and seeds (less than 1 mm). It grows only in the Sahel zone of West Africa, from Senegal to Sudan. It is a natural colonizer and is found in disturbed places like seasonally dry stream beds, roadsides, abandoned fields and human habitations.

Shibra is an intermediate form between the wild progenitor and the cultivated species. It can have intermediate morphological characters but it is often difficult to distinguish from the cultivated form before maturation, as it mimics the specific characters of the cultivated plant it grows next to. It mixes up with cultivated plant but spreads its seeds at maturity. Shibras grow in most of the culture area of pearl millet in Africa, but they are less frequent in mesic zones, which are not the originating area of pearl millet but where cultivated pearl millet has been adapted. Shibras have not been found in India. To sum up, shibra is generally found in places where the wild progenitor grows. The origin of shibra is unclear. A first study (Brunken et al., 1977) set that these forms have likely been selected by human intervention: as men removed all weeds present in cultivated fields, especially the wild form, intermediate forms, very alike to cultivated plants but still able to spread seeds without man intervention, were selected. A genetic analysis (Oumar et al., 2008) suggested on the contrary that shibra can be the result of hybridization between wild and cultivated plants. In fact, some accessions considered as wild or cultivated revealed to have hybrid genome between wild and cultivated genomes. This information could be interesting for selection because it implies that parts of the wild genome could be easily introgressed into cultivated accessions.

The main morphological differences between wild and cultivated pearl millet, called the domestication syndrome, are quite typical of cereals. Cultivated forms have a lower number of tillers, an increased spike length, both resulting from an increase of apical dominance, the lost of spikelet shedding, the reduction of bracts size, parallel to the increase of seed size, leading to uncoated seed and the lost of seed dormancy (Poncet et al., 1998). Significant signatures of selection associated with domestication were also found in genes controlling flowering time and especially in genes associated with the circadian clock (Clotault et al., 2012).

The origin of domesticated pearl millet has long been localized in Africa, but its exact origin remained unclear until recently. Three potential domestication places were initially suggested (Brunken et al., 1977), the Sahel zone of West Africa being fostered. Between 5000 and 3000 BC, Sahara was wetter than it is now. This allowed the spread of cereal cultivation in this region, coming from the Near East by the way of Egypt. Mediterranean cereals like wheat or barley were widely cultivated by the beginning of the climate aridification, around 3000 BC. But this climate change compromised the success of the Mediterranean crops,

which probably led people to try agricultural practices with their local grasses. The domestication origin of pearl millet was therefore suggested to be along the Southern margins of the central highlands of Sahara, between 3000 and 2000 BC. A more recent study, based on genetic analysis of a large number of wild and cultivated accessions (Oumar et al., 2008) clarifies this domestication place to a zone comprised between Niger and Mali. The domestication period, however, is suggested to be around 8000 BC. Another recent study dealing with pearl millet domestication focuses on a specific region in North-Eastern Mali (Manning et al., 2011). In spite of reevaluating the domestication period to around 4500 BC, it details two phases in the domestication process. The first step was the non-shattering character of the spikelet, which facilitate harvest. After this event, small-seeded domesticated pearl millet spread quickly in Africa and up to India, and later phases of grain-size increase occurred in several places, including India. Latest analysis of genetic diversity in wild and cultivated pearl millet accessions refines the domestication event to around 4800 BC (Clotault et al., 2012). It also estimates to 1.4% the amount of gene fluxes from the wild to the cultivated form. In conclusion, due do this gene fluxes and the existence of the shibra form, the domestication history of pearl millet is still hard to date and describe precisely.

1.3 Genomics

Pearl millet is a diploid annual (2n = 2x = 14). Its genome size is estimated to 1.76 Gb (unpublished data). Pearl millet genome has a large number of gross structural chromosomal rearrangements relative to rice, the model cereal, and this number is greater in pearl millet than in any other grass genome analyzed to date, even foxtail millet (*Setaria italica*), which is phylogenetically very close to pearl millet (Devos et al., 2000). Comparative genetic helps to predict the location of genes underlying traits of interest already mapped in other plants and specificities may appear for pearl millet in terms of gene position due to this high level of rearrangement. The percentage of repetitive DNA in pearl millet genome is estimated to 80%, which is a bit less than maize (> 85%) but much higher than sorghum (~ 61%), foxtail millet (~ 40%) and rice (~ 42%) genomes (Bennetzen et al., 2012; Paterson et al., 2009). The most abundant repetitive DNA class is long-terminal repeat retrotransposons, comprising over 50% of the nuclear genome. Gene number is estimated to 38,579 with an average transcript size of 3,945 bp and an average coding sequence size of 687 bp. Identification of regions with depleted diversity in the cultivated but not wild genome indicated potential locations for genes selected during domestication. Among the genes that experienced the most striking diversity loss, putative functions are associated with regulation of response to hormones like auxin and ethylene, regulation of the circadian clock and morphogenesis, along with transcription factors (unpublished data).

1.4 Economics

Agricultural data at world level may be hard to find because pearl millet data are often pooled with all kind of cereals called millet, as finger millet, proso millet or foxtail millet. According to statistics from the International Crop Research Institute for the Semi Arid

Tropics (ICRISAT), pearl millet fields cover an area of 31 million hectares worldwide (ICRISAT, 2013). The first world producer is India, with over 8.3 or 11 million tons in 2014 according to ICRISAT or FAO data respectively. This crop occupies 9.3 million hectares in India (FAO, 2014). West Africa is also a major production zone, with nearly 15 million cultivated hectares. The main producers in this area are Niger, with over 3 million tons produced in 2014, Mali, Nigeria and Burkina Faso with over 1 million tons each (FAO, 2014). Senegal comes in 6th position among West African producer with 400.000 tons produced in 2014. Eastern and Southern Africa regions also cultivate pearl millet but the total surface occupied by pearl millet in this area is only 2 million hectares (ICRISAT, 2013).

In these areas, pearl millet is usually grown as part of a mixed cropping system, alternate with legumes, such as groundnuts or cowpea, or with cereals such as sorghum or maize. Beside this staple crop usage, pearl millet is also grown in some parts of Brazil as a mulch crop in no-till soybean systems. The plant is not grown for its yield but for its ability to produce dense mulch in acidic soils. Mulch crop offers a permanent soil cover that recycles nutrient, limits erosion and weed growth. In central Asia, pearl millet is being tested as a rotational crop after wheat to increase cropping intensity and incomes and to limit soil erosion. These examples show that, apart from its major use as a staple crop, unique properties of pearl millet such as tolerance to drought and to acidic soils allow the emergence of novel uses for this cereal.

Pearl millet yields are low comparing to other cultivated cereals: around 900 kg/ha in 2014 at the worldwide level (FAO, 2014) comparing to 1.5 tons/hectare for sorghum, 3.3 tons/hectare for wheat and 5.6 tons/hectare for maize. Short cycle varieties generally produce lower yields but reduced cycle length is not the only factor limiting yield in pearl millet, as Indian F1 hybrids were reported to yield 3 to 4 tons/ha in 80 days in optimal conditions (Bidinger and Hash, 2004). The world production is mainly consumed locally, the amount of international trade staying below 0.5 million tons in 2014. The first exporter is India, whereas African countries keep all their production for local consumption. The exchange price is around 250 $/ton.

1.5 Nutritional data

Pearl millet is a highly nutritious cereal with high protein content (about 10% and up to 24% for some cultivars) and a 5% fat content (Andrew and Kumar, 1992). Its amino acid profile is better than that of maize or sorghum. It tends to have higher nutritional value than sorghum grown in equivalent culture conditions (Andrew and Kumar, 1992). Its micronutrient content is also good, with high iron (from 60 ppm iron for improved varieties to over 80 ppm iron in germplasm and breeding lines), zinc (around 30 ppm) and magnesium contents (up to 170 mg/100 g; Souci et al., 2000). Pearl millet seeds are usually eaten as porridge or flatbread. Pearl millet is also used to feed animals, after harvest or directly in the field by grazing, which limits costs and losses of nutrients associated with harvesting, processing, storing and feeding. It gives good results for feeding poultry, sometimes better than maize, and seems also suitable for pigs and beef cattle, especially by grazing (Andrew and Kumar, 1992). Despite its high

nutritional interest, average yield stays under 1 ton/ha in 2014 (FAO, 2014) and production is uncertain.

1.6 Factors limiting pearl millet production

Pearl millet is mostly grown in areas where the rainfall does not exceed 800 mm per year (Guigaz, 2002), the lower limit being around 150 mm per year. The soil is usually sandy and therefore drains water quickly, deep, with low soil organic matter (SOM) content and with low phosphorus (P) level. It is often grown in areas where no other cereal would grow. A number of abiotic or biotic factors limit peal millet yield.

1.6.1 Abiotic factors

1.6.1.1. Drought stress

The main physiological stress is water scarcity and randomness of rainfall, especially at the beginning and at the end of the growing season. The Sahelian climate is made of a rainy season that lasts from two to four months and a dry season that lasts the rest of the year, but the length of the rainy season varies from one year to another. This may lead to early and late drought stresses that threaten crop establishment and grain filling respectively (Eldin, 1993). Seeds are usually sown just before the first rain and germinate when this first rain occurs. But while this event symbolizes the beginning of the rainy season, it is not necessarily directly followed by other rain events in the next days. The young seedling, which benefited from the initial water input to germinate, can therefore be submitted to water shortage during several days. It has been pointed out that pearl millet is usually grown in deep sandy soils with low SOM content. This kind of soil has low water retention capacity and water can drain quickly out of it. Moreover, the bare soil surface temperature can reach up to 45°C in some places, so it becomes clear that the soil surface dries out very quickly, leaving the seedling with very few water resource. This can lead to early crop loss. Models predict that climate change will lead to increased precipitation in West Africa (Li et al., 2012). However, they also predict an increase in extreme events as heavy rains, drought or flooding and an increased year-to-year variability of precipitations (Sultan and Gaetani, 2016).

There is a wide variability of growth cycle length amongst pearl millet varieties, varying from 45 days for some very early varieties up to more than 140 days for very late varieties. These varieties have various appellations depending on places and local dialect. For instance they are called “Souna” for the early varieties and “Sanio” for the late ones in Senegal. Early varieties are usually grown in the Northern part of the growing area, where the length of the rainy season is short, in order to maximize the chance of success for the crop. On the contrary, the rainy season is longer in the South and it is therefore possible to grow late varieties in order to optimize the use of all the available water resource and therefore to maximize the yield potential. As it is possible to adapt the variety chosen to the expected length of the rainy season, and therefore to the amount of water averagely available, the randomness of this length can be a bigger problem for the crop success than the actual amount of rain.

1.6.1.2 Nutrient limitation

Pearl millet is grown on soils with a low SOM and fertilizer use is low or absent. In most part of West Africa, the most limiting nutrient is phosphorus (Chien et al., 1990; Payne et al., 1991). It is sometimes considered that the lack of nutrient is the main limiting factor for pearl millet growth, because its occurrence creates or reinforces the existing drought stress. This effect occurs because the lack of nutrients limits the development of the root system, thus preventing the plant from an optimal use of soil water resource. In addition, farmers tend to limit plant density on poor soils, leading to a greater evaporation and then lower water use efficiency. In a sense, water stress can then be considered as a consequence of low nutrient availability. Thus, the low availability of phosphorus in the soil could affect the success of the development of culture. After phosphorus, nitrogen is the second mineral limiting plant growth. This constraint limits crop yield but, unlike water or phosphorus, it does not jeopardize its establishment.

1.6.1.3 Other abiotic factors

Amongst other factors that may affect the culture, high temperatures play an important role. Their impact on culture is strongly linked to the state of the plant water status. Indeed, transpiration in leaves limits the excessive rise in temperature of the plant cover, but this phenomenon is only possible when water is available. Mechanical stress, which takes the form of a compact soil, hard to penetrate for the roots, is usually not a major problem for pearl millet. Sandy soils generally remain light and oppose little resistance to mechanical penetration. This constraint may nevertheless occur, especially when plowing led to the formation of a harder horizon under the plowed horizon, called hard pan. Soil acidity is also a limiting factor, although pearl millet is usually very tolerant to this phenomenon (Scott-Wendt et al., 1988). Soil salinity may also reduce pearl millet yield.

1.6.2 Biotic stresses

The main biological threats to pearl millet production, according to ICRISAT (2013), include:

- Weeds: weedy wild relatives were already mentioned. The main weed in pearl millet fields is striga (*Striga hermonthica*), a parasitic plant. Its incidence increases with phosphorus deficiency and the shortage of this element for the crop is therefore a double punishment because, on top of lacking an essential micronutrient, it is also more likely to be parasitized. Striga has a strong impact on yield, going up to 100% of yield loss, and it affects about 40% of the cereal-producing area in sub-Saharan Africa (Gurney et al., 2006; Kountche et al., 2013).
- Various fungal and pseudo-fungal diseases, especially downy mildew (caused by *Sclerospora graminicola* and *Plasmopara penniseti*), blast (caused by *Pyricularia grisea*), smut (caused by *Moesziomyces penicillariae*), ergot (caused by *Claviceps fusiformis*) and rust (caused by *Puccinia substriata* var. *penicillariae*).
- Bacterial diseases as bacterial spot (*Pseudomonas syringae*) and bacterial leaf streak (*Xanthomonas campestris* pv. *pennamericanum*).
- Insect pests, including millet head miner and stem borers.

- Parasitic nematodes.

Many constraints limit pearl millet production and abiotic conditions play a central role among them, especially water and nutrient limitations. Improving pearl millet root system could help optimizing their uptake and therefore increase yield in limiting conditions, without resorting on greater inputs. A good knowledge of root system structure and functioning is necessary to identify relevant traits to improve. Knowing the genetic basis controlling the establishment of this root system may allow the use of marker assisted selection, a powerful tool that fasten breeding on selected traits (Steele et al., 2006).

2. The root system of cereals

A root is defined as a highly differentiated multicellular axis found only in the sporophytes of vascular plants that typically has a rootcap, endodermis, pericycle and lateral roots (Seago and Fernando, 2013). The root system is the network formed by all the roots of a plant. Its main functions are anchorage of the plant body to its substrate and absorption of water and dissolved minerals to support growth and development. In some cases, it also fulfills storage and vegetative reproduction.

2.1 Root system organization

The root system is formed of a plurality of root types:

- the primary root is derived from the radicle that emerges from the seed. The destiny and the importance of that root vary widely depending on the plant.
- seminal roots are embryonic roots formed within the scutellar node of the plant embryo in some monocotyledonous plants (Plant Ontology). Rice primary root is also often designed as “seminal root” (Rebouillat et al., 2009).
- adventitious roots are post-embryonic roots emerging from non-root tissue. They have different names according to the tissue from which they originate. Typically, crown roots are shoot-borne roots emerging from a stem node (Plant Ontology). They can be induced by exogenous factors, like sugar in *Arabidopsis thaliana* (Takahashi et al., 2003) or be produced ontogenetically.
- lateral roots emerge from a mature root that can be a primary, seminal, adventitious or lateral root. They may be referred as branch roots or secondary roots.

Root system organization differs between Monocots and Dicots. In Dicots such as *A. thaliana*, the primary root persists over time and is the major axis of the mature root system. This gives rise to a so-called taproot root system. In contrast, in Monocots such as cereals the importance of the primary root is limited and it regresses quickly. Adventitious roots form most of the root system, forming what is called a fibrous root system. The components of the root system of a young Monocot are presented in **Figure In-3**, based on the example of maize root system.

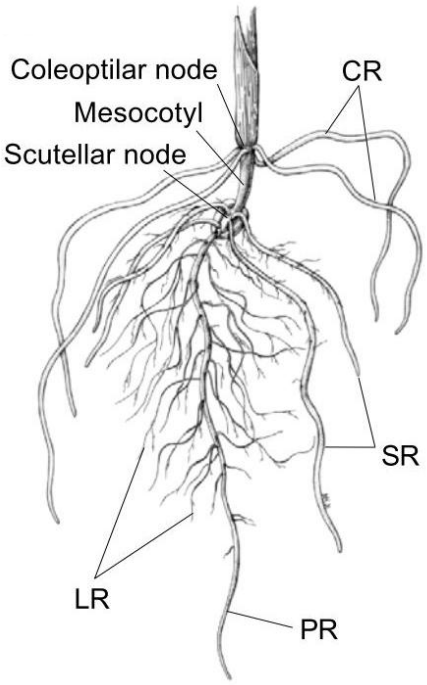

Figure In-3: Maize root system as example of cereal root system. 14-day-old maize seedling displaying primary (PR), seminal (SR), shoot-borne crown (CR) and lateral (LR) roots.
Reproduced from (Hochholdinger and Feix, 2002).
Drawing by Miwa Kojima (Iowa State University).

2.2 Genetic control of cereal root system development

Root system architecture depends on:

- the growth of individual root types,
- the formation of new roots, emerging from a root (lateral roots) or from a non-root tissue (adventitious roots),
- root angles.

Root system development in cereals includes development of the primary root and lateral roots, which are common between Monocotyledonous and Dicotyledonous plants, and crown root development, which is characteristic of Monocots. While the genetic bases of root development have been largely explored in the model plant *Arabidopsis*, they are less well known in cereal crops. Genetic studies on root system development in Monocot were mostly performed on the model plant rice (*Oryza sativa*) and on maize (*Zea mays*).

2.2.1 Primary root growth

Genes controlling primary root growth have been identified in rice. They are mostly involved in root apical meristem maintenance and cell elongation, two processes that mainly drive root growth. The *srt1 (short root 1)* and *rrl1 (reduced root length 1)* mutants have reduced root growth, due to reduced cell elongation (Ichii and Ishikawa, 1997, Inukai et al., 2001). *RRL1* was proposed to promote the beginning of cell elongation (Inukai et al., 2001b) but the exact nature of the protein coded by this gene is not documented yet. *RRL2* (*REDUCED ROOT LENGTH 2*) inhibits the transition of the cell from division to elongation.

Accordingly, the *rrl2* mutant has reduced root growth, due to a reduced cell length but also to a shorter root apical meristem and a smaller cell flux (Inukai et al., 2001b). Similarly, the *shoebox* (*shb*) rice mutant has shorter and fewer cells in the root meristem (Li et al., 2015). *SHB* encodes an AP2/ERF transcription factor that directly activates transcription of a gibberellic acid (GA) biosynthesis gene and therefore GA production. Accordingly, the *shb* phenotype can be rescued by GA application or phenocopied by application of a GA biosynthesis inhibitor. This indicates that GA regulates root meristem size (through cell division and elongation) in rice (Li et al., 2015).

Conversely, the *crl2 (crownrootless 2)* mutant has longer cell size, longer apical meristem and higher cell flux (Inukai et al., 2001b). *CRL2* promotes the transition of meristematic cells from division to elongation. *SRT6 (Short Root 6)* positively controls primary root growth. It was suggested that *SRT6* plays a role in abscisic acid (ABA) perception or signal transduction (Yao et al., 2003). The *srt5 (short root 5)* mutant has a very short root system at one week, but it recovers after 45 days. The *SRT5* gene was first suggested to be involved in ABA biosynthesis (Yao et al., 2002) but further studies suggested that *srt5* phenotype was sugar-dependant and that ABA regulation of root growth in this mutant was mediated by sugar (Yao et al., 2004). Retarded seedling root growth in this mutant might be due to deficient sugar transport from photosynthetic leaves to seeds during their maturation, underlying the fact that early root growth is also determined by seed traits.

Phosphorus-starvation tolerance 1 (*PSTOL1*) is a gene identified in Kasalath, responsible for a major quantitative trait locus (QTL) for phosphate deficiency tolerance (Gamuyao et al., 2012). It was isolated in a traditional rice variety and is absent from the rice reference genome and modern rice varieties, that are intolerant to phosphorus starvation. This gene codes for a protein kinase and acts as an enhancer of early root growth, enabling plants to acquire more phosphorus and other nutrients. This demonstrates the importance of root characters for abiotic stress tolerance.

Our current knowledge of the genes regulating root growth in cereals, with rice as model, is summarized in **Figure In-4**.

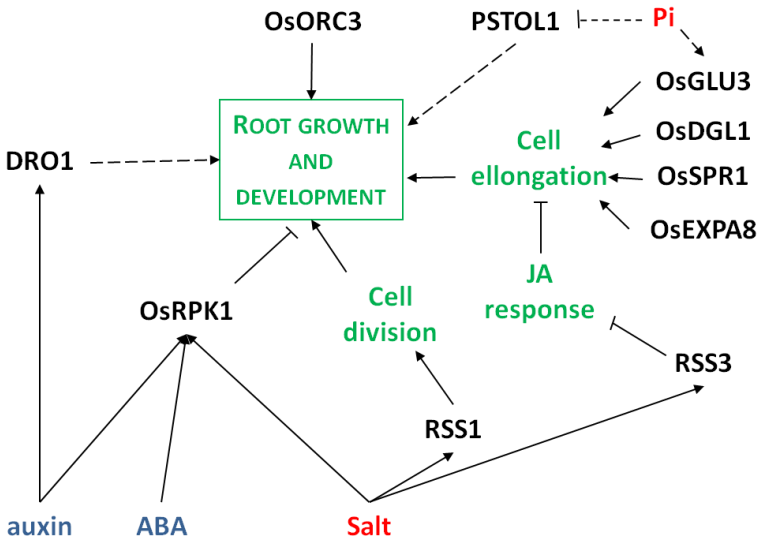

Figure In-4: Gene networks controlling root growth in rice. Arrows represent the positive regulatory action of one element of the network on another one. A line ending with a trait represents

the negative regulatory action of one element of the network on another one. Dotted line represent hypothetical link between two elements. Text color code: genes, black; hormones, blue; signals, red; biological processes, green.
Modified from (Mai et al., 2014).

2.2.2 Lateral root formation

Lateral roots arise from divisions of specific cells within the parent root. In maize, rice, barley and wheat, these lateral root founder cells originate from pericycle and endodermal cells located opposite to phloem poles (Casero et al., 1995; Hochholdinger et al., 2004). Lateral root development follows an acropetal sequence, the youngest primordia forming closest to the root tip. In rice, lateral root primordia are first observed between 3 and 6 mm to the root tip but lateral root priming is supposed to happen as close as 1 mm to the root tip (Takehisa et al., 2012). Primordia are first observed 10 to 15 mm from the root tip in maize (MacLeod, 1990) and 10 to 20 mm from the root tip in barley (Babé et al., 2012).

Lateral root initiation has been extensively studied in *A. thaliana*. In this model plant, the phytohormone auxin plays a central role in this developmental process (reviewed in Lavenus et al., 2013). It also plays a central role in lateral root development in cereals (Orman-Ligeza et al. 2013). Indeed, the majority of cereal mutants affected in lateral root initiation and development are related to auxin. A parallel between the gene regulatory networks controlling crown root and lateral root initiation in rice and lateral root initiation in Arabidopsis is presented in **Figure In-5**.

In rice and maize, lateral root initiation requires local auxin accumulation that is dependent on the specific activity of auxin efflux carriers encoded by the *PIN-FORMED* (*PIN*) gene family (Wang et al., 2009, Jansen et al 2012). Mutation in *CROWN ROOTLESS 4* (*CRL4*), also known as *OsGNOM1*, leads to a reduced number of lateral roots and the absence of crown roots (Liu et al., 2009). OsGNOM1 is a large guanine nucleotide exchange factor (GEF) for ADP-ribosylation factor that regulates the intracellular trafficking of the PIN auxin efflux carriers. The expressions of *OsPIN2*, *OsPIN5b*, and *OsPIN9* are also altered in *crl4* (Kitomi et al., 2008; Liu et al., 2009).

Auxin perception mechanisms have been well characterized (Salehin et al., 2015). It involves a co-receptor made of a member of the TRANSPORT INHIBITOR RESPONSE1 (TIR1)/ AUXIN SIGNALING F-BOX (AFB) protein family and an Aux/IAA protein. *Aux/IAAs* are early auxin response genes that encode repressor of auxin response. Upon auxin binding to the co-receptor, Aux/IAAs are degraded and this leads to de-repression of AUXIN RESPONSE FACTOR (ARF)-mediated transcription of auxin-responsive genes (Salehin et al., 2015). In maize, auxin perception in lateral root founder cells is mediated by the *Aux/IAA* gene *ZmIAA10* also known as *ROOTLESS WITH UNDETECTABLE MERISTEM1* (*RUM1*). RUM1 represses auxin responsive genes via the interaction with the ZmARF25 and ZmARF34 transcription factors (Von Behrens et al., 2011). Accordingly, the dominant negative *rum1* mutant is impaired in LR initiation in the primary root (Woll et al., 2005). High level of auxin in pericycle founder cells lead to the degradation of RUM1 proteins which activates the expression of downstream auxin response genes and leads to the cell division and lateral root initiation. In rice, *OsIAA13* controls the expression of genes that are

required for lateral root initiation in a similar way as *ZMIAA10* (Kitomi et al., 2012). *OsIAA11* and *OsIAA30* have similar sequences and expression patterns as *OsIAA13*, suggesting that they may have redundant function in lateral root initiation (Jain et al., 2006; Zhu et al., 2012). Altogether, the auxin-mediated pathway controlling lateral root formation seems to be conserved between *Arabidopsis* and model cereals (rice and maize). This was further confirmed by comparative transcriptomics studies that revealed a common transcriptional regulation during lateral root initiation in *Arabidopsis* and maize (Jansen et al., 2013). This suggests that the genetic pathways regulating root development discovered in *Arabidopsis* could be translatable in cereal crops.

Other phytohormones regulate lateral root formation. In rice, cytokinin treatment inhibits lateral root initiation but increases lateral root growth (Debi et al., 2005). However, the genes implied in these responses are hardly known in cereals. ABA treatment leads to initiation of lateral root primodia in the tips of young seminal rice roots (Chen et al. 2005) through an increase in cytoplasmic Ca^{2+} that activate downstream signaling components, such as calcium/calmodulin-dependent protein kinase or phosphatase via a Ca^{2+}-calmodulin complexe. This changes the phosphorylation status of actin depolymerization factor and causes rearrangement of the cytoskeleton during cell growth leading to root tip swelling, root hair formation and lateral root formation (Chen et al., 2005).

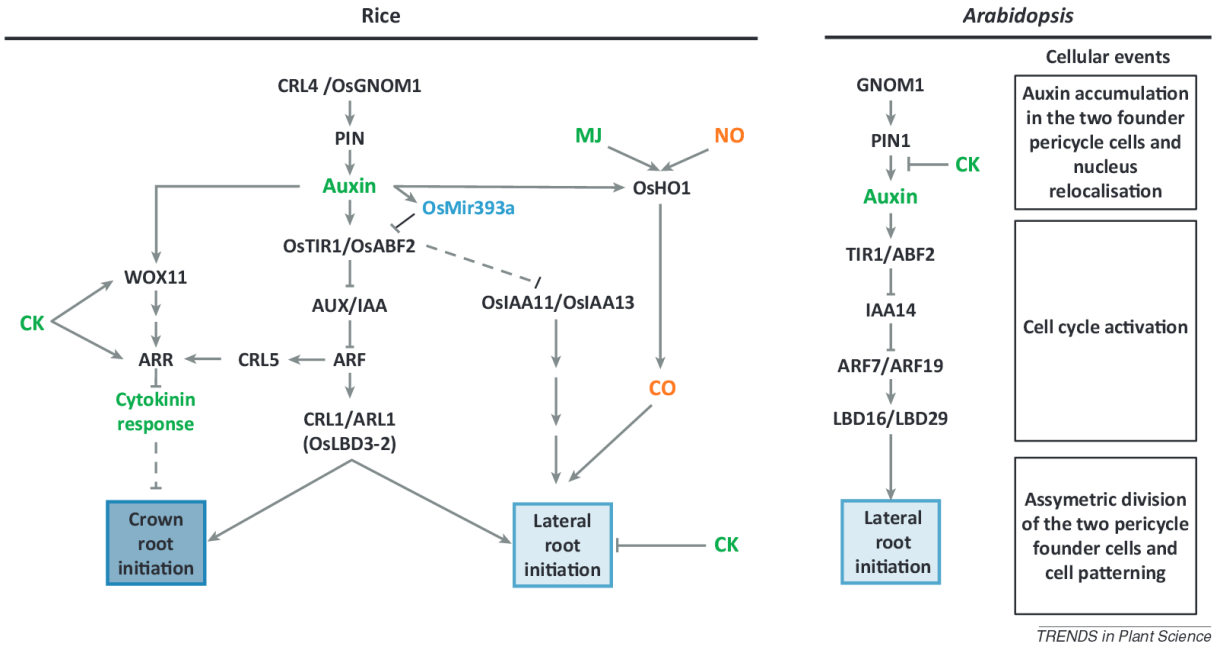

Figure In-5: Gene regulatory networks controlling crown root and lateral root initiation in rice and lateral root initiation in Arabidopsis. The corresponding early cellular events of root initiation in Arabidopsis are noted. Arrows represent the positive regulator y action of one element of the network on another one. Genes are denoted in black, hormones in green, miRNA in blue and regulatory molecules in red. A line ending with a trait represents the negative regulatory action of one element of the network on another one. Dotted lines represent hypothetical links between two elements. Abbreviations: AFB2, auxin signalling F-box2; ARF, Auxin Response Factor; ARL, adventitious rootless; ARR, type-a response regulator2; AUX/IAA, auxin/indole-3-acetic acid; CK, cytokinin; CO, carbon monoxide; CRL, crown rootless; GNOM1, membrane-associated guanine nucleotide exchange factor of the ADP-ribosylation factor G protein (ARF-GEF); HO1, heme

oxygenase 1; LBD, lateral organ boundaries domain; MJ, methyl jasmonate; NO, nitric oxide; PIN, pin-formed auxin efflux carrier proteins; TIR1, transport inhibitor response 1; WOX11, WUSCHEL-Related Homeobox 11.
(Orman-Ligeza et al., 2013).

2.2.3 Crown root formation

Genes involved in crown root formation are largely common with those regulating lateral root development. Once again, auxin plays a central role through a pathway similar to the lateral root initiation pathway described in *Arabidopsis* (**Figure In-5**). However, some differences have been reported between lateral and crown root formation.

In terms of auxin signaling, *CROWN ROOTLESS 1* (*CRL1*) is required for crown root primordia initiation in rice (Inukai et al., 2001a). It codes for a protein of the LATERAL ORGAN BOUNDARIES (LOB) family also known as LOB DOMAIN 3-2 (OsLBD3-2) (Coudert et al., 2013) and its expression is induced by auxin, via the de-repression of OsARF1 (Inukai et al., 2005). *RTCS (rootless for crown and seminal roots)* is a maize orthologous of *CRL1* that codes for a LOB-domain protein and is involved in embryonic seminal and crown root emergence but not in lateral root initiation (Hetz et al., 1996; Taramino et al., 2007).

Crown root initiation also implies cytokinin and this pathway is better known than for lateral root initiation. In rice, two genes from the *APETALA2* / *ETHYLENE RESPONSIVE FACTOR* (*AP2*/*ERF*) transcription factor family were found to be implied in cytokinin pathway. The first one, *CROWN ROOTLESS 5 (CRL5)*, is expressed in response to auxin, as direct target of *OsARF1* (Kitomi et al., 2011). It is close to the *Arabidopsis* gene *AINTEGUMENTA* (*ANT*), which regulates growth during lateral organ development. CRL5 positively regulates *OsRESPONSE REGULATOR1* (*OsRR1*) and *OsRR2*, two type-A cytokinin-responsive regulator genes, expression. This pathway is only implied in crown root emergence, as *crl5* produces fewer crown root but has a normal amount of lateral roots (Kitomi et al., 2011). The second one, *ERF3*, binds *OsRR2* in crown root primordia (Zhao et al., 2015). In emerging crown roots, the *WUSCHEL-related Homeobox* gene *WOX11* is expressed, it interacts with ERF3 and binds to OsRR2, leading to inhibition of ERF3 function or direct repression of OsRR2 and enhanced cytokinin signaling that promotes crown root growth (Zhao et al., 2009, 2015). There are two parallel pathways regulating *OsRR1* and *OsRR2*, one implying *CRL1*/*CRL5* and the other *ERF3* and *WOX11*. They lead to the repression of cytokinin signaling and promotion of cell division during crown root initiation.

2.2.4 Root angle

Crown root angle plays an important role in the shape of the root system, as high crown root angles to the vertical result in an increase in deep rooting. In rice, crown root growth direction is positively correlated with apical diameter (Araki et al., 2002) and genotypic variation has been evidenced for root growth angle in upland fields (Kato et al., 2006). *DEEP ROOTING 1* (*DRO1*) gene was shown to influence crown root angle by mediating root gravitropic response (Uga et al., 2013). Indeed, it promotes cell elongation and is degraded by auxin, which is distributed to the lowest part of the root in response to gravity (Band et al.,

2012). *DRO1* is thus degraded in the lowest side of the root, leading to a slower growth of downward cells compared to upper ones. IR64, a leading paddy cultivar with shallow rooting, transformed with the *DRO1* allele of Kinandang Patong, an upland cultivar from the Philippines that shows deep rooting, showed deeper rooting due to an increased root angle and had enhanced drought tolerance. A noticeable fact for this gene is that this transformation did not lead to different root biomass.

2.3 Pearl millet root system

Few studies were published on pearl millet root system. A general description was given by Maiti and Bidinger (1981) defining different root types:

- the seminal or primary root, derived directly from the radicle;
- adventitious roots, which develop from nodes at the base of the stem;
- crown (or collar) roots, which originate from several lower nodes of the stem at or above the soil surface.

2.3.1 Developmental dynamics

Lateral roots and adventitious roots start to appear respectively 3-4 days after germination on the primary root and 6-7 days after germination in the nodal region at the base of the seedling stem (Maiti and Bidinger, 1981). In the field, adventitious roots were first spotted at the 5-leaf stage, 9 to 10 days after germination (Chopart, 1983). Their number varies from three to five per shoot and they are thicker than the primary root (Maiti and Bidinger, 1981). The crown roots appear in the lower nodes of the stem near the soil surface approximately 30 days after germination. The crown roots stay unbranched during several days before developing many lateral branches by the time of flowering (Maiti and Bidinger, 1981). Regular measures of average diameters in the field revealed that at 30 days, the average diameter stays high, meaning that the root system does not have many lateral roots at this stage (Chopart, 1983).

The primary root system, formed by the primary roots and all its laterals, leads the growth of the root system during the first 15 days, at an average speed of 2 cm/day, and is then outdistanced by the adventitious root system, that grows at an average speed of 3.5 cm/day during 50 days (Chopart, 1983). Pearl millet roots were found at up to 2 meters in depth (Brück et al., 2003a) and more than 3 meters laterally from the stem (Chopart, 1983). The primary root system remains functional up to 45 to 60 days after germination, before decaying (Maiti and Bidinger, 1981). This correlates with a peak of root system biomass observed two months after germination in well-watered plants grown in pots (Payne et al., 1991). The decline of root biomass observed after that date was attributed to root dying and carbon translocation to shoots.

2.3.2 Root function

Adventitious roots rapidly develop a very extensive system of secondary and tertiary branches and are the main pathway for supplying water and nutrients to the plant during most

of its life and in particular during flowering and grain filling (Maiti and Bidinger, 1981). Crown roots are considered to serve mainly as support for the stem but their lateral roots appear to be active in the uptake of water and nutrients.

2.3.3 Response to limiting conditions

Both water and phosphorus supply have a positive influence on root system growth compared to situation with limited access to these two resources (Payne et al., 1991). In water stressed conditions, root biomass was increased by P supply, but this increase did not depend on the dose of P applied, which suggests that, above a minimal P supply, root biomass was limited more by water than P. Conversely, root biomass was increased by P supply in well-watered conditions. The authors conclude that water supply under dry conditions cannot be effectively managed for pearl millet production without addressing soil fertility constraints. Another study confirmed that root length is positively correlated with P supply, which suggests that low P availability could increase pearl millet sensitivity to drought stress, due to a reduced root system development (Brück et al., 2003b). Pearl millet root system responds to drought by growing longer crown roots (Rostamza et al., 2013). In the case of water experimentally supplied only to primary root system, which could mimic a situation where water is available in depth but the subsoil is very dry, crown roots grew anyway, possibly with phloem-delivered water coming from the primary root system. A sufficient water uptake by primary root system in depth could therefore help the plant maintain its development, even if the topsoil is extremely dry. This situation may happen at the beginning of the growing season, when rain events may be spaced. Pearl millet is very resistant to drought but is in return very sensitive to waterlogging (Zegada-Lizarazu and Iijima, 2005). This justifies that pearl millet is nearly often grown on sandy and draining soils and is replaced by other cereals (sorghum, maize or rice) as soon as the soil is susceptible to waterlogging.

2.3.4 Comparison with other species and existing diversity

Pearl millet roots were shown to be longer than sorghum's in pot experiments (Rostamza et al., 2013). Pearl millet has also been compared to other millet species, a group of small-seeded cereals, in different watering conditions (Zegada-Lizarazu and Iijima, 2005). It appeared that pearl millet was the most resistant plant to drought compared to other millets. This was explained by high water use efficiency in this condition but not by increased water uptake efficiency in deep soil layers as compared to barnyard millet, another drought-resistant millet species. This suggests that deep water uptake could be improved in pearl millet. On the opposite, it was the most sensitive species to waterlogging, with the largest decrease of water use efficiency in this condition.

Inside pearl millet species, substantial genotypic variation were found among eight different varieties for root length density for root dry matter and total root length but not for depth of rooting or partitioning of roots between topsoil and subsoil (Brück et al., 2003b).

2.3.5 Ideas for improving the root system adaptation to main abiotic constraints

The main abiotic constraints the root system may help coping with are water and nutrient limitation. In particular, survival of the young seedling can be critical due to both phosphorus and water scarcity. Interestingly, an ideal root system phenotype for water and phosphorus uptake was suggested (Chopart, 1983). Water uptake requests that the roots grow rapidly in depth because of the quick water drainage of the sandy soils where millet is usually grown. On the contrary, phosphorus nutrition would request the formation of a dense root system in the topsoil where phosphorus is present. This might seem contradictory but as phosphorus uptake can only occur in a wet soil layer, which is not always the case for the topsoil, the ideal phenotype would be a root system that grows rapidly in depth and produces a dense lateral root system all along the soil profile. Comparing the actual root system to the ideal one leads to conclude that improving the early growth speed would be beneficial for pearl millet crops. This hypothesis seems supported by previously cited studies, showing that pearl millet has low water uptake in depth compared to other millet species resistant to drought (Zegada-Lizarazu and Iijima, 2005) and that water uptake from the primary root system can be sufficient to maintain seedling development in case of very dry topsoil (Rostamza et al., 2013).

Objectives of the thesis

Water and nutrient availability are two major factors limiting pearl millet growth, in particular in Africa. As root system architecture is a critical factor for the acquisition of these elements, breeding of adapted root systems is a promising strategy to improve pearl millet tolerance to drought and low soil fertility. However, very little is known about pearl millet root system development and function. Its general developmental dynamics has been described but variability exists among pearl millet cultivars and it has been poorly explored. Moreover, previous studies mainly considered the root system as a whole and did not separate primary, crown and lateral roots, although their functions are different. Furthermore, these studies mainly used destructive methods to study the root system. Modern phenotyping techniques now allow non-destructive studies and thus precise measurement of temporal characters associated to root development.

In this context, the first aim of my work was to produce a precise description of pearl millet root system. We therefore performed a general morphologic description of early root system development, obtained quantitative data on root system development dynamics as well as anatomical description of the different types of root. We also evaluated the diversity existing among a panel of diverse pearl millet lines. These results are presented in **Chapter 1**.

Our data showed that variability existed among lateral root growth. Hence we designed a pipeline to efficiently measure growth profiles of a large number of lateral roots and used a statistical model to classify lateral roots according to these growth profiles. This classification was used to characterize this variability and to condense it. This reduction of temporal complexity allowed to probe the relationship between lateral root growth behavior and other characters, especially root anatomy. It also allowed to characterize the repartition of these different lateral root types along the primary root and to assess the local influence of root types on neighbor lateral roots. These results are detailed in **Chapter 2**. This work was conducted in parallel on two species, pearl millet and maize, allowing us to underline specificities for each species.

Little is known about the genetic control of root development in pearl millet. We initiated a genetic study (using a genome wide association study approach) to identify genes involved in primary root growth. A large diversity panel was phenotyped for primary root growth rate and each accession was genotyped by sequencing. **Chapter 3** presents the methodology used and the results obtained after phenotyping and genotyping.

Chapter 1

General characterization of pearl millet root system

This chapter is composed of three parts. The first part is a journal article (Passot et al., 2016) that was published in Frontiers in Plant Sciences. The general aim of this paper was to provide a morphological and anatomical description of pearl millet root system, especially in early stages. A new nomenclature for roots was also needed, as the existing names for pearl millet root (Maiti and Bidinger, 1981) were in contradiction with Plant Ontology, which is the most broadly shared reference for naming plant elements. This paper provides a dynamic description of early stages of pearl millet root system architecture and an anatomical description of the different types of roots. It revealed the existence of three types of anatomically distinct lateral roots. It also evidenced the existence of a large diversity in early primary root growth and lateral root density among a small diversity panel of pearl millet inbred lines thus serving as a proof of concept for genetic analyses.

The second and third parts are supplementary results. The detailed root set up dynamics of two pearl millet inbred lines with contrasted root traits identified during the high throughput phenotyping experiment are compared in the second part. The root systems of plants grown in well-watered or drought-stressed conditions, observed with X-ray microcomputed tomography, are compared in the third part.

1. Characterization of pearl millet root architecture and anatomy reveals three types of lateral roots

Sixtine Passot[1,2], Fatoumata Gnacko[1], Daniel Moukouanga[1,3], Mikaël Lucas[1,3,4], Soazig Guyomarc'h[5], Beatriz Moreno Ortega[6], Jonathan A. Atkinson[7], Marème Niang Belko[3,8], Malcolm J. Bennett[7], Pascal Gantet[5], Darren M. Wells[7], Yann Guédon[2], Yves Vigouroux[1,3], Jean-Luc Verdeil[9], Bertrand Muller[6], Laurent Laplaze[1,3,4,*]

[1] UMR DIADE, Institut de Recherche pour le Développement (IRD), Montpellier, France
[2] UMR AGAP, Centre International de Recherche Agronomique pour le Développement (CIRAD) & Virtual Plants, Institut National de Recherche en Informatique et en Automatique (Inria), Montpellier, France
[3] Laboratoire mixte international Adaptation des Plantes et microorganismes associés aux Stress Environnementaux, Dakar, Sénégal
[4] Laboratoire Commun de Microbiologie IRD/ISRA/UCAD, Dakar, Sénégal
[5] UMR DIADE, Université de Montpellier, Montpellier, France
[6] Laboratoire d'Ecophysiologie des Plantes sous Stress Environnementaux (UMR LEPSE, INRA-Supagro), Montpellier, France
[7] Centre for Plant Integrative Biology, School of Biosciences, University of Nottingham, Sutton Bonington, UK
[8] Centre d'Etude Régional pour l'Amélioration de l'Adaptation à la Sécheresse (CERAAS), Institut Sénégalais des Recherches Agricoles, Thiès, Sénégal
[9] Plateforme PHIV, UMR AGAP, Centre International de Recherche Agricole pour le Développement (CIRAD), Montpellier, France

*** Correspondence:** Dr. Laurent Laplaze**,** IRD**,** UMR DIADE**,** 911 Avenue Agropolis**,** 34394 Montpellier cedex 5**,** France
laurent.laplaze@ird.fr

Abstract

Pearl millet plays an important role for food security in arid regions of Africa and India. Nevertheless, it is considered an orphan crop as it lags far behind other cereals in terms of genetic improvement efforts. Breeding pearl millet varieties with improved root traits promises to deliver benefits in water and nutrient acquisition. Here, we characterize early pearl millet root system development using several different root phenotyping approaches that include rhizotrons and microCT. We report that early stage pearl millet root system development is characterized by a fast growing primary root that quickly colonizes deeper soil horizons. We also describe root anatomical studies that revealed 3 distinct types of lateral roots that form on both primary roots and crown roots. Finally, we detected significant variation for two root architectural traits, primary root length and lateral root density, in pearl millet inbred lines. This study provides the basis for subsequent genetic experiments to identify loci associated with interesting early root development traits in this important cereal.

Keywords

Lateral root, root growth, metaxylem, root architecture, breeding

1.1 Introduction

In Africa, most of the recent increase in agricultural production has been due to the expansion of cultivated lands rather than an increase in yields (Bationo *et al*, 2007). Moreover, several climate models predict that global changes may reduce the potential productivity of cereals (Berg *et al.*, 2013). For example, millets potential productivity is predicted to decrease by 6% in the driest cultivated regions. In order to achieve future food security in Africa, it is therefore necessary to improve crop productivity through breeding and improved agricultural practices.

Pearl millet (*Pennisetum glaucum (L.) R. Br.*) is the sixth most important cereal grain in the world (FAO, 2014). It accounts for 6% of the total cereal production in Africa, and 14% in West Africa alone (FAO, 2014). Pearl millet grain is a significant source of micronutrients such as iron and zinc with contents higher than those in other cereals (Souci *et al.*, 2000). Both in sub-Saharan Africa and India, it potentially represents one of the cheapest food sources of these micronutrients and proteins when compared with other cereals and vegetables. In addition, pearl millet is well adapted to dry climates and is mostly grown in areas with limited agronomic potential characterized by low rainfall, in the 200-500 mm range, and marginal soils (Guigaz, 2002). These facts make millet an important food staple over much of the African continent, especially in the semi-arid areas of the Western Sahel where other crops tend to fail because of inadequate rainfall and poor soil conditions. Thus pearl millet is an important cereal in arid and semi-arid regions where it contributes to food

security and is expected to have an increased importance in the future adaptation of agriculture to climate change in sub-Saharan Africa.

Despite its importance, pearl millet is considered as an orphan crop because it has received very little support from science, industry and politics while other crops such as wheat, rice or maize were subjected to intense efforts of genetic and agronomic improvement. As a result, it lags behind sorghum and far behind the other major cereals in its genetic improvement. Its average grain yields barely reach 900 kg/ha, compared to 1500 kg/ha for sorghum (FAO, 2014). Moreover, production has increased by only 0.7% a year in West Africa during the last two decades, the lowest growth rate of any food crop in the region and far less than the population's growth rate of nearly 3% per year (United Nations Statistics Division, 2016). However, its untapped genetic potential is vast and could be used to improve pearl millet tolerance to some environmental factors that are the main limitations to its growth potential. For instance, pearl millet is mostly grown in marginal soils such as sandy soils in Western Sahel where low water and nutrient (particularly phosphate) availability are major limiting factors. Moreover, root establishment in poor soil is essential to ensure efficient use of available water.

The importance of root architecture for water and nutrient acquisition has been well documented in both monocots and dicots, and could be successfully used for root trait-targeted genetic improvement. For example, targeted modifications of root architecture in pea to increase P acquisition efficiency were achieved (Lynch, 2011). Pearl millet is a monocot species displaying a fibrous root system in which different categories of roots can contribute to a various extent in root system growth, branching and tropism dynamics as well as to water transport. Importantly, substantial differences in root traits were reported for 8 pearl millet varieties grown in soil in Niger (Brück *et al*., 2003) indicating a potential genetic diversity that could be used for breeding and selecting new varieties with improved root systems. However, the detailed structure and dynamics of pearl millet root system has not been described and very little is known about root growth and anatomy.

Here, we analyzed root architecture during the early phase of pearl millet development. Furthermore, we identified and characterized the anatomy of the different root types. Finally, we compared two root development parameters in 16 pearl millet inbred lines and show that there is a large diversity of phenotypes that could be exploited in later breeding studies.

1.2 Material and Methods

1.2.1 Plant material

Pearl millet (Pennisetum glaucum (L.) R. Br.) inbred lines (Saïdou et al., 2009) originating from Indian, West and Central African landraces were used in this study. Seeds were surface sterilized with 5% hypochlorous acid for two minutes, rinsed three times in sterile water, then immerged in 70% ethanol for two minutes, rinsed three times again and kept for ten minutes in sterile water. Seeds were put in Petri dishes containing wet filter paper for 24 hours in the dark at 30°C for germination. The age of the plants are given in DAG (Days after Germination) i.e. the number of days from the date of seed- transfer onto the filter paper for germination.

1.2.2 Root phenotyping

For analysis of root development, rhizotrons were built according to Neufeld et al. (Neufeld *et al*., 1989). They were composed of a 400 x 700 x 20 mm aluminum frame, and, from rear to front, a 5 mm extruded polystyrene layer, a 20 mm layer of substrate, a cellulose acetate tissue layer (40 µm mesh) and a 5 mm plexiglass (**Figure 1-1A**). In this system, the root system grows in two dimensions between the fabric and the plexiglass (**Figure 1-1B**). The cellulose acetate was chosen because it is both non-deformable, preventing roots to grow through (this was confirmed at harvest), and allows roots to remain hydrated. The water content of the substrate was evaluated at the onset of the experiment and later maintained above stressful threshold by daily weighing the rhizotrons and watering from the top. The substrate used was composed of 30% fine clay, 25% peat fibers, 5% blond peat and 40% frozen black peat (Klasmann-Deilmann France SARL). The average SWC (Soil Water Content) of the substrate was 56% (w:w). At one DAG, one germinated seedling (displaying a primary root of about 1 cm long) was transferred to the top of each rhizotron, in a layer of wet sphagnum. This layer permanently maintained wet in order to prevent the seedlings from drying out during the early stages of growth. The plants were placed in a 1 m² growth room with a 14 hour photoperiod, a temperature of 28°C/ 24°C during days/nights and a VPD of 1.5 kPa. From the second day of growth onwards, rhizotrons were scanned (Epson Expression 10000XL) every day at a fixed time at a resolution of 600 DPI. Root system outlines were then extracted using SmartRoot (Lobet *et al.*, 2011). These outlines comprised information on all root lengths, branching position and angle for every scan.

For high-throughput root phenotyping, a paper-based system was used (**Figure 1-1C**) according to Atkinson et al. (Atkinson *et al*., 2015). One DAG-old seedlings were transferred into pouches and then maintained in a growth room with a 14 hours photoperiod (28°C during day and 24°C during night). Pictures of the root system were taken every 2 days for 6 days with a D5100 DSLR camera (Nikon) at a resolution of 16 M pixels. The camera was fixed on a holder to maintain the same distance between the lens and each root system. At six DAG, the root tip of the "fastest-growing" plants reached the bottom of the pouches. The experiment was repeated 4 times independently. Root traits (primary root length, lateral root density along the primary root and number of crown roots) were extracted using RootNav (Pound *et al*., 2013).

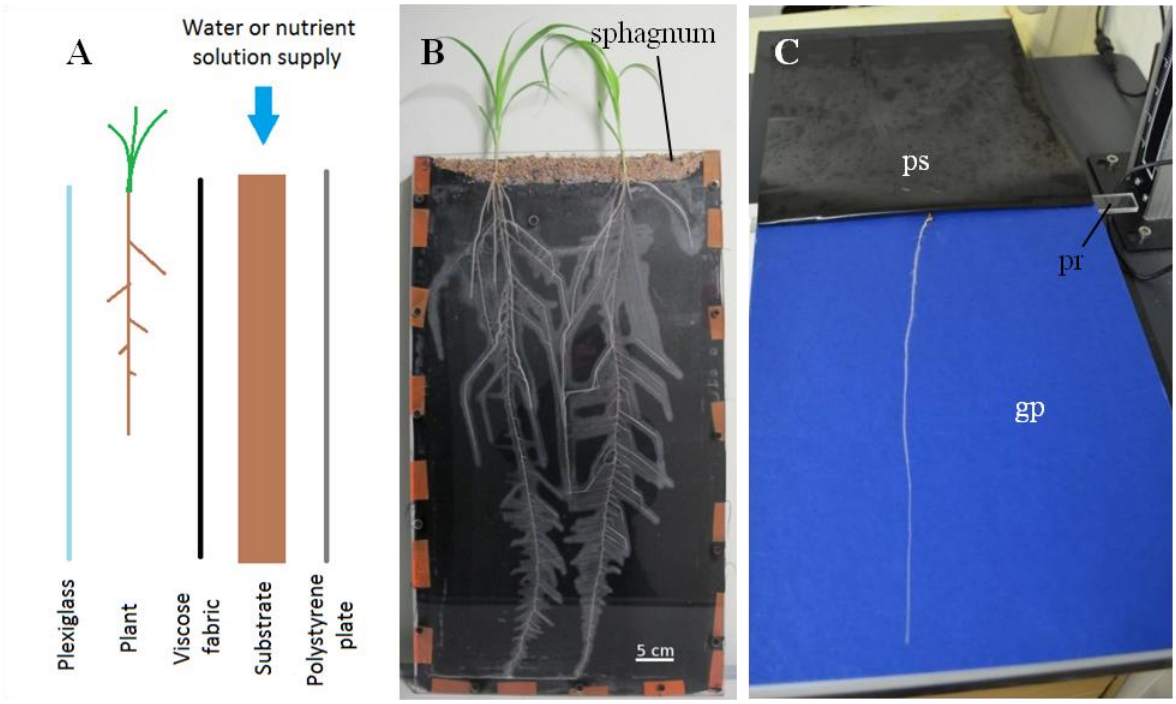

Figure 1-1: A: Scheme of the rhizotron used. B: A rhizotron at the end of an experiment. Scale bar: 5cm. C: One of the pouches used in the high-throughput phenotyping system. ps: plastic sheet, pr: plastic rod, gp: germination paper. These three elements are held together by foldeback clips (not visible here).

1.2.3 Root sections and microscopy

One DAG-old seedlings were transferred in a hydroponic system containing quarter strength Hoagland medium (Hoagland and Arnon, 1950) or put on the top of seed germination paper (Anchor Paper Company, USA) rolled on itself with the base immerged in distilled water (Hetz *et al*., 1996). The plants were kept in a growth chamber (12 hour photoperiod, a temperature of 27°C and an hygrometry of 60%) for 10 to 20 days. For sections of fresh material, 1-cm long samples were collected at the root apex and every 5 cm along the root and were embedded in agarose blocks (3% v/v in water) before sectioning, as described in Lartaud *et al*., (2014). The sampling positions were recorded. Transverse root sections (thickness 60 µm) were obtained using a HM 650V vibratome (Microm) and observed directly under the epifluorescence microscope. Some section were stained with Safranin and Alcian blue (FASGA, Tolivia & Tolivia, 1987).

For thin sections, samples were fixed and dehydrated as described by Scheres *et al*. (1994). Samples were then embedded in Technovit 7100 resin (Heraeus Kulzer) according to the manufacturer's instructions. Thin longitudinal sections (5 µm) were produced with a HM355S microtome (Microm). Sections were stained for 15 min in aqueous 0.01% toluidine blue (pH=6,8) solution and mounted in Clearium Mountant (Surgipath). Sections were visualized using a Leitz DMRB epifluorescence microscope (objectives used: 10x, numerical aperture (NA)=0,3; 20x, NA=0,5; 40x, NA=0,75). Pictures were taken using a Retiga SRV FAST 1394 camera (QImaging) and the QCapture Pro7 software (QImaging). Vessel dimensions were measured using ImageJ.

1.2.4 X-ray microcomputed tomography

Plants were transferred to pots (50 mm diameter and 120 mm height) containing "Newport Series Loamy Sand" soil (sand 83.2%, silt 4.7%, and clay 12.1%; organic matter 2.93%; pH= 7.13; Nitrate= 5.48 $mg.L^{-1}$; Phosphorus = Defra index of 3 (29.65 $mg\ kg^{-1}$)) one DAG. Plants were maintained throughout the experiment at a soil water content of ~26% (w:w), which corresponds to 75% of field capacity. The SWC was monitored daily by weighing the pots. Plants were scanned with a v|tome|x M scanner (Phoenix/GE Systems), with a maximum energy of 240 kV, 4 times over an 18 days period (4, 8, 14 and 18 DAG) to image the root structure. Root systems were segmented manually from the image stacks using the VGStudio Max software (Volume Graphics GmbH).

1.2.5 Statistical analyses and heritability estimates

Statistical analyses were performed using R (R Development Core Team, 2008). An analysis of variance was performed to detect an effect of the line on the variability of the different root traits measured. When an effect was detected, a Tukey's HSD (Honest Significant Difference) test was used to group lines of homogeneous means for the trait of interest.

Broad sense heritability was computed by dividing the variance associated with line with the total variance of the character (variance associated with line + environmental variance + residual variance).

Average seed weight for each line was evaluated and a Spearman's rank correlation coefficient was computed to detect a putative correlation between seed weight and root trait.

1.3 Results

1.3.1 Early development of pearl millet root system

The emergence and development of different roots in pearl millet seedling was studied in different growth conditions. Different roots observed at early stage are named according to the nomenclature presented in **Figure 1-2A**, based on the nomenclature used for maize root systems (Hochholdinger and Tuberosa, 2009). The first root to emerge from the seed, initially called the radicle, is then called the primary root. A small segment, called the mesocotyl, links the seed and the base of the shoot. At later stages of development, crown roots emerge from the base of the shoot. Branches that appear on the primary or crown roots are called lateral roots. The lateral roots can branch themselves, these ramifications being called secondary lateral roots.

The developmental dynamics of the root system was studied more finely on pearl millet line LCICMB1 (line 109 of the panel). In all of the plants that we analyzed in rhizotrons (n = 28), the early root system of pearl millet was made up of a single primary root that has emerged from the seed 12 to 24 hours after seed rehydration. This primary root grew vertically at an increasing rate during the first 6 DAG, reaching a maximum of 9.1 $cm\ day^{-1}$. After that date, the primary root growth rate slightly slows down, but remains *ca.* 7 $cm\ day^{-1}$ at 11 DAG (**Figure 1-2C**). The average primary root length at 11 DAG was 66.3 cm. Crown

roots and lateral roots started to emerge respectively from the shoot base and on the primary root at 6 DAG. The average number of crown roots per plant is shown in **Figure 1-2D**. Crown roots started to emerge 6 DAG and were in average two per plant at the end of the experiment. This number is quite low and this experiment only captured the very beginning of crown root emergence period. Average crown root growth rate was 3.7 cm day^{-1}. The number of lateral roots emerging each day on the primary root is shown on **Figure 1-2E**. Lateral roots started to emerge on the primary root 6 DAG. Their emergence rhythm increased until the end of the experiment, quickly up to 8 DAG and then slowly between 8 and 11 DAG. Lateral root density on the primary root was 4.2 roots cm^{-1}. Lateral root growth rates were heterogeneous, reaching up to 3 cm day^{-1}. Interestingly, crown roots and lateral roots started to appear at 6 DAG, when primary root growth rate reached its maximum, and correlates with the emergence of the third leaf.

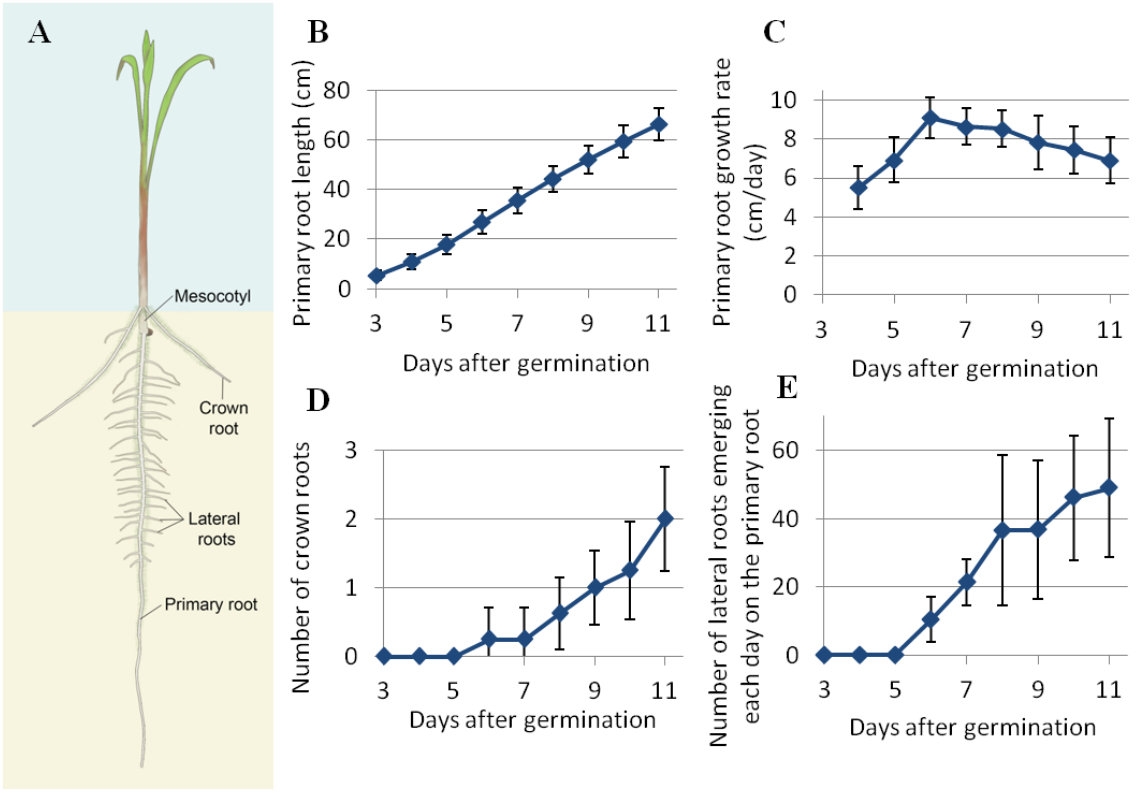

Figure 1-2: A: Scheme of the various roots of a pearl millet seedling. B: Daily average length of the primary root. C: Daily average primary root growth rate. D: Daily cumulative number of lateral roots along the primary root. E: Daily cumulative number of crown roots. N = mean +/- standard deviation.

Early root development was also analyzed in 3D in soil using micro-computed x-ray tomography (**Figure 1-3**). LCICMB1 plants were grown in small soil columns (5 cm diameter x 12 cm high) and scanned at 4, 8, 14 and 18 DAG. As in the rhizotrons, only primary root was visible at 4 DAG and crown and lateral roots could be detected from 8 DAG onwards. This indicated that these roots emerged between 4 and 8 DAG, but the time resolution was too rough to identify a precise emergence date. However, this time interval is consistent with their emergence time observed in rhizotron, of 6 DAG. This observation therefore supports the hypothesis that rhizotrons provide a realistic assessment of root architecture development in

natural conditions. The 3D images also gave us information about the organization of the different roots in space. The primary root, first to emerge, grew nearly vertically into the soil volume. On the contrary, crown roots grew at an angle of between 20° and 40° to vertical. This angle appeared conserved for the first centimeters of crown root growth, but the small diameter of the pots scanned constraining root growth to just a few centimeters after emergence, did not allow us to check whether this angle could be maintained. Crown root emergence sites were distributed regularly in space around the stem base.

Hence, early root system development in pearl millet is characterized by a fast growing primary root that quickly colonizes deeper soil horizons, while lateral and crown roots only start to emerge 6 DAG.

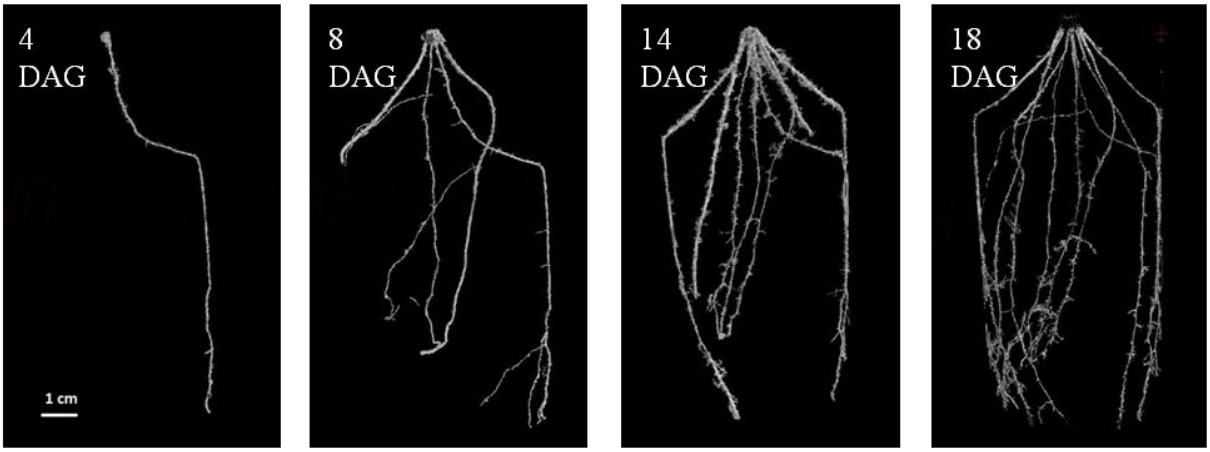

Figure 1-3: Establishment of the architecture of a soil grown pearl millet root system using X-Ray CT: 2D projection of a 3D image of the root system architecture. Images at 4, 8, 14, and 18 DAG (days after germination). Scale bar: 1 cm.

1.3.2 Anatomy of the different root types

We next analyzed the cellular organization of primary, crown and lateral roots of young pearl millet plants (LCICMB1 line) grown on germination paper or in hydroponics. Root fragments were harvested at different positions along the root and transverse sections were obtained using a vibratome. As root characteristics did not vary strongly in the zone we sampled (Supplementary Figure 1-1 for example of stele diameter) we considered all the samples we had to define the anatomical features of the different root types (**Table 1-1**).

Primary roots were characterized by a large diameter metaxylem vessel located at the center of the stele (**Figure 1-4**). Their ground tissue contained 3 to 5 layers of cortical cells. Aerenchyma differentiation was observed in mature parts of the root. Crown roots were thicker than primary roots with a significantly larger stele that contained 2 to 5 (3 in most cases) large metaxylem vessels separated by parenchyma cells (**Figure 1-4, Table 1-1**). They also showed 3 to 5 layers of cortical cells and aerenchyma. In both cases, cell wall autofluorescence was lower in the stele close to the root tip and increased particularly in the endodermis as the root matures, presumably because of cell wall lignification and suberization accompanying casparian strip formation.

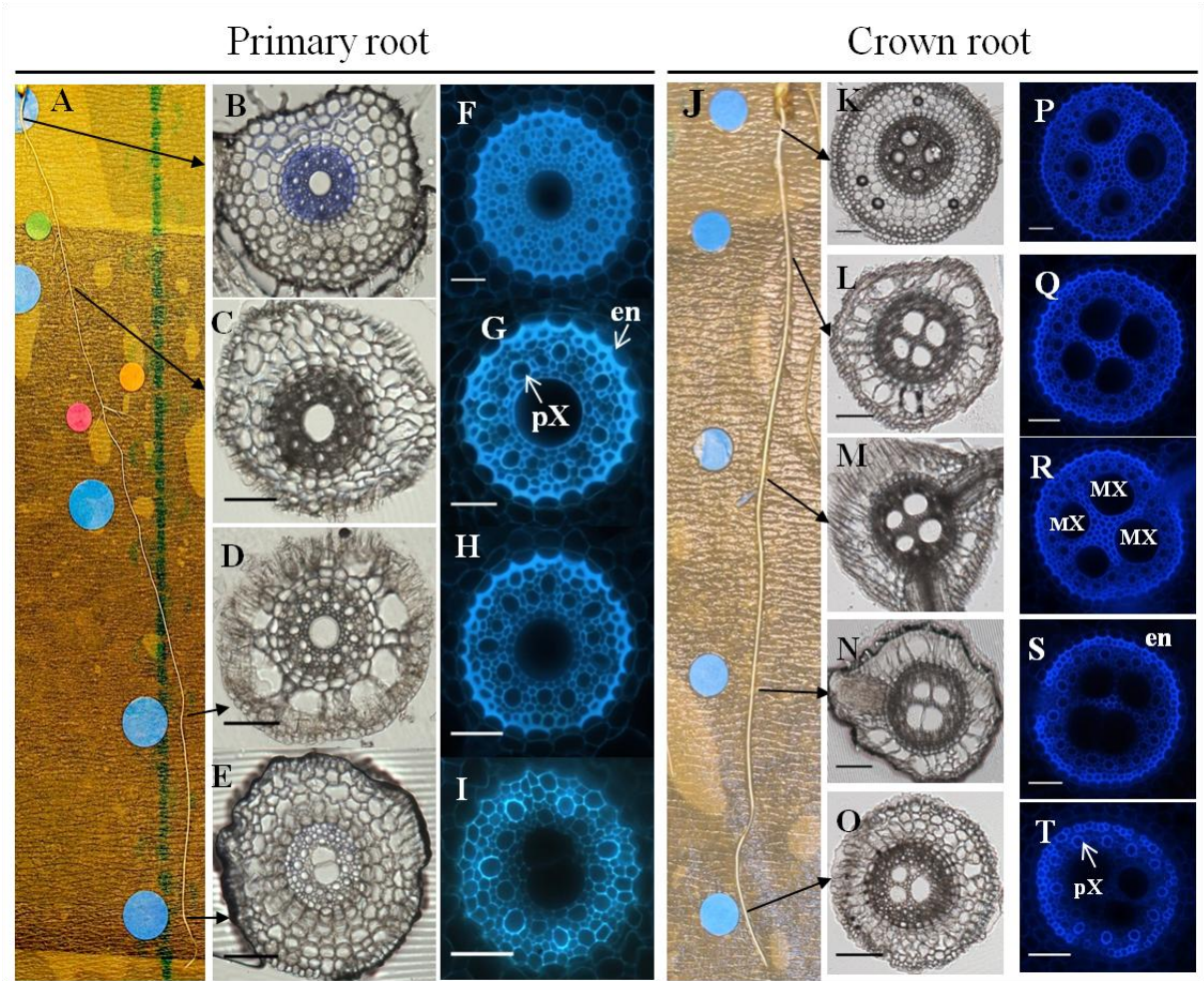

Figure 1-4: Anatomical organization of a primary root (B-I) and a crown root (K-T), 11 and 15 days after germination respectively. Transverse sections were performed every 5 centimeter, from the root apex to the root basis. A: general view of a primary root with the sampled zones marked by an arrow. B-E : transverse section of primary root observed in transmitted light (scale bar: 100µm). F-I : transverse section of primary root focused only on the root stele, observed in epifluorescence (natural autofluorescence at 460-480nm) (scale bar: 50µm). J: general view of a crown root with the sample zones marked. K-O : transverse section of crown root observed in transmitted light (scale bar: 100µm) P-T : transverse section of crown root focused only on the root stele, observed in epifluorescence (natural autofluorescence at 460-480nm) (scale bar: 50µm) co: cortex, ae: aerenchyma, MX: metaxylem, pX: peripheric xylem vessel, en: endodermis.

In order to localize secondary deposition (lignin or suberin) in the cell wall, we performed FASGA staining on transverse sections of primary and crown roots (**Figure 1-5**). The formation of a typical horseshoe-shaped Casparian strip could be visualized in the endodermis of both primary and crown roots as they differentiated. In addition, the FASGA staining revealed 6 xylem poles, alternating with 6 phloem poles in the primary root (**Figure 1-5E**), while we observed 12 to 16 xylem poles in crown roots (**Figure 1-5D**). Mature parts of crown roots displayed a sclerenchyma, surrounded by a hypodermis and a rhizodermis (**Figure 1-5A**).

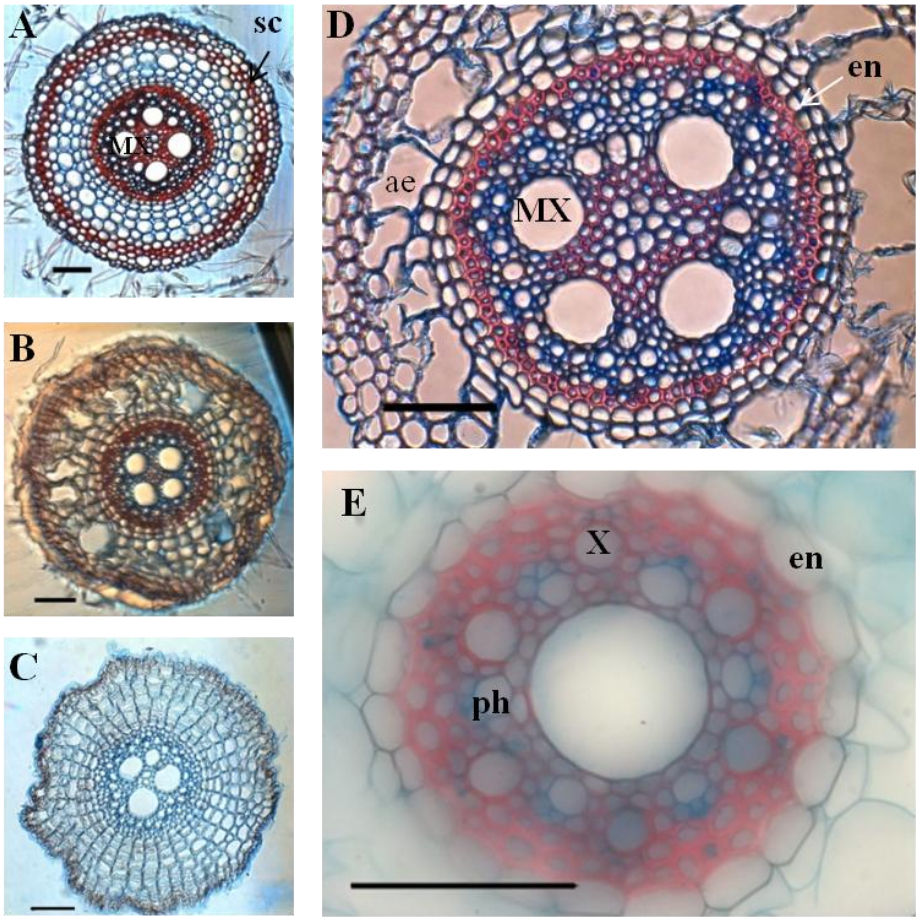

Figure 1-5: Transverse section of crown roots and primary root stained with FASGA. Sections were performed at various level along the roots axis. A-C : transverse section of crown root, after FASGA staining. D: transverse section of a crown root after FASGA staining, focused on the stele (scale bar: 100 µm) sc: schlerechyma, en: endodermis, X: xylem vessel, MX: metaxylem vessel, ph: phloem vessel, ae: aerenchyma.

Longitudinal sections (5 µm) through the primary root meristem revealed a closed meristem organization with cell files converging to a small group of cells whose location and size are consistent with those of quiescent center cells (**Figure 1-6A**). The metaxylem differentiated and expanded radially close to the putative initial cells. Cortex parenchyma cells accumulate metabolites, possibly starch grains, but further investigation is needed to identify the nature of this deposit. Longitudinal sections through the crown root meristem showed a similar closed meristem organization with a larger stele (**Figure 1-6B**).

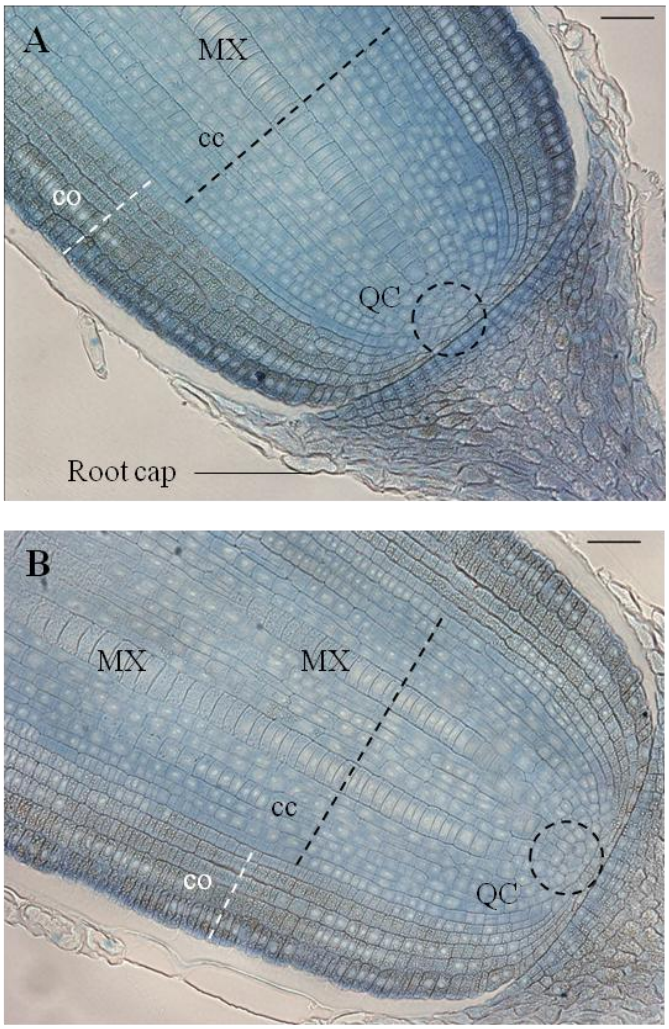

Figure 1-6: Anatomical organization of primary root and crown apices observed on a longitudinal section, stained with toluidine blue, sampled 5 days after germination. A: Longitudinal section of a primary root apex. B: Longitudinal section of a crown root apex. QC: quiescent center, cc: central cylinder, co: cortex, MX: metaxylem vessel. (scale bar: 100 µm)

Transverse sections through first order lateral roots (n = 33) branching from either primary or crown roots revealed distinct organizations. Interestingly, lateral roots could be classified into three types based on their anatomy (**Figure 1-7, Table 1-1**). Type 1 lateral roots are very thin (68-140 µm diameter) with an anatomy characterized by a diarch (2 protoxylem poles) stele without any central metaxylem vessel. Ground tissues include an endodermis, a bi-layered cortex, and epidermis, but neither sclerenchyma nor aerenchyma (**Figure 1-7A, D, G, J**). Type 2 lateral roots have a medium diameter (235-291 µm), show one small (16 µm diameter in average) metaxylem vessel and 3 layers of cortical cells. Like type 1, type 2 lateral roots have no sclerenchyma or aerenchyma (**Figure 1-7B, E, H, K**). Finally, type 3 lateral root exhibit the largest diameter (328-440 µm similar to primary root) and the same organization as primary roots, independently of the root from which they emerge (i.e. primary root or crown root) (**Figure 1-7C, F, I, L**). Hence our anatomical studies have revealed that there are 3 distinct types of lateral roots that form on both the primary root and crown roots in pearl millet.

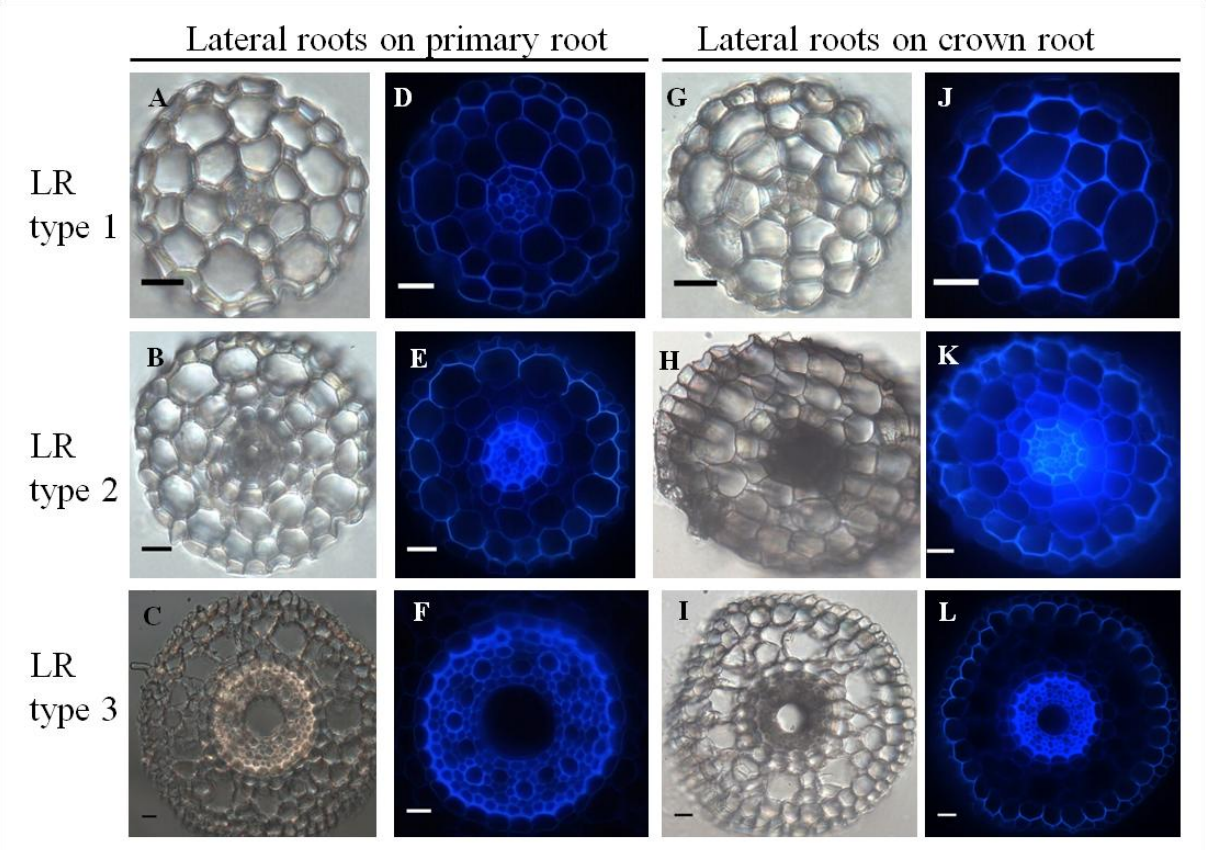

Figure 1-7: Comparative anatomical organization of lateral roots (left: transmitted light, right: autofluorescence). A-F : lateral root emerging from primary root. Picture F only shows the root stele. G-L: lateral root emerging from crown root. 3 root types are identified, independent of the mother root: Type I: small root diameter and no metaxylem (A, D, G & J), Type II: medium root diameter and small diameter metaxylem vessel, (B, E, H & K), Type III: large root diameter and large diameter central metaxylem vessel: (C, F, I & L). Scale bar: 20 µm

1.3.3 Diversity in pearl millet root development

We next addressed whether there was significant variation in pearl millet root architecture. We selected 16 lines from a panel of pearl millet inbred lines (Saïdou et al., 2009). As our objective was to maximise diversity, these lines were sampled to represent the whole diversity observed in the phylogenetic tree of 90 inbred lines (Saidou *et al*., 2009), taking also into account a sufficient seed set availability and good germination rate. We analysed the root system of these plants using a germination-paper-based phenotyping platform (Atkinson *et al*., 2015).

We observed large variation in primary root growth and lateral root density along the primary root among the individuals screened of this panel (**Figure 1-8**). In both cases, a significant part of this variability was explained by the genetic line variable (ANOVA $p < 0.01$). The lines could be separated into groups of homogeneous means with a Tukey's HSD test. For primary root length, the group identification showed some clear outliers with especially large or small values, associated with a group of lines with intermediate and quite homogeneous values (**Figure 1-8A**). For lateral root density, no clear outlier was observed, the values for all the lines forming a rather smooth continuum between small and large values (**Figure 1-8B**). The broad-sense heritability was equal to 0.72 for primary root length and to

0.34 for lateral root density. We tested whether the variability in early primary root growth was due to differences in available seed reserves (Supplementary Figure 1-2) by computing the Spearman's rank correlation coefficient between average seed weight and primary root length for each line. The Spearman's rank coefficient correlation was equal to 0.22. This value was not significantly different to zero (p = 0.21), indicating that no correlation could be found between seed weights and primary root length in our experiments. As seed mainly contains reserves, this result suggests that the differences we observed are not simply due to available reserves.

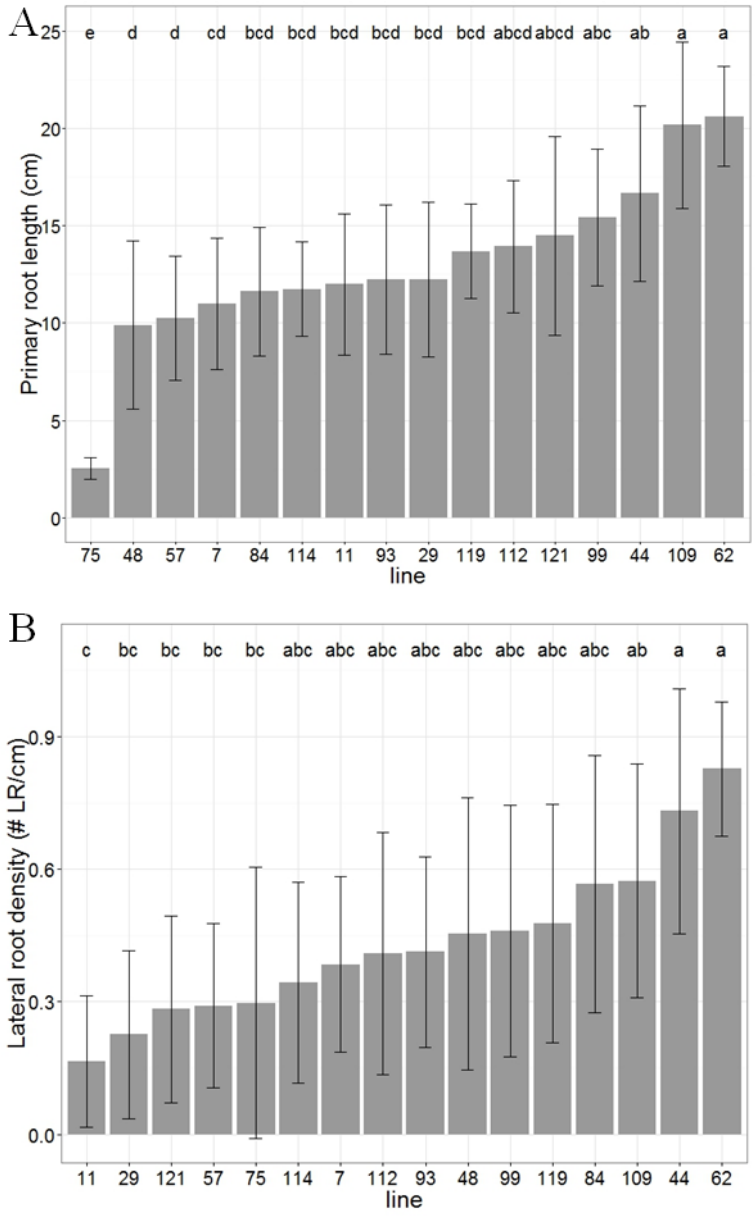

Figure 1-8: High throughput pearl millet root phenotyping: distribution of primary root length (A) and lateral root density (B) among 16 pearl millet from a panel of inbred lines covering a large genetic diversity. Error bars represent standard deviation, letters represent Tukey's HSD groups.

1.4 Discussion

Here, we analyzed root system architecture at early stages of the pearl millet life cycle. We named the different roots following the current standards in terms of monocotyledonous root nomenclature (Hochholdinger *et al*., 2004). One striking feature of early pearl millet root development is the very rapid emergence and vertical growth of the primary root (7 cm day^{-1} in our experimental conditions) compared to other cereals (3 cm day^{-1} for maize and wheat ; Muller *et al*., 1998; Pahlavanian and Silk, 1988; Pritchard *et al*., 1987). In contrast, root branching started relatively late after seedling germination (6 DAG). The X-ray CT experiment confirmed this global dynamics of early root system formation. Traditionally, pearl millet is sown at the very start of the rainy season. As it was domesticated in Sahel (Oumar *et al*., 2008) and is mostly grown in areas characterized by light soils with a low carbon content and water retention capacity, we hypothesize that the observed developmental pattern can be favorable to the rapid colonization of deep soil horizons that retain some water. This might therefore be an important adaptive strategy to deal with early drought stress. The observed anatomy of pearl millet roots is consistent with those found in other cereals such as rice (Rebouillat *et al*., 2009), wheat, barley and triticale (Watt *et al*., 2008) or maize (Hochholdinger, 2009). A striking difference between the different root types comes from the number of central metaxylem vessels: one (or two) in the primary root, always more than two in the crown roots, including the root emerging from the scutellar and coleoptile node. Interestingly, our analyses identified three different lateral root types on the basis of their diameter and radial anatomy. Variation in lateral root anatomy has been reported in other cereals, with numbers of distinct types varying from two in rice (Rebouillat *et al*., 2009) to five in wheat (Watt *et al*., 2008). Recently, a more detailed characterization of cortex cell layers present in rice lateral roots revealed that 3 types of lateral roots exist in rice (Henry *et al*., 2016). These anatomical distinctions share similar features across species, the smallest root type having a very simple organization, with only two (or three) xylem vessels and no aerenchyma, and the bigger type having an organization similar to a primary root. One can hypothesize that these different lateral root types have different roles: type 1 lateral roots may be involved in the exploitation of resources close to the root whilst type 3 lateral root could be involved in the branching of the root system and the exploration of new soil volumes. The role of type 2 lateral roots is still unclear. Nevertheless, the functional relevance of these differences in anatomy needs to be explored. Similarly, it will be interesting to unravel how these different lateral roots develop and how their formation is controlled by environmental factors. Whilst the molecular mechanism controlling lateral root development has been extensively studied in the model plant *Arabidopsis thaliana* (see Lavenus *et al*., 2013 for review), how these mechanisms are modified to form different types of lateral roots in Monocots is completely unknown.

Root phenotyping of different pearl millet inbred lines revealed a high variability for two root traits within the panel, consistent with an earlier study (Brück, *et al.*, 2003). Here we showed that this variability was also visible *in vitro* at a very early stage of growth (6 DAG). This finding together with the high heritability of the primary root length could be exploited to identify the genetic determinants of primary root growth, a potentially beneficial root trait for pearl millet early establishment. For instance, screening of natural variability of the primary root length have been done at the cellular level in *Arabidopsis thaliana* and led to the

identification of a root meristem regulator gene (Meijón *et al.*, 2014). Beside, it will be interesting to exploit the large diversity we observed for primary root growth to test the adaptive value of this character for early drought stress tolerance. In conclusion, our analysis opens the way to dissecting the genetic determinants controlling key root phenes and the characterization of their impact on yield and stress tolerance in pearl millet.

1.5 Author contributions

SP, PG, DW, JLV, YV, YG, BM, LL designed the study. SP, FG, DM, ML, SG, BMO, JA, MNB, LL performed the experiments. SP, ML, SG, BMO, MJB, DW, JLV, YG, BM, LL analyzed the data. SP, JLV, YG, LL wrote the paper. All authors read and approved the manuscript.

1.6 Conflict of interest statement

The authors declare that the research was conducted in the absence of any commercial or financial relationships that could be considered as a potential conflict of interest.

1.7 Acknowledgments

This work was funded by IRD, Cirad, the French Ministry for Research and Higher Education (PhD grant to SP) and the NewPearl grant funded in the frame of the CERES initiative by Agropolis Fondation (N° AF 1301-015 to LL, as part of the "Investissement d'avenir" ANR-l0-LABX-0001-0l) and by Fondazione Cariplo (N° FC 2013-0891). We also acknowledge the support of Agropolis Fondation (project N° 1404-001, as part of the "Investissement d'avenir" ANR-l0-LABX-0001-0l to LL), the Bill and Melinda Gates Foundation (2013 AWARD fellowship to MNB) and European Research Council Advanced Grant funding (294729: "FUTUREROOTS") to MJB, DMW and JAA. Root phenotyping experiments at the University of Nottingham were supported by a grant from the European Plant Phenotyping Network (EPPN Pearl project to LL).

1.8 References

Atkinson, J. A., Wingen, L. U., Griffiths, M., Pound, M. P., Gaju, O., Foulkes, M. J., et al. (2015). Phenotyping pipeline reveals major seedling root growth QTL in hexaploid wheat. J. Exp. Bot. doi:10.1093/jxb/erv006.

Bationo, A., Kihara, J., Vanlauwe, B., Waswa, B., and Kimetu, J. (2007). Soil organic carbon dynamics, functions and management in West African agro-ecosystems. Agric. Syst. 94, 13–25. doi:10.1016/j.agsy.2005.08.011.

Berg, A., De Noblet-Ducoudré, N., Sultan, B., Lengaigne, M., and Guimberteau, M. (2013). Projections of climate change impacts on potential C4 crop productivity over tropical regions. Agric. For. Meteorol. 170, 89–102. doi:10.1016/j.agrformet.2011.12.003.

Brück, H., Sattelmacher, B., and Payne, W. A. (2003). Varietal differences in shoot and rooting parameters of pearl millet on sandy soils in Niger. Plant Soil 251, 175–185.

FAO (Food and Agriculture Organization of the United Nation) (2014). FAOSTAT database. Available at: http://faostat3.fao.org/browse/Q/*/E.

Guigaz, M. (2002). Memento de l'Agronome. Quae eds. CIRAD-GRET and Ministère des Affaires Etrangères.

Henry, S., Divol, F., Bettembourg, M., Bureau, C., Guiderdoni, E., Périn, C., et al. (2016). Immunoprofiling of Rice Root Cortex Reveals Two Cortical Subdomains. Front. Plant Sci. 6, 1–9. doi:10.3389/fpls.2015.01139.

Hetz, W., Hochholdinger, F., Schwall, M., and Feix, G. (1996). Isolation and characterization of rtcs, a maize mutant deficient in the formation of nodal roots. Plant J. 10, 845–857. doi:10.1046/j.1365-313X.1996.10050845.x.

Hoagland, D. R., and Arnon, D. I. (1950). The Water-Culture Method for Growing Plants without Soil. Calif. Agric. Exp. Stn. Circ. 347.

Hochholdinger, F., Park, W. J., Sauer, M., and Woll, K. (2004). From weeds to crops: Genetic analysis of root development in cereals. Trends Plant Sci. 9, 42–48. doi:10.1016/j.tplants.2003.11.003.

Hochholdinger, F., and Tuberosa, R. (2009). Genetic and genomic dissection of maize root development and architecture. Curr. Opin. Plant Biol. 12, 172–177. doi:10.1016/j.pbi.2008.12.002.

Lartaud, M., Perin, C., Courtois, B., Thomas, E., Henry, S., Bettembourg, M., et al. (2014). PHIV-RootCell: a supervised image analysis tool for rice root anatomical parameter quantification. Front. Plant Sci. 5, 790. doi:10.3389/fpls.2014.00790.

Lavenus, J., Goh, T., Roberts, I., Guyomarc'h, S., Lucas, M., De Smet, I., et al. (2013). Lateral root development in Arabidopsis: Fifty shades of auxin. Trends Plant Sci. 18, 1360–1385. doi:10.1016/j.tplants.2013.04.006.

Lobet, G., Pagès, L., and Draye, X. (2011). A novel image-analysis toolbox enabling quantitative analysis of root system architecture. Plant Physiol. 157, 29–39. doi:10.1104/pp.111.179895.

Lynch, J. P. (2011). Root Phenes for Enhanced Soil Exploration and Phosphorus Acquisition: Tools for Future Crops. Plant Physiol. 156, 1041–1049. doi:10.1104/pp.111.175414.

Meijón, M., Satbhai, S. B., Tsuchimatsu, T., and Busch, W. (2014). Genome-wide association study using cellular traits identifies a new regulator of root development in Arabidopsis. Nat. Genet. 46, 77–81. doi:10.1038/ng.2824.

Muller, B., Stosser, M., and Tardieu, F. (1998). Spatial distributions of tssue expansion and cell division rattes are related to irradiance and to sugar content in the growing zone of maize roots. Plant. Cell Environ. 21, 149–158.

Neufeld, H. S., Durall, D. M., Rich, P. M., and Tingey, D. T. (1989). A rootbox for quantitative observations on intact entire root systems. Plant Soil 117, 295–298.

Oumar, I., Mariac, C., Pham, J.-L., and Vigouroux, Y. (2008). Phylogeny and origin of pearl millet (Pennisetum glaucum [L.] R. Br) as revealed by microsatellite loci. Theor. Appl. Genet. 117, 489–97. doi:10.1007/s00122-008-0793-4.

Pahlavanian, A. M., and Silk, W. K. (1988). Effect of Temperature on Spatial and Temporal Aspects of Growth in the Primary Maize Root. Plant Physiol. 87, 529–532.

Pritchard, J., Tomos, A. D., and Wyn Jones, R. G. (1987). Control of Wheat Root Elongation Growth. J. Exp. Bot. 38, 948–959.

R Development Core Team (2008). R: A language and environment for statistical computing. R Foundation for Statistical Computing, Vienna, Austria Available at: http://www.r-project.org.

Rebouillat, J., Dievart, A., Verdeil, J. L., Escoute, J., Giese, G., Breitler, J. C., et al. (2009). Molecular genetics of rice root development. Rice 2, 15–34. doi:10.1007/s12284-008-9016-5.

Saïdou, A. A., Mariac, C., Luong, V., Pham, J. L., Bezançon, G., and Vigouroux, Y. (2009). Association studies identify natural variation at PHYC linked to flowering time and morphological variation in pearl millet. Genetics 182, 899–910. doi:10.1534/genetics.109.102756.

Scheres, B., Wolkenfelt, H., Willemsen, V., Terlouw, M., Lawson, E., Dean, C., et al. (1994). Embryonic origin of the Arabidopsis primary root and root meristem initials. Development 2487, 2475–2487. doi:10.1038/36856.

Souci, S. W., Fachmann, W., and Kraut, H. (2000). Food composition and nutrition tables. 6th editio. Medpharm Scientific Publishers Stuttgart.

Tolivia, D., and Tolivia, J. (1987). Fasga : a new polychromatic method for simultaneous and differential staining of plant tissues. J. Microsc. 148, 113–117.

United Nations Statistics Division (2016). UNData. Available at: http://data.un.org/Data.aspx?q=population&d=PopDiv&f=variableID%3a12.

Watt, M., Magee, L. J., and McCully, M. E. (2008). Types, structure and potential for axial water flow in the deepest roots of field-grown cereals. New Phytol. 178, 135–146. doi:10.1111/j.1469-8137.2007.02358.x.

Root type	Root diameter (µm)	Stele diameter (µm)	# metaxylem vessels	Metaxylem vessel diameter (µm)	n
Primary root	429 ± 103 [ab]	181 ± 34 [b]	1	58 ± 11 [a]	10
Crown root	517 ± 76 [a]	229 ± 54 [a]	3	56 ± 9 [a]	8
LR type 1	112 ± 27 [d]	32 ± 8 [e]	0	NA	14
LR type 2	264 ± 22 [c]	74 ± 9 [d]	1	16 ± 2 [b]	7
LR type 3	367 ± 66 [b]	145 ± 16 [c]	1	50 ± 6 [a]	12

Table 1-1 : Anatomical features of the different root types in pearl millet. Mean and standard deviation of all sections. Letters correspond to groups formed by Tukey's Honest Significant Difference test (alpha = 0.05). n: sample size.

2. Comparison of early root system development in two contrasted pearl millet inbred lines

2.1 Material and Methods

2.1.1 Plant material

Two lines were selected among the inbred panel described in part 1 according to three root traits evaluated in the high-throughput phenotyping (**Table 1-2**). Line LCICMB1 (109 in the panel) showed high length of primary root at 6 DAG, large numbers of crown roots and lateral roots per plant. On the opposite, line ICMB 98222 (57 in the panel) showed low values for these three traits. Another selection criterion was the high number of individuals phenotyped for these two lines during the experiment, ensuring a good representativeness of the values relative to the line.

LCICMB 1 was derived by selfing from Nigerian landraces and selected for downy mildew resistance. It is dwarf, long-headed and medium-early in maturity, with a moderate level of photoperiod sensitivity. ICMB 98222 was bred in India from Togolese landrace.

Line	No. of plants	Primary root length (cm) Mean (sd)	No. of crown root Mean (sd)	No. of lateral root Mean (sd)
57	46	10.3 (6.4)	0.17 (0.68)	3.1 (3.9)
109	76	20.2 (8.6)	0.54 (1.1)	14.1 (14.3)

Table 1-2: Means and standard deviations –s.d.- of the root traits of the two contrasted lines selected

2.1.2 Root phenotyping

Seeds belonging to both lines were individually weighted and sterilized before germination. Plants were then phenotyped in rhizotrons following the protocol detailed in Passot et al. (2016). After 11 days of growth, rhizotrons were opened and aerial and root parts were collected. Leaves were scanned and leaf area measured using ImageJ (Schneider et al., 2012). Shoot and root biomasses were estimated after 72 hours of dehydration at 70°C.

2.1.3 Statistics

Differences of mean trait values between the two lines were assessed using Student's t-tests.

2.2 Results

2.2.1 Root system development

Detailed results for line 109 are presented in Passot et al. (2016). This part focuses on the differences existing between the lines 109 and 57. Primary root growth rate followed the

same dynamics for the two lines, with a maximum at 6 DAG followed by a plateau (**Figure 1-9A**). Line 109 had significantly higher primary root growth rates ($p < 0.01$) at all times.

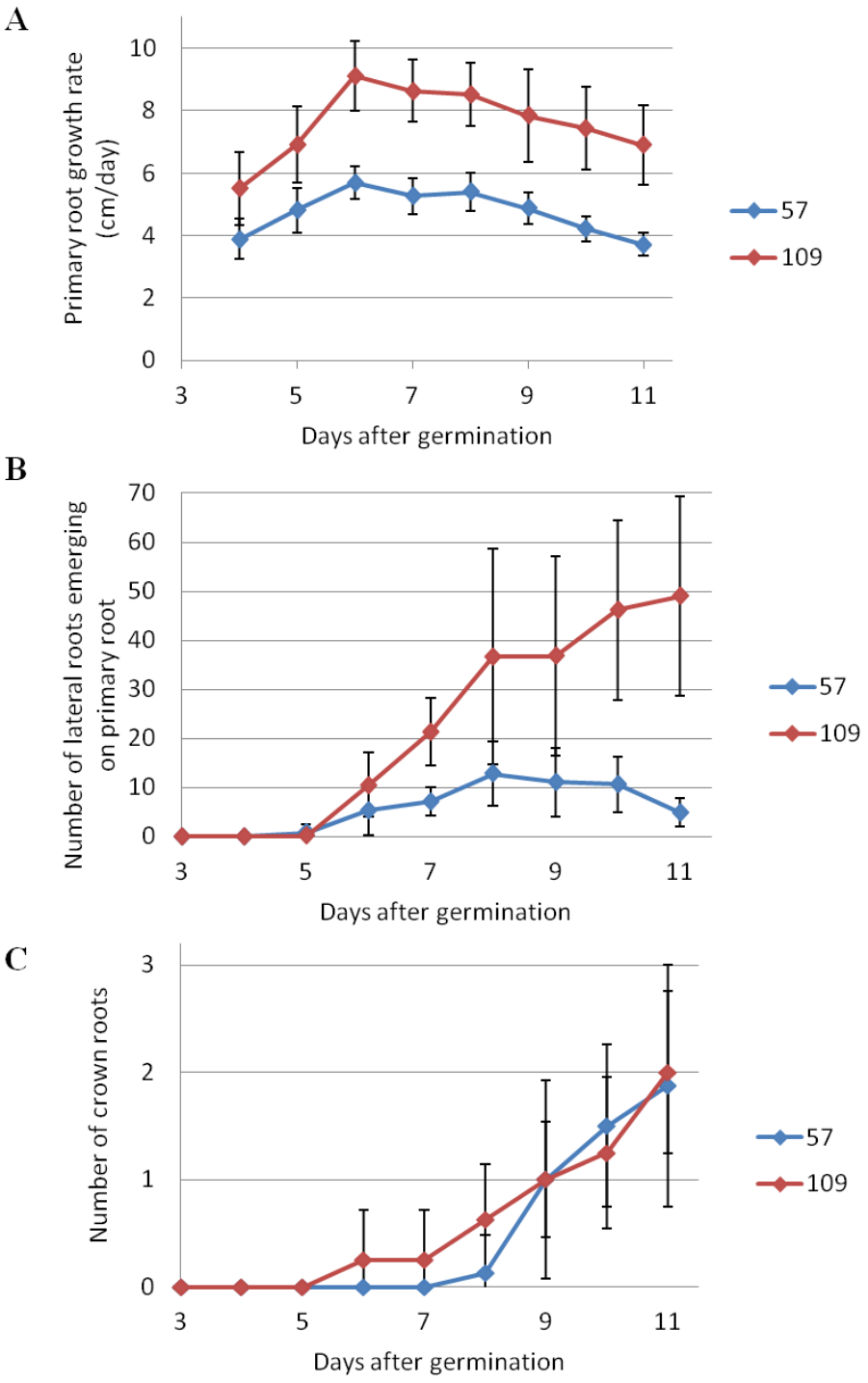

Figure 1-9: A: Daily average primary root growth rate for line 57 and 109. B: Daily cumulative number of lateral roots along the primary root for line 57 and 109. C: Daily cumulative number of crown roots for line 57 and 109. N = mean +/- standard deviation.

Lateral root emergence rates show different profiles for the two lines. The number of lateral roots emerging on the primary root for line 109 increased all along the experiment duration whereas emergence rate for line 57 increased up to 8 DAG, before decreasing up to

the end of the experiment (**Figure 1-9B**). Emergence rate was significantly higher for line 109 ($p < 0.05$) at all days between 7 and 11 DAG. The number of crown roots showed very similar profiles for the two lines (**Figure 1-9C**). The number of emerged lateral roots observed in rhizotron at 6 DAG was consistent with the numbers observed in pouches. The numbers of emerged crown roots at 6 DAG in rhizotron were very low, which is also consistent with the numbers found in pouches.

2.2.2 Other biological traits

Leaf areas were significantly different between the two lines ($p < 0.01$), as well as shoot biomasses ($p < 0.05$) and root biomasses ($p < 0.01$) (**Table 1-3**). Average seed weights were significantly different between the two lines ($p < 0.01$), but there was no significant correlation between individual seed weight and final primary root length among each line ($p = 0.20$ for line 57 and $p = 0.57$ for line 109) (**Figure 1-10**).

Line	Leaf area (cm²)	Shoot biomass (mg)	Root biomass (mg)
57	819 (224)	24.6 (6.4)	6.9 (1.0)
109	1172 (220)	31.9 (6.3)	13.0 (3.1)

Table 1-3: Physical parameters after harvest for the two lines. Means and standard deviations.

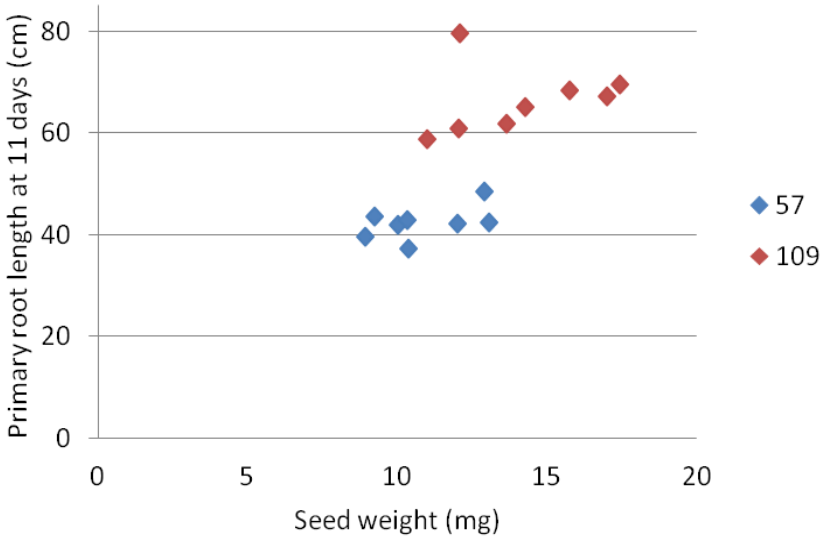

Figure 1-10: Individual seed weight against final primary root length for line 57 and 109

2.3 Discussion

Two inbred lines were selected for their contrasted root phenotypes measured on pouches during the high-throughput phenotyping. This finer phenotyping experiment confirmed the differences between the two lines, with line 109 having a faster growing primary root and more lateral roots than line 57. On the contrary, crown root phenotypes were similar for the two lines during this experiment. However, as the experiment ended just at the beginning of crown root formation, differences in crown root number might appear later. The

two lines should be grown during a longer period to assess whether their crown root phenotypes are different or similar on a longer term. If crown root phenotypes appear similar, a comparison of these two lines in the field or under a drought stress would provide very interesting information on the role of primary root and lateral roots. Indeed, it would able to compare two lines with different primary root and lateral root phenotypes but similar crown root phenotypes.

We were interested in finding the biological explanations for such differences between the two lines. There is no apparent compromise between primary root elongation and lateral root initiation, as line 109 has the highest values for both these traits. Such compromise between root growth in depth and branching has been found in maize, where smaller lateral root density was associated to deeper rooting and greater drought tolerance in the field (Zhan et al., 2015). This greater "vigor" for line 109 was associated with a higher average seed weight compared to line 57. However, individual seed weights were not correlated with initial primary root growth within each line. This suggests that a higher seed weight might not be the only factor responsible for this greater early vigor. Line 109 also showed higher leaf area and shoot biomass.

The fine phenotyping of these two lines will be used to extract root development parameters to develop functional-structural models of root development in those two contrasted lines (A. Ndour PhD thesis). In fact, modeling is a way to assess the role of different morphological and physiological root parameters on plant functioning, particularly water uptake (Xu et al., 2011). This can be done by using sensitivity analysis approaches (York et al., 2016). Here, the two studied lines have contrasted architectural root traits, but further experiments should be performed to assess whether they also differ in terms of anatomy. Indeed, root anatomical traits can greatly influence water acquisition (Lynch et al., 2014). A model was already designed and implemented to study water uptake in a young root system, based on the data measured on line 109 (**Figure 1-11**). This model takes into account the root system architecture and the hydraulic properties of the root system. The data acquired with the phenotyping in rhizotrons and the histological sections were used to parameterize the model, together with hydraulic conductivities estimated with a pressure chamber (Javot et al., 2003). After validation, the model will be used to test the impact of differential root growth and branching on water acquisition *in silico*, using the contrasted architectural parameters of lines 57 and 109. The predicted differences will be validated experimentally with soil water potential measurements as predictors of water fluxes in the soil (Doussan et al., 2002).

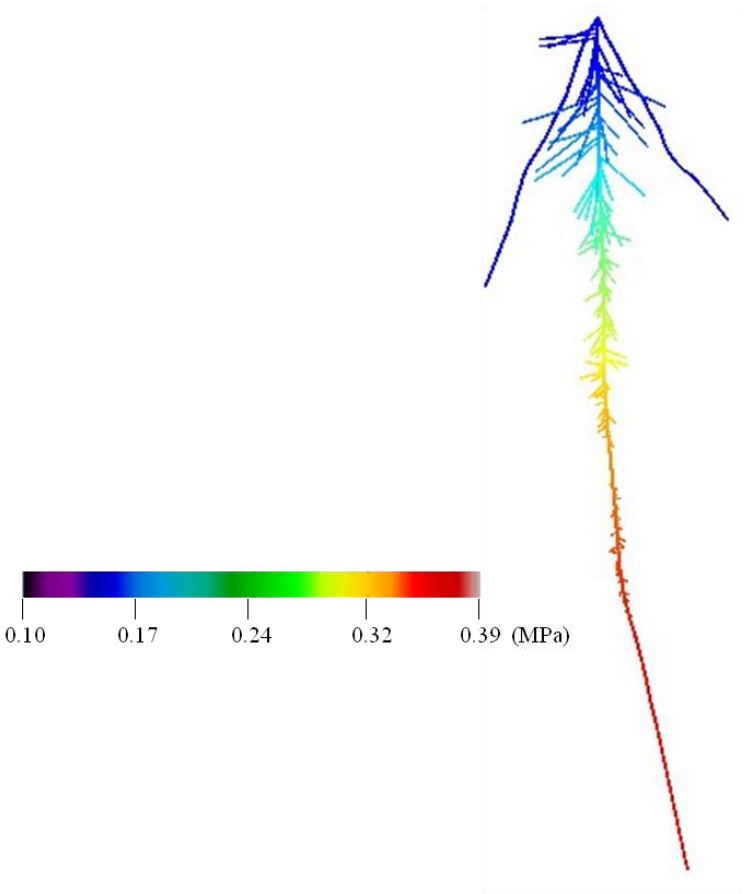

Figure 1-11: Simulation of water potentials using the first FSPM of pearl millet root system hydraulics. (Adama Ndour)

3. Impact of drought stress and mycorrhization on early root system development assessed by X-ray microcomputed tomography

An experiment was set up to test whether pearl millet root system development changes in response to drought. Different protocols exist to monitor precisely drought, for example supplementing a hydroponic growth medium with polyethylene glycol to decrease the nutrient solution water potential by increasing osmotic pressure, without changing ion availability for the plant (Lagerwerff et al., 1961). We chose to simply reduce soil water content when growing plants in pot. Mycorrhization with symbiotic fungi as *Rhizophagus irregularis* is supposed to help plants tolerate drought stress (Jayne and Quigley, 2014). We therefore tested whether mycorrhization had an effect on root system architecture, especially in a context of drought stress.

3.1 Material and methods

Pearl millet line LCICMB 1 was used in this experiment. The seeds were surface-sterilized by a 2 minute immersion in 10% hypochlorous acid followed by 2 minutes in 70% ethanol. Each bath was followed by 3 rinses in deionised water. Then the seeds were germinated in Petri dishes at 30°C in the dark for 24 hours. Germinated seedlings were transferred to pots (50 mm diameter and 120 mm height) containing "Newport Series Loamy Sand" soil (sand 83.2%, silt 4.7%, and clay 12.1%; organic matter 2.93%; pH = 7.13; Nitrate = 5.48 mg.L^{-1}; Phosphorus = Defra index of 3 (29.65 mg kg^{-1})) one DAG. Half of the soil was inoculated with spores of *Rhizophagus irregularis*. Spores originated from 3 Petri dishes containing transformed carrot roots, cultivated on phytagel at room temperature (20°C) until the hyphae covered all the dishes. Presence of spores was assessed using a stereomicroscope and phytagel was dissolved in sodium citrate solution (10 mM, pH = 6) at 35°C to retrieve hyphae bearing the spores. Retrieved fungus material was rinsed with sterile watered and stored until inoculation. This was done by mixing the spores with 4.5 kg of soil. Half of the plants were maintained throughout the experiment at a soil water content of ~26% (w:w), which corresponds to 75% of field capacity. The other half was maintained at a SWC of ~9% (w:w) corresponding to 25% of field capacity. Overall, 4 treatments were tested on 6 plants each: well-watered without inoculation, well-watered with inoculation, drought-stressed without inoculation and drought-stressed with inoculation The SWC was monitored daily by weighing the pots. Plants were scanned with a v|tome|x M scanner (Phoenix/GE Systems), with a maximum energy of 240 kV, 4 times over a 18 days period (4, 8, 14 and 18 DAG) to image the root structure. Two days after the last scan, the aerial parts of the plants were collected, oven dried during 72 hours and weighted. The root system of each plant was washed and fixed at 95°C in a 10% KOH solution. The roots were then rinsed with water and stored in a 10% acetic acid solution. They were dyed 3 minutes at 90°C in a staining solution containing 5% Schaffer ink and 5% acetic acid to stain mycorrhizal (fungal) structures (Vierheilig et al., 1998). The roots were rinsed with water and stored at 4°C in Petri dishes before observation. The observations were made with a stereomicroscope (Zeiss).

Root systems were segmented manually from the image stacks produced by the scanner using the VGStudio Max software (Volume Graphics GmbH). In order to extract some

information about the nutrient harvesting performance of different root systems, we wrote a Python script to compute the volume of soil exploited by the 3D root architectures obtained (Appendix 1-1). We considered 3 distances (3 mm, 12 mm and 50 mm) that correspond to resources with poor (e.g. phosphate ions), intermediate (e.g. potassium) and high (e.g. nitrate or water) mobility in the soil (Pagès, 2011). Our script allowed us to compute the soil volume exploited globally and at different depths.

3.2 Results

3.2.1 General considerations

The main objective of this experiment was to study a root system growing in 3 dimensions in a real soil using microcomputed tomography. The opportunity to study plants in a real soil allowed us to grow them in conditions impractical for *in vitro* studies: soil inoculated with an arbuscular mycorrhiza and drought. We wanted to have 3D data on plants growing in soil and to compare them between different conditions. The general results obtained for well-watered plants are described in Part 1. We observed that, as pearl millet has a rapid root growth, the limited pot volume was rapidly limiting root growth. Indeed, primary and crown roots touched the pot side shortly after emergence and stayed in contact with the pot side while growing after that moment. At the bottom of the pot, soil was maintained by a thin sieve roots could not go through. At that point, roots thickened and changed direction to grow horizontally. Interestingly, in some high-resolution scans we were able to observe the presence of aerenchyma in some roots (**Figure 1-12**).

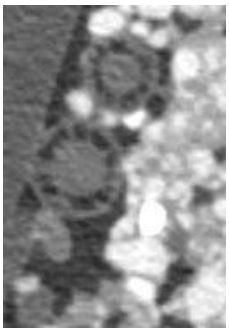

Figure 1-12: Enlargement of X-ray image showing 2 pearl millet roots observed transversally. Aerenchyma is visible in the cortex of the roots.

3.2.2 Effect of drought treatment on root development

The explored soil volumes at different depths were computed with a dedicated Python script (**Figure 1-13**). There was no significant difference between the two treatments if we considered the whole soil volume. When separated in different depth, differences ($p < 0.05$) in explored soil volumes appeared:

At 14 DAG, in the 30-60 mm horizon, for a foraging distance of 3 mm,

At 8 DAG, in the 60-90 mm horizon, for the foraging distance of 12 mm,

At 8 DAG, in the 60-90 and 90-end horizons, for the foraging distance of 50 mm.

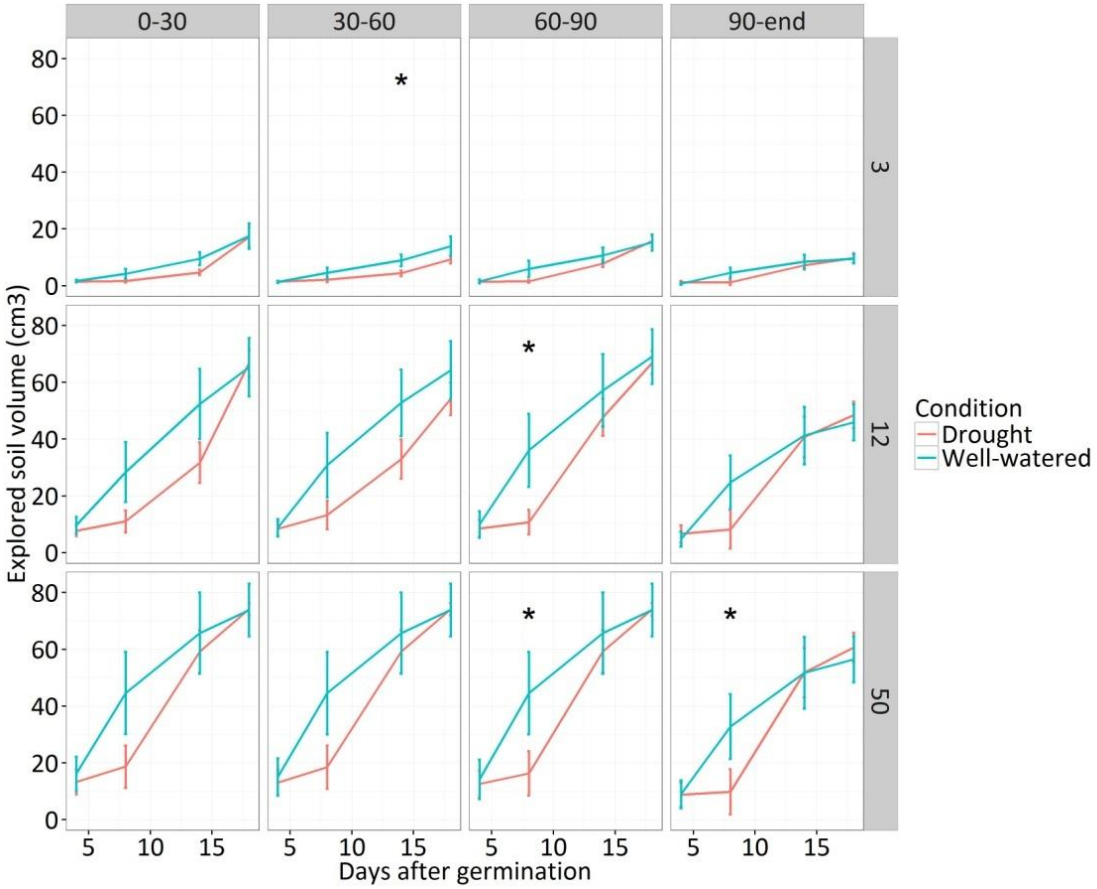

Figure 1-13: Calculated soil volumes explored by the root system at 3 distances and 4 depths in two culture conditions. N = mean +/- standard deviation. *: significant difference between drought-stressed and well-watered plants ($p < 0.05$)

At later time points, the soil volume explored by drought-stressed plants systematically caught up with the soil volume explored by well watered-plants. Comparison of root systems at different time points for well-watered and drought-stressed plants confirm that root growth is first inhibited between 4 and 8 DAG and then is stimulated in response to drought (**Figure 1-14**). We did not observe any difference in the number of crown roots between the root system of drought-stressed versus well-watered plants. The drought-stressed plants presented a significantly reduced shoot biomass 20 days after germination ($p < 0.05$) (**Figure 1-15**).

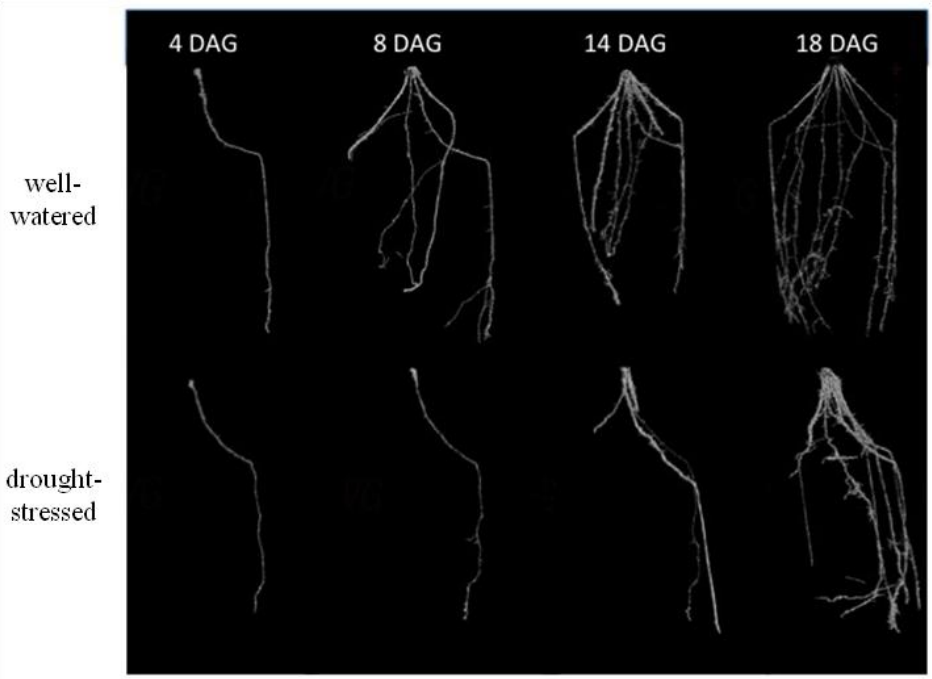

Figure 1-14: Comparison of the root system architectures of a well-watered and a drought-stressed pearl millet plant using X-Ray CT: 2D projections of 3D images. Images at 4, 8, 14, and 18 DAG (days after germination).

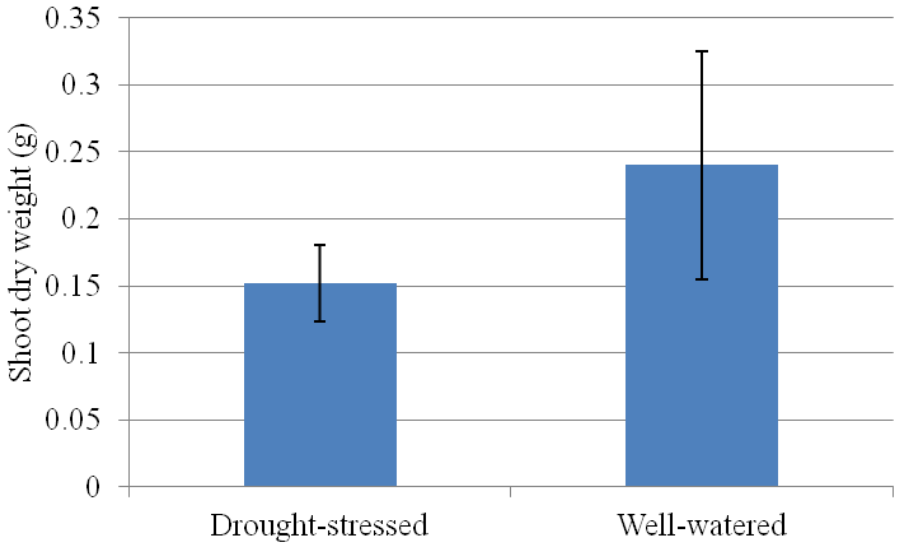

Figure 1-15: Shoot dry weights after 20 days of growth of plants grown in drought stressed or well-watered conditions. N = mean +/- standard deviation.

3.2.3 Effect of soil inoculation

Soil inoculation with *Rhizophagus irregularis* spores was meant to assess whether mycorrhization has an effect on root system architecture, especially in the case of drought stress. The observation of stained roots did not allow to observe any mycorrhization, either in the inoculated or not inoculated treatment.

3.3 Discussion

We used X-ray tomography to analyse pearl millet root system growth in soil and its response to drought stress and interaction with the arbuscular mycorrhizal fungus *R. Irregularis*. We observed a temporary reduction of the soil volume explored by the root system in response to water deficit, depending on the distance studied and the depth. This suggests that after an early inhibition of root growth by drought between 4 and 8 DAG, root growth was stimulated at later stages to reach similar soil exploration at 18 DAG. Another option is that due to the small volume of the pot, the root growth of well-watered plants is restrained and the explored soil volume stabilizes. This root growth seems to be homogeneous in depth and not limited to a certain soil depth. Together with the reduced shoot biomass, this suggests a reallocation of resources for root growth in conditions of drought stress. However, these conclusions are to be taken cautiously and need to be confirmed by other approaches due to the limited soil volume used in the experiment and the limited number of samples.

It appeared that the drought imposed to half of the seedling was too strong regarding their developmental stage, leading to the death of a large number of seedlings. In fact, the soil dried very quickly in small pots and many drought-stressed seedlings dehydrated and died. Future drought stress experiment should allow the seedling to be in a wet environment for a few days after germination, to prevent this plant loss. Because of this, the experiment was conducted on fewer repetitions than what was initially planned.

We wanted to test the effect of the inoculation of the arbuscular mycorrhiza *Rhizophagus irregularis* but the experiment did not allow to see any effect of inoculation. Very few fungi were found in the roots after staining and, due to the absence of sterilization for the soil, they were found in the two inoculation treatments (with or without). We hypothesize that the duration of the experiment (20 days) was too short to see an effect of inoculation on root development. Indeed, arbuscular mycorrrhizal infection was reported to be low up to 30 days after germination in wheat, barley and rye, becoming significantly noticeable only 45 days after germination (Castillo et al., 2012). However, another study stated that mycorrhization was established 36 days after germination in wheat and that mycorrhizal fungi participated very significantly in P uptake at this stage, even without any difference in plant biomass (Li et al., 2006). This indicates that mycorrhization could be beneficial at early stages even if no effect was detected in our experiment and supports the interest of studying the effect of arbuscular mycorrhizal fungi on pearl millet, which is frequently cultivated in soils with low available phosphate.

There is still no automation for root system segmentation from the stack of images generated by the scanner. The image analysis is therefore a time consuming and tedious manual process, compromising any scaling of this particular experimental setup for high-throughput phenotyping. Moreover, the scan definition was not sufficient to detect all lateral roots, and in particular thin ones which represent 80% of pearl millet lateral root were not detected (see **Chapter 2**). This may be improved by a fine contrast adjustment associated with adequate image treatment. The development of an algorithm for automatic segmentation of roots from soil scans will be compulsory for high-throughput use of this technique. Other three dimensional imaging techniques, like magnetic resonance imaging (MRI), might also skirt this segmentation issue (van Dusschoten et al., 2016).

Chapter 2

Spatio-temporal analysis of early root system development in two cereals, pearl millet and maize, reveals three types of lateral roots and a stationary random branching pattern along the primary root

The work presented here has been done in collaboration with the Laboratoire d'Ecophysiologie des Plantes sous Stress Environementaux (LEPSE). Two PhDs were conducted in parallel with one common advisor and we chose to develop a comparative study of two cereal species, pearl millet (my PhD) and maize (PhD of Beatriz Moreno Ortega, LEPSE). Protocols for plant culture and anatomical analyses have been shared between species and a single pipeline has been designed for analyzing the phenotyping data of the two species. This permitted to benefit from synergic effects of shared work and to compare two cereals grown and analyzed in the same conditions.

This chapter is a manuscript in a pre-submission format. It has been written following submission guidelines of the focused journal and the results and discussion sections are therefore presented before the material and methods section.

Authors contributions

Sixtine Passot contributed to all the experiments concerning pearl millet, except histological sections, analyzed the data and wrote the manuscript.
Beatriz Moreno-Ortega contributed to all the experiments concerning maize, except histological sections, analyzed the data and wrote the manuscript.
Daniel Moukouanga performed histological sections for pearl millet and maize and contributed to plant culture for pearl millet.
Crispulo Balsera contributed to rhizotron preparation and plant culture for both species.
Soazig Guyomarc'h contributed to plant culture for pearl millet.
Mikael Lucas contributed to plant culture for pearl millet.
Guillaume Lobet updated SmartRoot and added specific functions for this study.
Laurent Laplaze designed the study and wrote the manuscript.
Bertrand Muller designed the study and wrote the manuscript.
Yann Guédon designed and implemented the statistical models, analyzed the data and wrote the manuscript.

Abstract

Recent progresses in root phenotyping focused mainly on increasing throughput for genetic studies while the identification of root developmental patterns has been comparatively underexplored. We introduce a new phenotyping pipeline for producing high-quality spatio-temporal root system development data and identifying developmental patterns within these data. This pipeline combines the SmartRoot image analysis system with statistical models for identifying developmental patterns. Semi-Markov switching linear models were applied to cluster lateral roots based on their growth rate profiles. This revealed three types of lateral roots with similar characteristics in pearl millet and maize. Correlation between these lateral root types and anatomical traits was strong for pearl millet and weak for maize. Potential dependencies in the succession of lateral root types along the primary root were then analyzed using variable-order Markov chains. The succession of lateral root types along the primary roots was neither influenced by the shootward neighbor root type nor by the distance from this root. This stationary random branching pattern was remarkably conserved despite the high variability of root systems in both pearl millet and maize. Precise recording and analysis of lateral roots spatio-temporal developmental patterns thus revealed strong similarities

between two cultivated cereals that are strongest than what anatomical comparisons would suggest.

1. Introduction

Cereal breeding has long ignored the belowground part of the plant but it is now acknowledged that root system represents an opportunity for improving plant efficiency and tolerance to abiotic stresses (Bishopp and Lynch, 2015). A better knowledge of root system structure and function is thus needed to open the way to root system improvement. Phenotyping, as the measure of plant traits in a given environment and in a reproducible manner, is one key approach to access this knowledge.

Recent progresses in plant phenotyping platforms, including plant handling automation and computer assisted data acquisition, has allowed an increase in phenotyping throughput (Fahlgren et al., 2015b). It was critical for association studies and gene discovery that benefit from the large number of plants studied in automated phenotyping system. Beside increasing throughput, another strategy chosen in some phenotyping systems is to improve on data dimensionality and structure (Dhondt et al., 2013). These systems increase the amount of data collected on a single plant, either by measuring several traits that can be of different nature, in control or special conditions, or by measuring the same trait at multiple time points to focus on physiological processes (Fahlgren et al., 2015a). Root architecture phenotyping present specific challenges as compared with phenotyping of aerial parts of plants. The root system is by nature hidden and root phenotyping systems have to make a compromise between the relevance of growth conditions and trait measurement feasibility. Most root phenotyping pipelines focus on the high throughput measurement of selected root traits on a large number of plants, with the objective of detecting QTL usable in breeding (Kuijken et al., 2015). For example, Atkinson et al. (2015) reported a phenotyping platform where root systems grew in 2D on a filter paper for a few days for QTL detection. Systems considering the 3 dimensions of root systems exist too (Iyer-Pascuzzi et al., 2010) but their objective are generally focused on QTL detection (Topp et al., 2013). The development of individual root axes during long periods of time is rarely studied, whereas temporal analyses are more developed for the aerial parts (see e.g. Lièvre et al., 2016). This kind of studies has been hampered by the difficulty of collecting individual root growth data. In addition, the analysis of structured data such as root growth rate profiles is more challenging than the analysis of simple root traits.

The variability in lateral root length among neighbor roots borne by the same root axis is a widely observed feature of root systems. It is proposed that this variability contributes to root system efficiency (Forde, 2009; Pagès, 2011). It is observed in annual as in perennial species (in oak (Pagès, 1995), in banana peach (Lecompte et al., 2005), in rubber tree (Thaler and Pagès, 1996), in sunflower (Aguirrezabal et al., 1994)) and even in the model species *Arabidopsis thaliana* (Freixes et al., 2002). It is also observed in monocots such as maize, where some studies reported a high variability among lateral root length (Jordan et al., 1993; Varney et al., 1991; Wu et al., 2016). However, most of these descriptions did not consider growth dynamically. When they did (Pagès, 1995; Thaler and Pagès, 1996), they generally considered that the variability of growth rate profiles forms a continuum but did not investigate a possible structuring into distinct classes. On the other hand, different lateral root

types have been described among cereals, but these classifications were based on anatomical traits or diameter. Four types were reported in maize (Varney et al., 1991), three in pearl millet (Passot et al., 2016) and rice (Gowda et al., 2011; Henry et al., 2016) and five in wheat, barley and triticale (Watt et al., 2008).

Here, we designed a phenotyping pipeline for producing high-quality spatio-temporal root system development data. This pipeline incorporates the SmartRoot image analysis system (Lobet et al., 2011) able to reconstruct consistent spatio-temporal data on the basis of successive snapshots of root system architecture. Our ultimate goal was the identification and characterization of root developmental patterns on the basis of these spatio-temporal data. To this end, we adopted a two-step approach. Lateral root growth rate profiles were first analyzed. This first temporal step relies on a model-based clustering of these longitudinal data using semi-Markov switching linear models; see Lièvre et al. (2016) for another application of similar statistical models. One strength of these statistical models is the capability to model growth phase lengths combining complete and censored growth rate profiles (since some lateral roots were still growing at the end of the experiment entailing growth phase censoring). This first step led us to identify lateral root types on the basis of growth rate profiles. The second spatial step thus consisted of analyzing the primary root branching pattern where the lateral roots were summarized by their types. The proposed root system phenotyping pipeline was used on two cultivated cereals, pearl millet (*Pennisetum glaucum*) and maize (*Zea mays*). Commonalities and differences between these two species regarding the growth patterns of lateral roots and the branching patterns along the primary root were investigated as well as their relation to anatomical (vessel numbers and dimensions) and morphological (apical diameter) features.

2. Results

In order to analyze early root system development and architecture in pearl millet and maize, daily images of growing root systems were recorded for 15 and 21 days respectively in a rhizotron system. The ability of SmartRoot (Lobet et al., 2011) to cross-link information corresponding to different time points was then used to build consistent spatio-temporal data of root system development and architecture on the basis of the corresponding series of images. We chose to decompose the analysis of these spatio-temporal data into two steps:

1. *temporal analysis*: we first analyzed growth rate profiles of lateral roots using dedicated statistical models for these specific longitudinal data, characterized by the short length of profiles and the high censoring level, since many lateral roots were still growing at the last date of measurement. Lateral roots were classified in three types as a byproduct or these longitudinal data analysis.

2. *spatial analysis*: The intervals between consecutive lateral roots and the succession of lateral root types along the primary root were then analyzed.

2.1 Model-based clustering of lateral root growth rate profiles reveals three growth patterns for pearl millet and maize lateral roots

2.1.1 Model building

After data curation, our dataset was composed of growth rate profiles of 1254 and 3050 lateral roots from 8 pearl millet and 13 maize plants respectively. These lateral roots were followed up to 10 and 17 days respectively after their emergence from the primary roots. The exploratory analysis of these growth rate profiles highlighted a strong longitudinal organization with growth rates either increasing or decreasing with lateral root age (**Figure 2-1**). The growth rate profiles were essentially divergent from the time origin and the growth rate dispersion increased with the lateral root age. Hence, lateral roots can be roughly ordered according to their growth rate profiles.

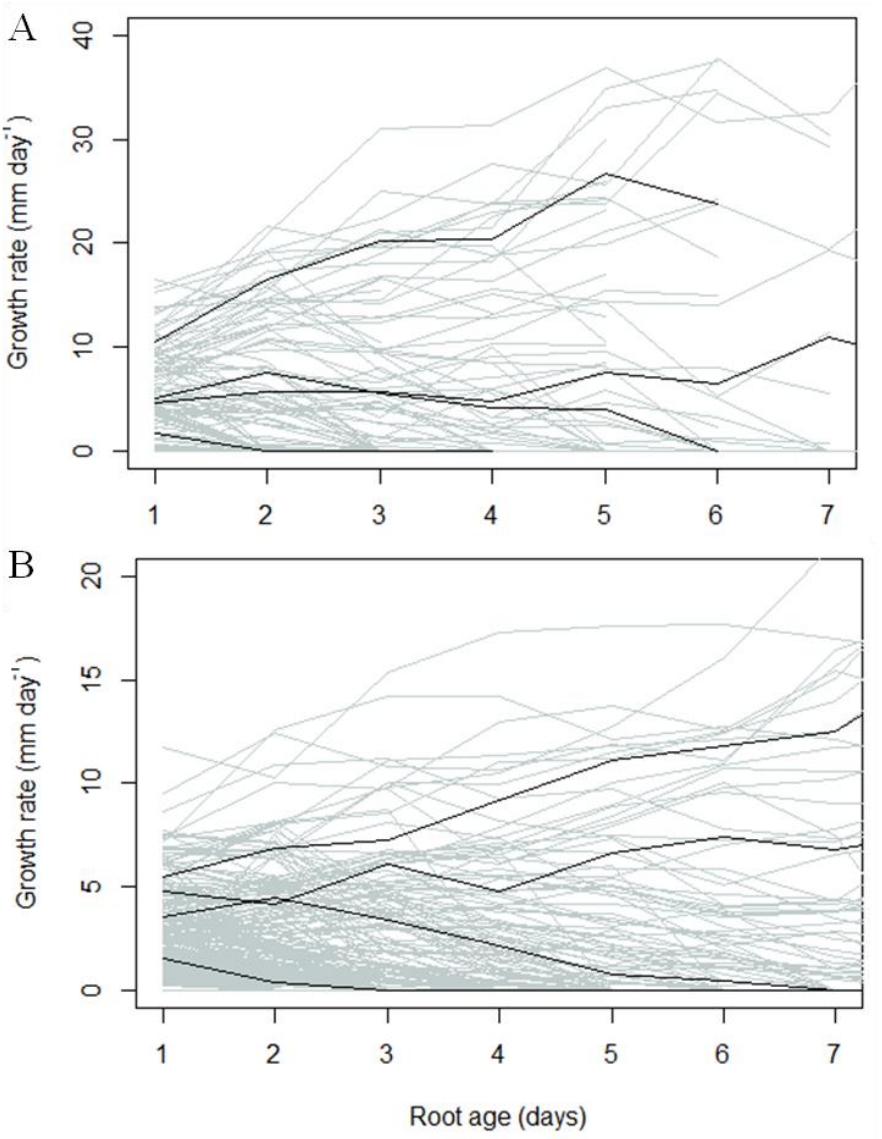

Figure 2-1: Growth rate profiles for individual lateral roots of one pearl millet (A) and one maize (B) plant. A selection of individual growth profiles have been highlighted (black lines) showing contrasted behaviors. Root age refers to the number of days following emergence.

This raises the question of a stronger structuring of these longitudinal data than a simple ranking of the lateral root growth rate profiles. We thus chose to investigate a model-based clustering approach for these longitudinal data. This raised two types of difficulties: (i) the growth rate profiles were longitudinally limited (up to 10 successive growth rates for pearl millet and up to 17 successive growth rates for maize) and (ii) the censoring level was high with a high proportion of lateral roots still growing at the end of the experiment. We thus designed a statistical model for clustering growth rate profiles, using only profiles lasting at least 5 days (corresponding to 652 lateral roots for pearl millet and 2029 for maize), based on the following assumptions:

- A growth rate profile is modeled by a single growth phase either censored or followed by a growth arrest.
- Changes in growth rate within a growth phase are modeled by a linear trend. This strong parametric assumption was a consequence of the short length of growth rate profiles. Hence, linear trend models should be viewed as instrumental models for clustering growth rate profiles rather than models for fitting each growth rate profile.

The proposed statistical model was composed of growth states, each corresponding to a lateral root growth rate profile type. A distribution representing the growth phase duration (in days) and a linear model representing changes in growth rate during the growth phase were associated with each of these growth states. Growth states were systematically followed by a growth arrest state. The overall model is referred to as a semi-Markov switching linear model (SMSLM; see **Methods and Appendix 2-1** for a formal definition and **Figure 2-2 and SupFigure 2-1** for an illustration in pearl millet and maize, respectively). This kind of integrative statistical model makes it possible to consistently estimate growth phase duration distributions combining complete and censored growth phases.

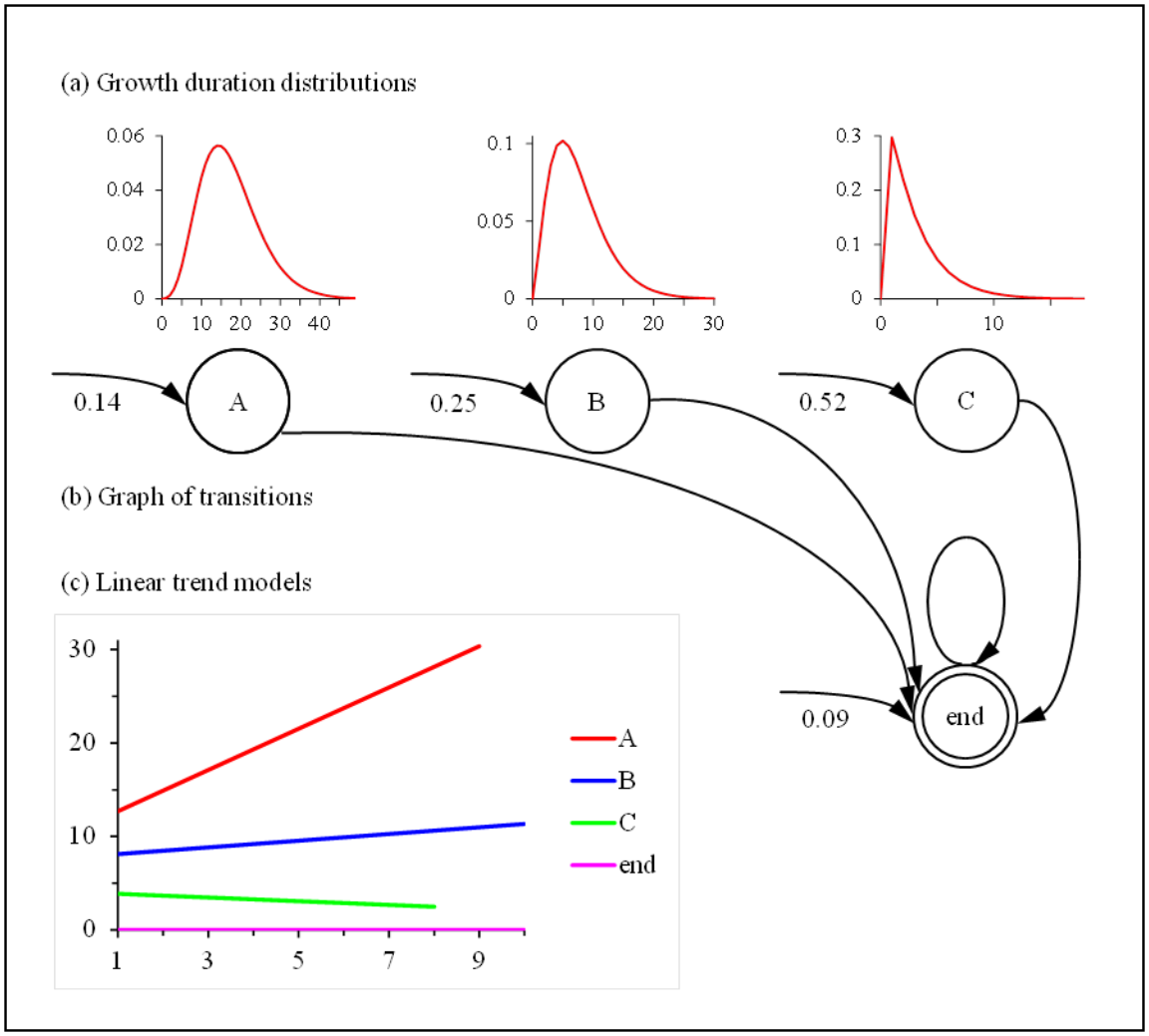

Figure 2-2: Four-state semi-Markov switching linear model estimated on the basis of pearl millet lateral root growth rate series: (a) Growth duration distributions; (b) Graph of transitions. The possible transitions between states are represented by arcs with the attached probabilities noted nearby when < 1. The arcs entering in states indicate initial states and the attached initial probabilities are noted nearby. **(c) Linear trend models estimated for each state.**

2.1.2 Selection of the number of lateral root types

We next had to define the number of growth states (i.e. the number of lateral root types). Because of the specific structure of the model where each state can be visited at most once, the usual model selection criteria such as the Bayesian information criterion do not apply. We thus had to design an empirical model selection method for selecting the number of growth states. This method detailed in **Appendix 2-2** combines the following criteria:

1. Posterior probabilities of the optimal assignment of each lateral root growth rate profile to a growth state (followed or not by the growth arrest state at a given age) i.e. weight of the optimal assignment among all the possible assignments of a given growth rate profile,
2. Comparison of location and dispersion measures of growth rate profiles for each lateral root type deduced from the optimal assignment of each lateral root growth rate profile,
3. Overlap between growth rate profiles for consecutive lateral root types.

We selected for both species 3 lateral root types that correspond to the best compromise between (i) the proportion of ambiguously assigned lateral roots, (ii) the relative dispersion of growth rate profiles for the most vigorous root type and (iii) the overlap between growth rate profiles for consecutive types.

2.1.3 Growth phases are similar in both species

Growth phase duration distributions for the three growth states estimated within the SMSLMs are shown in **Figure 2-3a** for pearl millet and **Figure 2-3b** for maize. The estimated growth phase duration distributions were very similar for the two species for each type (A, B or C), with mean growth durations of 17.3 and 15.2 days for type A, 7.6 and 6.8 days for type B and 3.2 and 3.0 days for type C for pearl millet and maize, respectively, and standard deviations equal to 7.6 and 7.7 for type A, 4.6 and 5.0 for type B, and 2.6 and 2.4 for type C. The censoring level is defined as the proportion of growth phase incompletely observed for a given lateral root type. The censoring level was computed for each growth state as a by-product of the estimation of the corresponding growth phase duration distribution within SMSLM. This censoring level takes into account all the possible assignments of growth rate profiles of length ≥ 5 incorporated in the training sample. We obtained 96% of censoring for state A, 54% for state B and 14% for state C in the case of pearl millet and 80% for state A, 36% for state B and 10% for state C in the case of maize. The growth rate profile length frequency distribution are superimposed to the estimated growth phase duration distributions shown in **Figure 2-3** to illustrate the censoring level for each species. The higher censoring level for pearl millet compared to maize was a direct consequence of the shorter growth rate profiles in average for pearl millet since the growth phase duration distributions were similar for the two species. It should be noted that the growth rate profile lengths were similar for the different lateral root types of a given species (see the corresponding cumulative distributions functions in **SupFigure 2-4**).

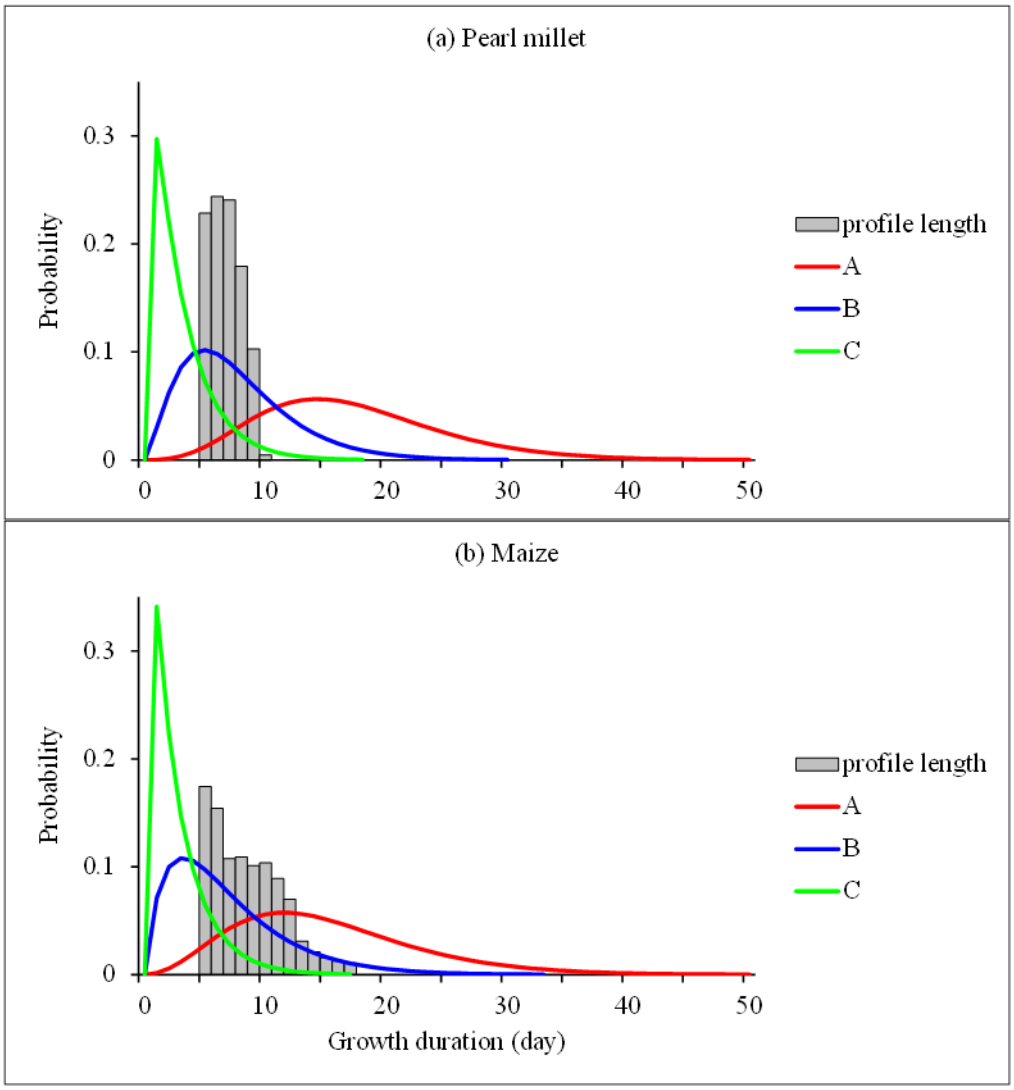

Figure 2-3: Growth duration distributions estimated within the 4-state semi-Markov switching linear model: (a) pearl millet; (b) maize. The growth rate profile length frequency distributions are drawn for illustrating the censoring level.

2.1.4 Classification of individual growth rate profiles

Only growth rate profiles of length ≥ 5 were used for the building of SMSLMs. Growth rate profiles of length < 5 were then assigned *a posteriori* to classes using the previously estimated SMSLM.

Daily median growth rate and associated mean absolute deviation for each class are shown in **Figure 2-4a and b** for pearl millet and maize respectively. In both species, daily median growth rate were divergent between the three types of lateral roots. Median growth profiles for type B and type C reached 0 mm day^{-1} by 7-8 and 3 days respectively, while type A median growth rate stayed positive and did not decrease in both species. The main difference between the two species, apart from different absolute growth rates, concerned type B lateral roots, where median growth rate stayed nearly constant up to day 5 in pearl millet whereas it started to decrease straight after emergence in maize, and type A lateral root, where median growth rate kept on increasing in pearl millet whereas it stabilizes after a few days in maize. Variability existed around these median profiles for each type. Mean absolute

deviations were rather similar between the two species for types B and C. Because the temporal sequences were longer in maize, we could observe a regular increase of mean absolute deviation with root age for type A, up to reaching nearly the same level as median growth rate at day 13. This is due to the presence in this class of lateral roots whose growth rate started to decrease at later stages while some lateral roots continued to increase their growth rate.

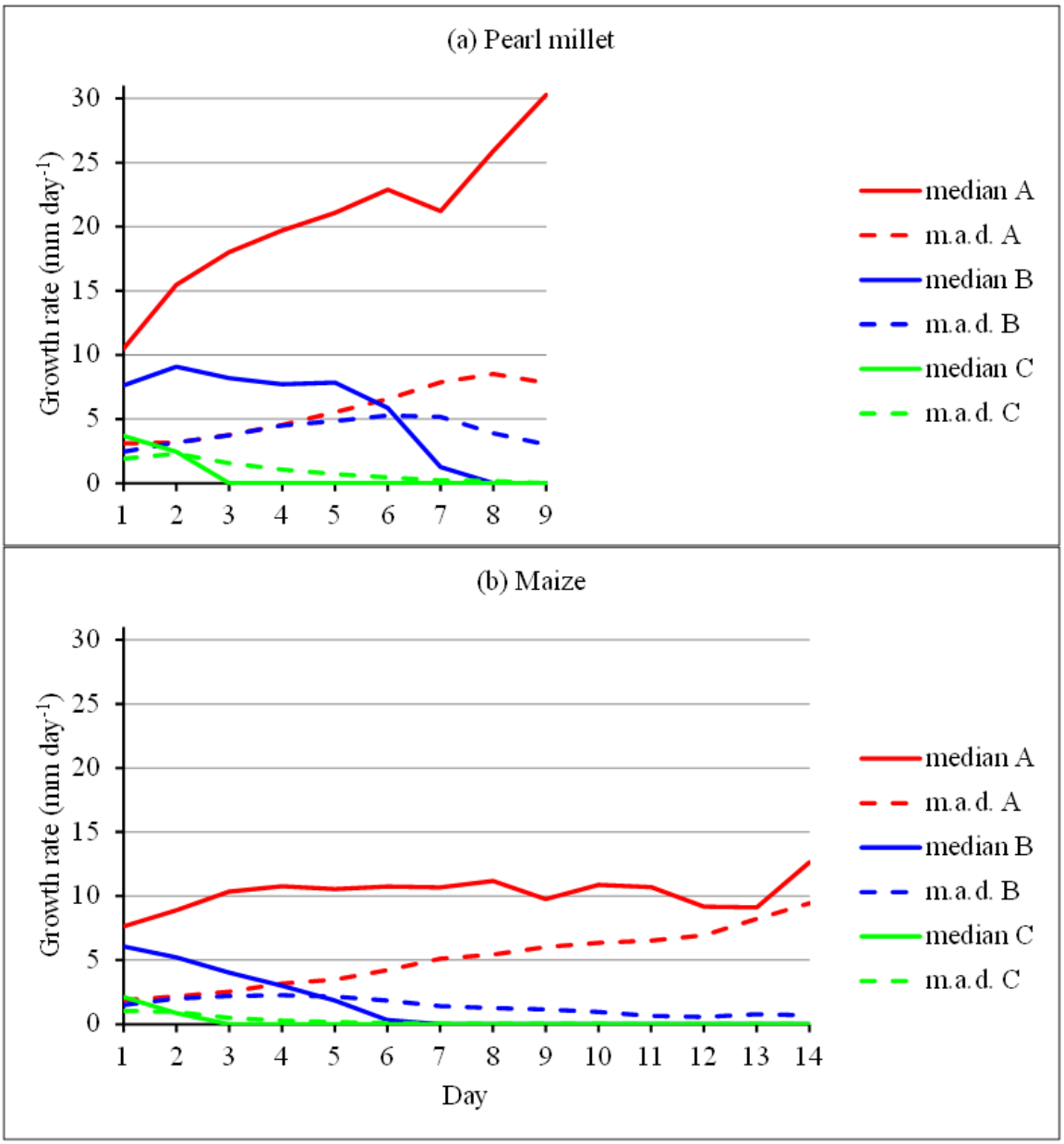

Figure 2-4: Daily median growth rate (and associated mean absolute deviation −m.a.d.−) for (a) pearl millet and (b) maize.

The growth rate profiles of all the lateral roots of a selected pearl millet and a selected maize plant colored according to the class they were assigned to are presented in **Figure 2-5**. This shows the variability of growth rate profiles within a class, the overlap between classes and the censoring level of growth rate profiles. Growth characteristics of the three lateral root types were very similar between maize and pearl millet. The main differences between maize and pearl millet root growth rate profiles concerned the absolute values of growth rates which were higher in pearl millet compared to maize.

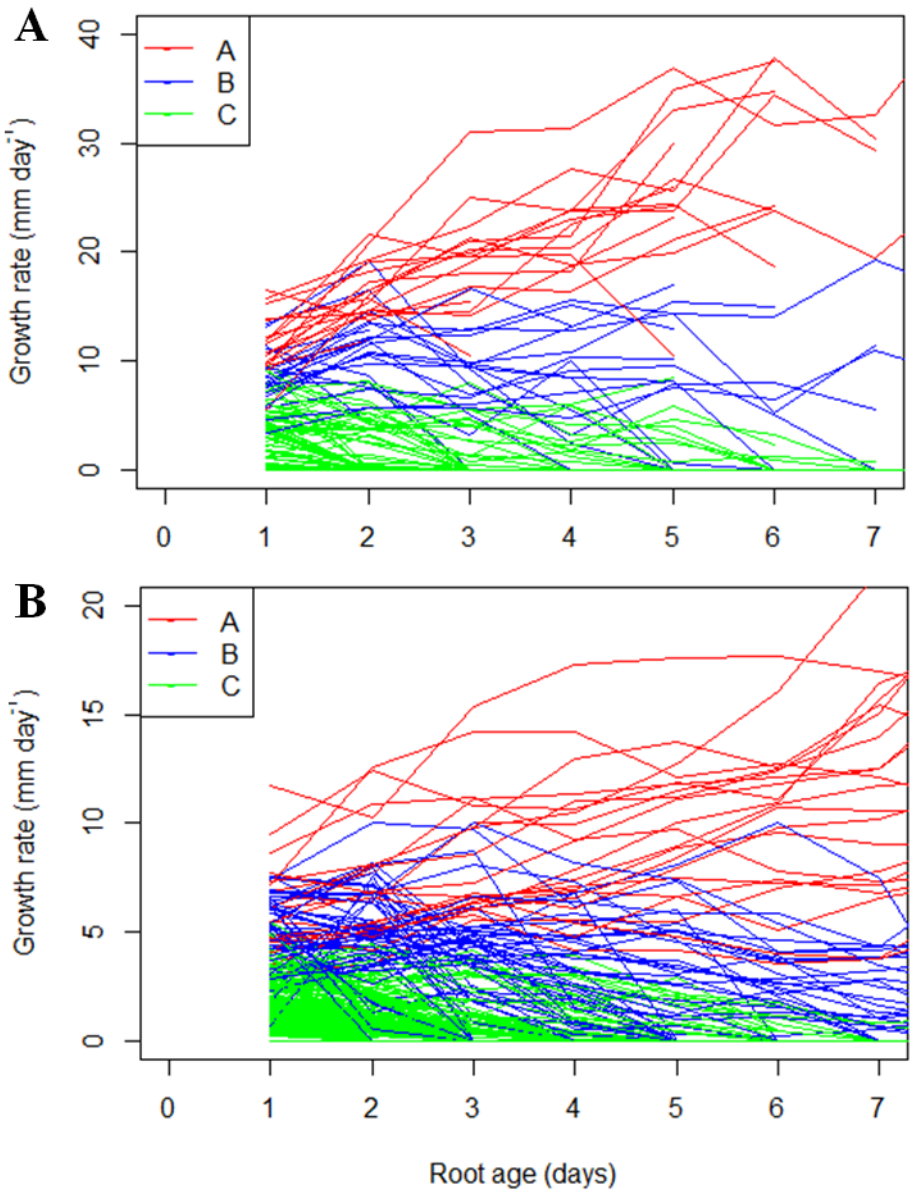

Figure 2-5: Growth rate profiles of individual lateral roots of a pearl millet (A) and maize (B) plant classified with SMSLM. Colors represent the different types identified with the model.

2.2 Comparison of apical diameter profiles and growth rate profiles for the 3 classes of lateral roots identified in maize

The optimal assignment of lateral roots to classes computed using the estimated 4-state semi-Markov switching linear model was used to compute median apical diameter profiles and associated mean absolute deviations per lateral root type. The median apical diameter profiles for the different lateral root types were far more stationary than the median growth rate profiles (**Figure 2-6**). Apical diameter profiles clearly distinguish type A from type B or C lateral roots but not type B from type C lateral roots (see the overlaps between apical diameter distributions for the successive ages in **Table S2-3**). Type B and C lateral root apical diameter decreased with time and converged towards a median apical diameter around 230 µm corresponding to a high proportion of arrested roots.

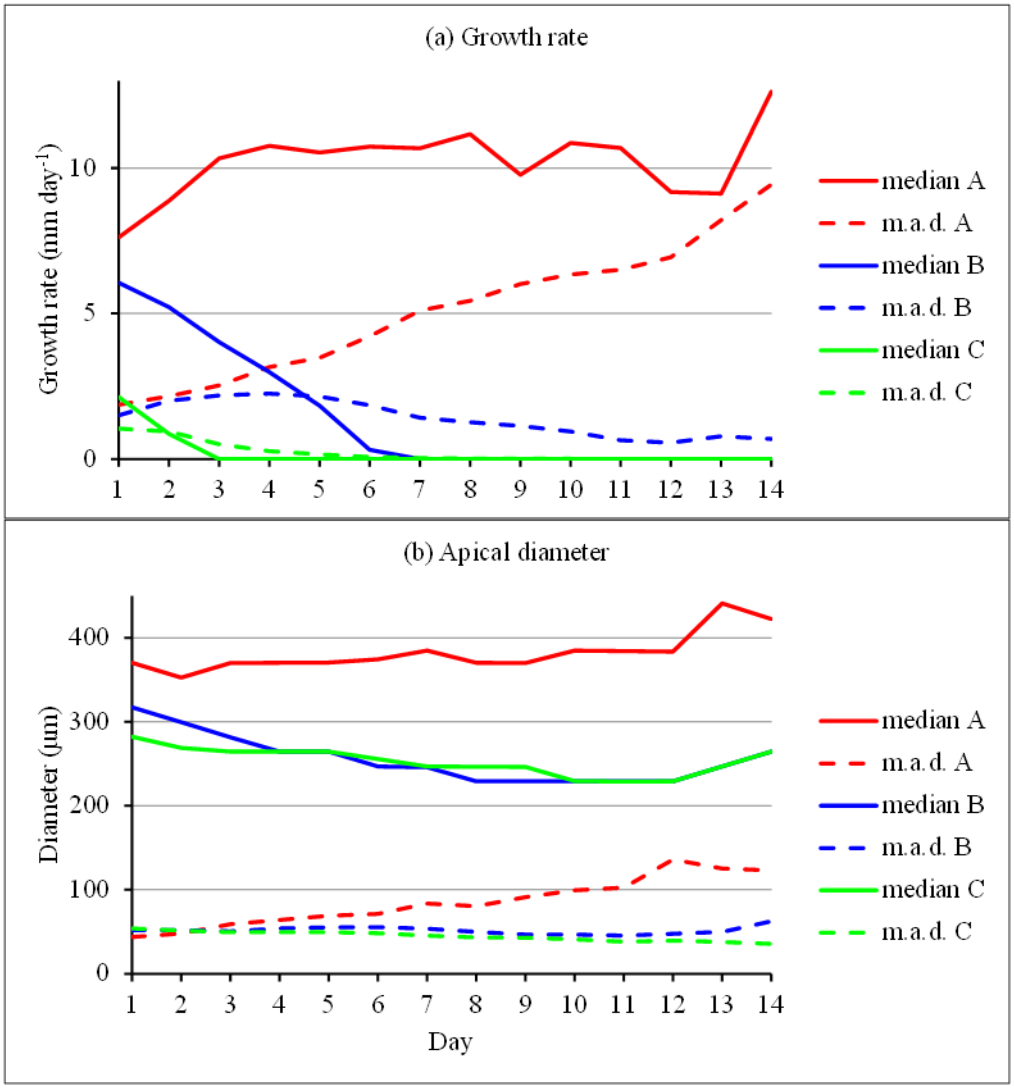

Figure 2-6: Maize: (a) daily median growth rate and (b) apical diameter (and associated mean absolute deviations −m.a.d.−) in the case of 3 groups.

2.3 Linking root growth profile with root anatomy

Previous studies have shown that different lateral root types can be defined in maize and pearl millet based on their anatomy (Varney et al., 1991; Passot et al., 2016). To explore the links between root kinetics and root anatomy, we performed root cross sections in 15 maize lateral roots and 35 pearl millet lateral roots with contrasting growth rate profiles. The roots originated from 3 maize plants and 5 pearl millet plants, having grown for 16 days after germination and 12 to 15 days after germination respectively. Lateral roots were assigned to one of the 3 classes defined previously, based on their growth rate profile. We measured 2 anatomical traits previously shown to be contrasting among individual roots (Passot et al., 2016), stele diameter and central xylem tracheary element (XTE) diameter. For pearl millet, the ABC classification of growth rate profiles was mirrored by a ranking of both stele diameter and XTE diameter, although there was some overlap between classes (**Figure 2-7**). By contrast, no clear trend could be detected in maize, in particular due to the low number (1) of type A roots, the large spread of anatomical dimensions in type B and type C roots and the

comparatively large anatomical dimensions of the type C roots. Globally, a consistent tendency was observed between stele diameter and XTE diameter that encompassed both species. These results suggest a correlation between anatomical traits and growth profile for pearl millet, but not for maize lateral roots. The small sample size for maize roots could explain the lack of observable relationship.

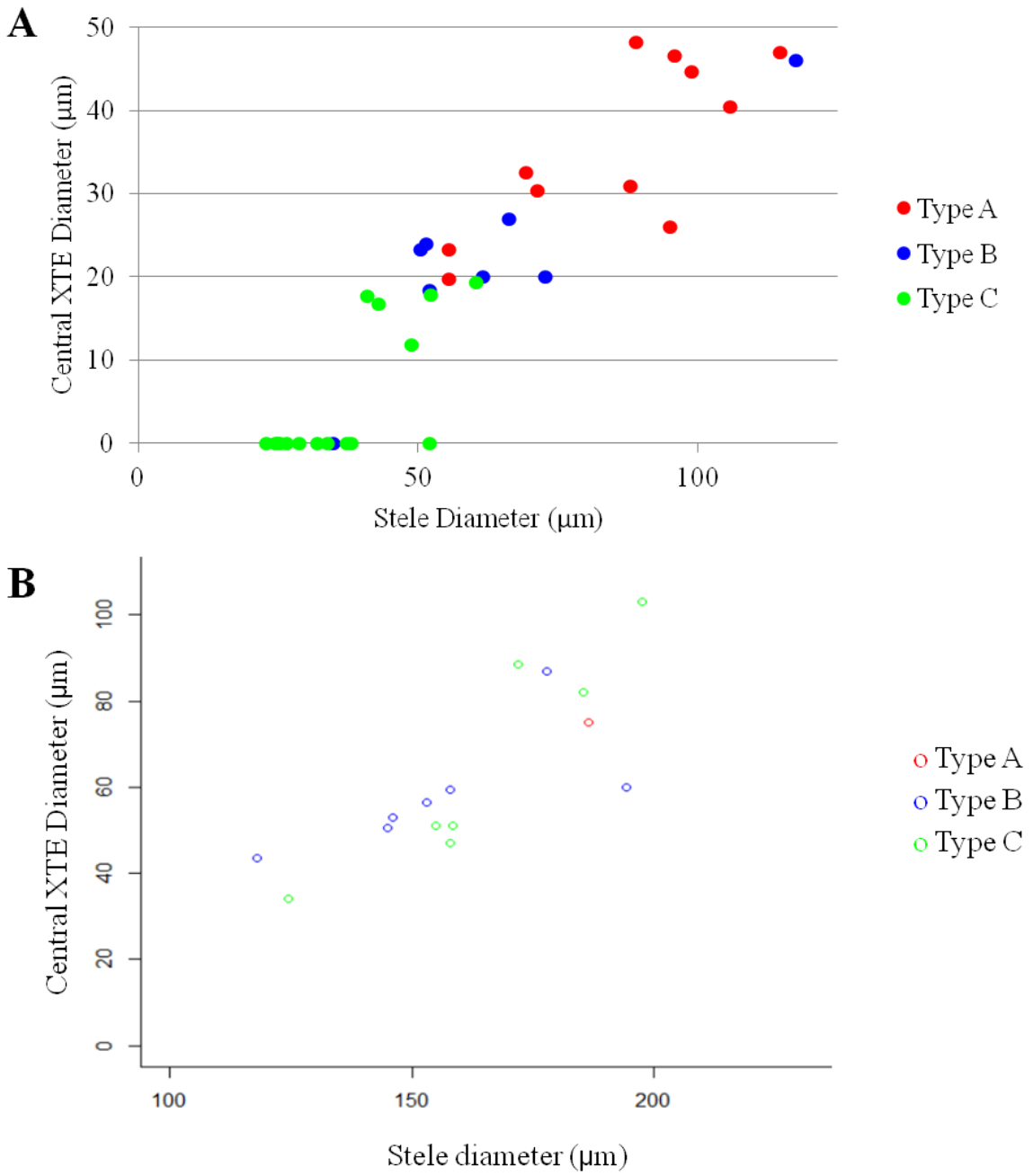

Figure 2-7: Relationship between stele and central XTE diameter of lateral roots in pearl millet (A) and maize (B). Colors indicate the estimated type based on the SMSLM.

2.4 Analyzing the primary root branching pattern

In order to explore whether lateral root type repartition along the primary root was random or somehow structured, we analyzed the distribution of lateral root types (A, B and C)

along the primary root. We first evaluated the impact of the root type on the length of the interval between a lateral root and its nearest neighbor in the rootward direction (Baskin et al., 2010). No difference was found between the mean interval length for the three root types in both species (ANOVA, p-value = 0.83 and 0.7 for pearl millet and maize respectively) (**Table 2-1**). The same type of analysis was conducted separating intervals into 9 groups, depending on the types of the two lateral roots delimiting the interval (**Table S4 and Table S5**). No effect of the lateral root types was found on the interval lengths (ANOVA, p-value = 0.52 and 0.39 for pearl millet and maize respectively). Hence, our results indicate that there is no influence of root types on interval lengths between two successive lateral roots.

Lateral root type in the shootward direction	A		B		C	
	Pearl millet	Maize	Pearl millet	Maize	Pearl millet	Maize
Sample size	165	237	296	814	785	1950
Mean (cm)	0.22	0.16	0.21	0.16	0.21	0.17
Standard deviation (cm)	0.27	0.16	0.27	0.15	0.19	0.15

Table 2-1: Length of the interval between successive lateral roots, classified according to the lateral root delimiting the interval in the shootward direction. No significant differences between the means were found (ANOVA, p = 0.83 and p = 0.70 for pearl millet and maize respectively).

We then questioned whether lateral root type sequences were random or somehow structured. We first computed the Spearman rank autocorrelation function for these sequences. The autocorrelation function for positive lags was within the confidence interval corresponding to the randomness assumption for most of the plants, indicating that the distribution of the different lateral root types along the primary root was stationary and suggesting no marked dependencies between successive lateral root types. This finding was consistent with the growth rate profile length frequency distributions being similar for the three types (**Supplementary Figure 2-4**). Since growth rate profile lengths directly depend on the emergence time of each lateral root and are thus related to the lateral root position on the primary root, this suggests that the proportions of the 3 types along the primary root were essentially stationary. We further analyzed primary root branching sequences applying a statistical modeling approach. To this end, we modeled potential dependencies between successive lateral root types described from the collar to the root tip. Three-state variable-order Markov chains, each state corresponding to a lateral root type, were built. The memories of variable-order Markov chains were selected (Csiszár and Talata, 2006) for each primary root branching sequence and for samples of branching sequences corresponding to each species. For all plants and for both species, a zero-order Markov chain was selected. This confirmed that the type of a lateral root was independent of the type of the previous lateral roots. Hence, our results indicate that there is no influence of the lateral root growth pattern on the distance to or on the growth pattern of the next lateral root.

We checked whether the length of the interval between successive lateral roots and the lateral root type proportions varied or not among individual plants. The mean interval lengths were not equal in all plants (ANOVA, $p < 10^{-5}$ for pearl millet and $p < 10^{-6}$ for maize). Plants were thus classified according to Tukey's Honest Significant Difference. Two overlapping groups were found, both for pearl millet and maize (**Figure 2-8**), with average interval length ranging from 0.31 to 0.21 cm in pearl millet, and from 0.25 to 0.14 cm in maize.

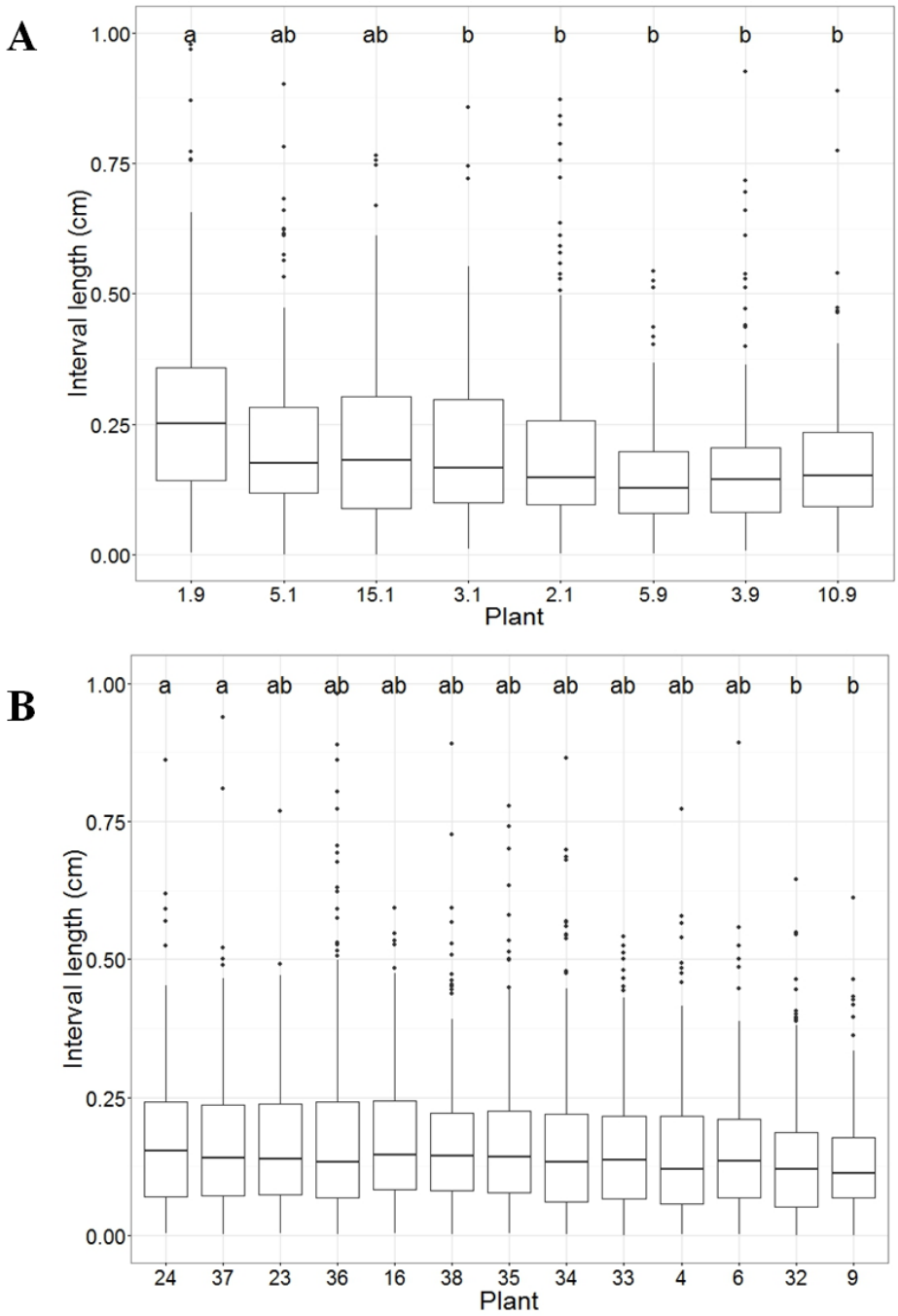

Figure 2-8: Distribution of interval lengths between successive lateral roots for each plant in pearl millet (A) and maize (B) species and plant group assignation according to Tukey's Honest Significant Difference test. Outliers above 1 cm were curtailed.

Significant differences among plants were also found for lateral root type proportions both for pearl millet and maize (Kruskal-Wallis test, $p < 10^{-10}$ and $p < 10^{-15}$ respectively,

Figure 2-9). For pearl millet, the 8 plants were separated into 3 significantly different groups with two overlapping. The proportion of type A roots ranged from 0.06 to 0.21 between these groups. The 13 maize plants were separated into 6 groups, with some overlaps between some groups, type A root proportion ranging from 0 to 0.2. These results indicated that both species show significant inter-individual differences in terms of interval lengths and lateral root type proportions. However, and despite individual differences between plants in terms of lateral root type proportions, the stationary random branching pattern was markedly conserved in all plants.

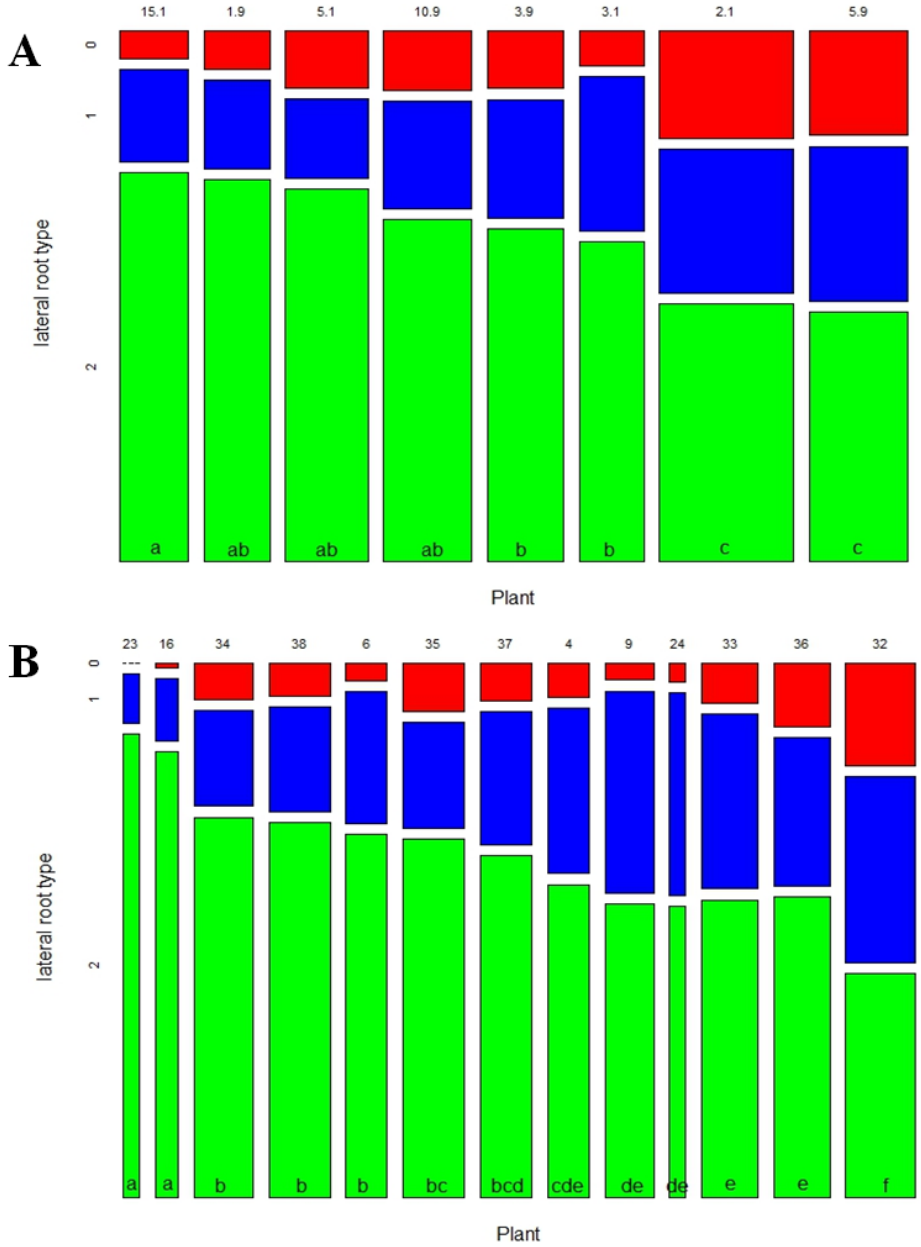

Figure 2-9: Proportion of root types for each plant in pearl millet (A) and maize (B) species and plant group assignation according to Kruskal-Wallis test. Tile areas are proportional to the number of roots in each category. Total lateral root number per plant ranged from 119 to 248 for pearl millet and from 82 to 352 for maize.

As all plants among species are supposed to be genetically homogeneous, we hypothesize that small environmental variations, either during the grain filling and maturation period or during the experiment itself, could explain differences in lateral root type proportions. The link between interval length and lateral root type proportions in each plant is explored in **Supplementary result 2-1**.

3. Discussion

3.1 An original methodology to classify lateral roots

In this study, we designed a pipeline for semi-automated analysis of lateral root growth profiles and primary root branching pattern and applied it to explore the diversity of lateral roots in two cereals, maize and pearl millet. Previous efforts to classify the diversity of lateral roots in cereal species into classes have been reported (Henry et al., 2016; Passot et al., 2016; Rebouillat et al., 2009; Varney et al., 1991; Watt et al., 2008) but these classes were often based on anatomical traits, mainly root diameters and vasculature. A first difficulty comes with the fact that some morphological traits change along lateral roots, typically root diameter (Wu et al., 2016), which was confirmed in our own data in maize. A different classification method, based on growth rates, was reported in rice (Rebouillat et al., 2009), where root growth rates were very contrasted among lateral roots but assignment to classes was based on expert knowledge. Here we assigned lateral roots to classes based on their growth profiles using a statistical model. Our approach revealed 3 similar classes of lateral roots in two different cereal species. Although absolute growth rates were different between lateral roots of the two species, general shapes of the three median growth rate profiles as well as relative proportion of the three lateral root types were similar between species. Growth durations in the three classes were also remarkably similar between the two species. In previous studies, three anatomical types of lateral roots were identified in pearl millet (Passot et al., 2016) and here these types were found to be partially related to the classes based on growth rate profiles. Link between growth rate profiles and anatomy was less clear in maize but maize root diameters were positively linked to growth rate profiles, confirming a general, but not systematical trend (Wu et al., 2016). However, diameter of internal root structures was larger for maize than for pearl millet, meaning that the relationship between root diameter and growth rate profiles is not transposable between species.

3.2 Origin and roles for the three lateral root types

The identification of 3 types of lateral roots raises questions on the origin of this variability and the potential functions of these three types. In rice, fast-growing lateral roots are also thicker and additional periclinal cell divisions in the endodermal cell layer producing additional ground tissue cell layers during the process of primordia establishment have been reported in these large lateral roots (Rebouillat et al., 2009). Variability among the size of lateral root primordia has been reported in maize (MacLeod, 1990) and could account for differences in apical diameter and root growth rate, at least at emergence. Along these lines, lateral root variability would be determined early in development and would be tightly

associated with morphology (diameter) and anatomy. The relationship between root anatomy (stele and central XTE diameter) and classes based on growth rate profile, evidenced in pearl millet goes in this direction. Root diameters at emergence were also ranked according to growth rate profiles in maize. Another possibility is that growth rate variability is determined after emergence and is controlled by different factors depending on the plant physiology (as local assimilate availability) and/or environmental sensing (local water and nutrients availability, local soil structure…). According to this hypothesis, root development may be more plastic. This hypothesis is for example supported by root apical meristem loss happening in most lateral roots of field grown maize (Varney and McCully, 1991). In this case, lateral roots are supposed to emerge without differences between each other and to lose their elongation potential after emergence, probably due to environmental conditions or internal clues. Our results showed that lateral root growth patterns are only partially determined by their initial growth rate, due to the divergent nature of the growth rate profiles. The parallelism between root diameter evolution and growth arrest in maize is also in favor of a link between structure evolution, post emergence growth and growth rate. These two hypotheses may not be exclusive and growth patterns may result from a combination of these two influences, pre- and post-emergence. Factors influencing initial growth rate, growth maintenance and growth arrest could also be different, therefore rendering the picture more complex and the overall patterns of lateral roots globally more plastic to face a variability of external and internal clues (Malamy, 2005).

The functions of these different lateral root types are not precisely known. Locally, each lateral root type could have a preferential function, like water uptake, absorption of certain nutrients, exudation or mycorrhization. In maize, apical meristem loss was suggested to facilitate water uptake (Varney and McCully, 1991). The three major macroscopic elements (N, P and K) for mineral nutrition are absorbed as ions whose diffusion coefficient in the soil widely differ (recalled by Pagès, 2011) and the different lateral root types could share their efforts into those distinct functions. Moreover, these roots may have also longer term functions. In rice, only one lateral root type is known to participate in higher level of branching (Gowda et al., 2011). In perennials, these long lateral roots contribute to the perennial structure of the plant (Coutts, 1987). The existence of different growth profiles is thus likely to contribute to the economy in root system construction. The different root growth patterns described here could be indeed an important component for the efficiency of soil exploration. The interest of such variations to enhance root foraging capacity was already suggested (Forde, 2009) while their cost/benefit advantage as compared to more homogenous lateral root patterns was demonstrated using simulated root systems (Pagès, 2011). Notably, growth cessation appears as an important strategy to avoid an excessive cost of root system. In our data, root type corresponding to indeterminate lateral root growth represented only 14% and 9% of the lateral roots in pearl millet and maize respectively. In annual cereal plants, the specific functions of these long roots is unknown, but we can imagine a role in further widening exploration in the horizontal dimension in opposition to exploration in depth covered by the primary and the limited horizontal exploration by nodal roots.

3.3 Positioning of the three lateral root classes is random along the primary root

One benefit of our approach is that it enables architectural analysis. All lateral roots were assigned to classes and precisely positioned on the primary axis. We showed that, both in maize and pearl millet, the longitudinal spacing of lateral roots was highly variable, both within and between root systems. Despite this variability, the average between-lateral-root distance was relatively conserved among plants for each species, being larger for millet than for maize. Our analyses showed that there was no relationship between the length of the interval between two successive lateral roots and the growth class of these lateral roots. That indicates that both fast-growing and slow-growing roots may be close or far from neighboring roots. The absence of relationship between lateral root spacing and growth rate suggests that lateral root initiation and development are regulated independently. Moreover, we found that the succession of lateral root types was random along the primary root, indicating that there were no local dependencies in root type succession. In other word, lateral roots appear to grow independently from each other since no local inhibition or stimulation could be observed. The absence of local dependencies can be related to the homogeneous soil in our experimental system. Indeed, the existence of soil heterogeneity is known to lead to spatial structuring, for example local proliferation of longer roots in response to nitrate-rich soil patches (Drew, 1975; Hodge, 2004). Our modeling approach opens the door to the exploration of the link between local root environment and proportion of the different root types on a stronger basis.

3.4 Extending the longitudinal modeling framework for studying the whole growth profile of type A lateral roots

The experiment duration constrained by the rhizotron dimensions made that only the beginning of type A lateral root growth could be observed. Hence most of the growth rate profiles assigned to type A lateral roots were censored in the corresponding growth state for both species. This makes a marked difference with type B or C lateral roots for which the whole growth profile, up to growth arrest, was observed for many individuals. Hence, it would be interesting to design larger rhizotrons or to change the growth conditions in order to study the whole growth of type A lateral roots and in particular the transition from increasing or stationary growth rate to decreasing growth rate. The proposed modeling framework can directly be extended by adding states in series for modeling successive growth phases for type A lateral roots. Such extension of semi-Markov switching models with states in series was recently developed for modeling successive developmental phase in *Arabidopsis* rosette in Lièvre et al. (2016). We may expect a single state with decreasing growth rate following the current increasing growth rate state A or an intermediate roughly stationary growth state between the increasing and decreasing growth rate states. Although mechanisms of lateral root growth arrest are documented for maize (Varney and McCully, 1991), the future of "indeterminate" lateral roots is not documented. If their growth duration appear to be really longer than what our experimental set up allowed to see, it could interfere with the decay of

primary root system reported in cereals, occurring for example within two months in pearl millet (Maiti and Bidinger, 1981).

3.5 A new look at lateral roots in future high-throughput phenotyping analyses?

To date, genetic improvement based on structural feature of the root system has essentially concentrated on deep vs shallow rooting (Saengwilai et al., 2014) as well as on structural feature such as the presence of aerenchyma in maize roots, suspected to decrease the carbon construction cost of roots without affecting their function (Zhu et al., 2010). Lateral roots have been comparatively overlooked although they represent the best example of the overall structural plasticity of the root system to face the variable and unpredictable nature of the soil encountered (Drew, 1975). Therefore, there could exist a mine of genetic variation to exploit (and not only in cereals) if relevant phenotyping pipelines for lateral roots were available. By combining image analysis and statistical modeling, our pipeline is a first step in that direction. Importantly, the structure of the model is flexible enough to accommodate variation in the structure such as the number of root types. Of course, while some steps such as image analysis are already semi-automated, some others will need to be automated to upscale the pipeline to study larger plant populations. Rhizotron handling and scanning could be automated with robot. Moreover, basic tasks could be automated, such as image reconstitution by stamping top and bottom part of the rhizotron, root system alignment from one day to another in SmartRoot or lateral root growth profile generation. The most limiting step appeared to be root tracing and dataset cleaning. Indeed, we found that data curation has a huge impact on the final results and was necessary. Curation minimized aberrant root growth profiles by modifying data without necessarily going back to the original image, in order to keep as many roots as possible. No clear criteria exist on what a “realistic” lateral root growth profile should look like and we therefore hypothesized that growth rate changes were smooth rather than steep to clean our database. Visual checking of aberrant growth profiles tended to confirm that our hypotheses on the sources of errors were often reasonable. This cleaning algorithm could be further improved by checking steep growth rate changes without stopping that were not taken into account in our algorithm.

In our experiment, with apparently uniform conditions among plants, variability in root type proportion appeared between plants, suggesting that proportion of each root type is very sensitive to small environmental variations, vigor differences between plants and/or differences among seeds. Based on sufficient replicate plants, our pipeline generates parameters that can be statistically compared among genotypes or environmental conditions, opening the door to high throughput phenotyping with a focus on this yet underexploited source of variation: lateral roots.

4. Materials & Methods

4.1 Experimental

Root observation boxes, called rhizotrons, were built according to Neufeld et al. (1989). The size of the frame was 400 x 700 so that they could be imaged with 2 contiguous A3 images using a scanner. The root system was sandwiched against a plexiglass surface by a layer of viscose that was impermeable to roots, but permeable to water and nutrients. Rhizotrons were made of (back to front) a 5 mm thick extruded polystyrene plate, a 2 cm layer of substrate, a layer of viscose and a 5 mm thick plexiglass plate, all joined together using aluminum U frame held by screws. The substrate used was composed of 30% fine clay, 25% peat fibers, 5% blond peat and 40% frozen black peat (Klasmann-Deilmann France SARL). The substrate was sieved before using. The rhizotrons were weighed individually before and after filling to determine the weight of substrate contained in each one and later to manage daily irrigation.

Maize seeds (*Zea mays*, hybrid B73xUH007) were surface sterilized with 6% hypochlorite for five minutes and rinsed in distilled water for one minute. Seeds were then germinated on moistened filter paper in Petri-dishes (20 x 20 cm) and placed vertically in a growth chamber in the dark at 20°C. Pearl millet germination was performed with a similar protocol, except that seeds were also cleaned with ethanol solution (70%) for 5 minutes after the first rinsing and germination temperature was set to 30°C. Germinated seedlings were transferred individually in the rhizotrons. A layer of wet sphagnum on the top of the rhizotrons maintained the seedlings and prevented them from drying. Rhizotrons were placed in a growth room with climatic conditions adapted to each species: a temperature of 28°C during day and 24°C during night for pearl millet and a constant temperature of 20°C for maize, with a 14-hour-photoperiod for both species. Light was provided by 6 mercury lamps (HQI, 250 W, Osram, Munich, Germany) and measured by a light sensor (SKP215; Skye Instruments, Llandrindod Wells, Powys, UK). Temperature and air humidity were recorded (HC2-SH, Rotronic, Bassersdorf, CH) for each growth room. The sphagnum was watered twice a day at the beginning of the experiment and from 6 days after germination onward, rhizotrons were watered daily using a 1/10 Hoagland solution to maintain the humidity of the substrate. The amount of watering was monitored by a daily weighting of the rhizotron.

4.2 Imaging and image processing

From the second day of growth, rhizotrons were scanned with an A3 scanner (Epson Expression 10000XL Pro, Japan) at 600 or 720 DPI. The histogram of the gray level intensities was adjusted to optimize the contrast on fine roots. As rhizotrons are twice the size of the scanner, two images (upper part and lower part of the rhizotron) were taken and aligned using Align_4 (http://www.mecourse.com/landinig/software/software.html) to recover an image of the entire root system, thanks to landmarks visible in both parts. These landmarks were either added intentionally on the rhizotron or were fortuitously present (water drops, mist, the root system itself).

The SmartRoot software (Lobet et al., 2011) was used to extract root system architecture at successive dates and root growth parameters because it supports time-lapse images and focuses on the analysis of individual root behavior. SmartRoot needs images where roots appear darker than background. An ImageJ (v.1.47v; Rasband, W.S., U. S. National Institutes of Health, Bethesda, Maryland, USA) macro was developed to automatically invert and adjust the contrast of the rhizotron images by scaling the image intensity histogram on a fixed range. The optimal contrast (min and max values of the intensity range) was determined empirically to reduce the number of errors when using the algorithm for automatic lateral root tracing provided by SmartRoot (see next section) using a subset of scan images, and was applied to the whole set of images using the macro tool.

4.3 Image analysis

SmartRoot enables semi-automatic root tracing. The primary root was drawn on the first image. For the next days, the root system traced on the previous day was imported and aligned, in such a way that the primary root elongated progressively, using automatic tracing. Crown and lateral roots were added as they appeared, either manually or using automatic detection. Their length increased progressively on the successive scans, as for the primary root.

When all roots were traced, the data were extracted with the batch export tool of SmartRoot. This tool provides several measurements including the length, the insertion position and the diameter for each root. Because the resolution was not sufficient for pearl millet lateral roots, we only considered root diameter for maize. Data were ordered and the ages of lateral root were computed at each day, age 0 being assigned to the first day of appearance of a lateral root. The root growth rates were extracted by differencing the length between 2 consecutive days. If the images were not evenly spaced in time, the growth rate computing was adapted to take into account the variable lengths of the time intervals.

4.4 Correction of growth rate profiles

In spite of manual supervision of root tracings, the exported dataset contained some digitalization errors. It was therefore necessary to characterize the implausible data points resulting from such errors and to clean out the dataset to ensure that any later analysis is performed on trustable data. We thus designed a data correction algorithm aiming at identifying implausible growth rate profiles that derive from errors in image analysis. The most typical errors were defaults in alignment, one-day missing root length increments or non-visible root tips in the case of roots encountering an obstacle. This kind of errors results in implausible trajectories for the root length at some time-point, which can be better identified by examining growth rate profiles. Depending on the type of error, growth rate profiles were either corrected or truncated before the first implausible growth rate. The proposed data correction algorithm is described in **Appendix 2-3**.

4.5 Model description

4.5.1 Definition of semi-Markov switching linear models

Semi-Markov switching linear models (SMSLMs) are two-scale models that generalize hidden semi-Markov chains by incorporating linear regression models as observation models. They are formally defined in **Appendix 2-1**. In our context, the succession and duration of growth phases (coarse scale) are represented by a non-observable semi-Markov chain while the growth rate trend within a growth phase (fine scale) are represented by observation linear models attached to each state of the semi-Markov chain. Hence, each state of the semi-Markov chain represents a growth phase. A *J*-state semi-Markov chain is defined by three subsets of parameters:

1. Initial probabilities $\left(\pi_j ; j = 1,\ldots, J\right)$ to model which is the first phase occurring in the series measured,
2. Transition probabilities $\left(p_{ij} ; i, j = 1,\ldots, J\right)$ to model the succession of phases,
3. Occupancy distributions attached to non-absorbing states (a state is said to be absorbing if, after entering this state, it is impossible to leave it) to model the growth phase duration in number of days. We used, as possible parametric state occupancy distributions binomial distributions B(d, n, p), Poisson distributions P(d, λ) and negative binomial distributions NB(d, r, p) with an additional shift parameter $d \geq 1$.

A SMSLM adds observations linear models to the non-observable semi-Markov chain:

4. We chose to model growth rate trends within growth phases using simple linear regression models because of the short length of growth phases (up to 10 successive growth rates for pearl millet and up to 17 successive growth rates for maize).

A SMSLM composed of parallel transient states followed by a final absorbing state was estimated on the basis of growth rate profiles corresponding to a given species. A state is said to be transient if after leaving this state, it is impossible to return to it. The final absorbing state represented the growth arrest and a degenerate linear model corresponding to a constant null growth rate was associated with this state. Each estimated model was used to compute the most probable state series for each observed growth rate profile (Guédon, 2003). This restored state series can be viewed as the optimal segmentation of the corresponding observed series into at most two sub-series corresponding to a given growth phase either censored or followed by a growth arrest. Because of the transient growth states in parallel, this restoration can be interpreted as a classification of the lateral roots on the basis of their growth rate profiles.

4.5.2 Definition of stationary variable-order Markov chain

Most of the methods for analyzing local dependencies in discrete series rely on high-order Markov chains. However, the number of free parameters of a Markov chain increases exponentially with its order, i.e. with the memory length taken into account. For instance, in the case of three states (corresponding to three lateral root types), the number of free parameters is 2 for a zero-order, 6 for a first-order, 18 for a second-order Markov chain, etc.

Since there are no models "in between", this very discontinuous increase in the number of free parameters causes the estimated high-order Markov chains to be generally overparameterized. This drawback can be overcome by defining sub-classes of parsimonious high-order Markov chains such as variable-order Markov chains (Bühlmann and Wyner, 1999; Ron et al., 1997) where the order is variable and depends on the "context" within the series, instead of being fixed. Stationary variable-order Markov chains are formally defined in **Appendix 2-4**.

4.6 Root anatomy

Plants were grown in rhizotrons as previously described. Stickers were placed on the viscose tissue previous to the plant transfer, evenly spaced near the position of the future root system to help roots tracking. Lateral root growth rate profiles were extracted before sampling, to determine the type of each root. Selected roots were harvested and fixed overnight in an acetic acid:ethanol solution (1:9) and conserved in 70% ethanol. For maize, two 8 mm long segments were cut from the apex (apical and subapical segments, respectively), as well as one segment at the root base (or basal segment). For short roots (< 8 mm), a single segment (considered basal) was analyzed. For pearl millet, samples were taken indifferently along the root at 12 to 15 DAG. Root segments were gently dried on a filter paper and imbibed in warm (30-45°C) liquid 3% agarose solution (SeaKem GTG Agarose, Lonza). 55 µm-thick sections were obtained from solidified agarose blocks using a vibratome (Microm HM 650V, Thermo Scientific, speed 30, frequency 60). Individual root sections were then collected, transferred to microscope slides and covered with a coverslip for direct observation.

Images were taken using a Leica DMRB microscope equipped with an epifluorescence filter (excitation range: UV; excitation filter: 460-480 nm). Two pictures were taken for each root section: one under visible light using Nomarsky optics and another using epifluorescence that takes advantage of the natural fluorescence of cell walls with secondary deposits. Images were taken using a Retiga SRV FAST 1394 camera and the QCapture Pro7 software. The RGB images were opened in ImageJ using the Bioformats importer plugin and transformed in gray level 8-bit images. A scale-bar was added to the images according to their magnification. Sizes of the stele and central XTE diameters and number of peripheral xylem vessels were recorded for each root section.

Chapter 3

Searching genes controlling primary root growth in pearl millet

This chapter is the beginning of an article. Further analyses are needed beyond the first exploratory analyses presented here to complete the results and to write a full article.

1. Introduction

Breeding new varieties is one strategy to obtain higher and more stable agricultural yields. Beside trying to improve crop performance in certain environments, breeding may be focused on improving or on modifying a specific trait. Improving root traits has recently raised interest as it offers new opportunities to enhance nutrient and water acquisition and therefore abiotic stress tolerance and crop resilience (Comas et al., 2013; Herder et al., 2010). Root breeding has been little used in the past, due to the hidden nature of the root system and its high environmental plasticity, which made difficult the phenotyping of large collection of diversity (Rich and Watt, 2013). However, root trait QTLs have been recently identified in cereals, largely thanks to the development of high-throughput phenotyping techniques for root characters in hydroponic condition (Clark et al., 2013). They mainly concern rice (e.g. Champoux et al., 1995), maize (e.g. Burton et al., 2014) or wheat (e.g. Bai et al., 2013). Root QTLs concern many different root traits, including morphological root traits such as root diameter, total root system depth, number of roots or root system dry weight, geometrical traits such as root angle, or even emergent traits such as convex hull area (Atkinson et al., 2015) or fractal dimension (Bohn et al., 2006). Some studies seek how root trait QTLs co-localize with aboveground QTLs like field performance (Atkinson et al., 2015) or plant height (Bai et al., 2013).

Further studies have led to the identification of some genes responsible for the QTL effect and the confirmation of the QTL influence on plant physiology by introgression into a control variety. A good example is *DRO1*, a rice gene responsible for a QTL involved in crown root angle (Uga et al., 2013). Its introgression into a drought sensitive cultivar led to an increase yield under drought stress by increasing deep rooting. The vast majority of these findings has been done using recombinant inbred population coming from the cross between two contrasted cultivars, but the advent of next generation sequencing now makes it possible to easily genotype large diversity panels in non-model plants (such as pearl millet) and to use genome wide association studiy to discover QTLs and genes controlling root traits. One example that can serve as proof of principle was reported recently in *Arabidopsis* and led to the discovery of *KURZ UND KLEIN* (*KUK*, from the German words for short and small), a gene controlling primary root elongation (Meijón et al., 2014).

We found previously that early pearl millet root system development is characterized by a fast growing primary root (Passot et al., 2016). We hypothesized that this might be an adaptative trait for early drought stress (Padilla et al., 2007). Our previous results suggest that there is a high heritability for this trait, which means that it has an important genetic control component.

Here we characterized a large panel of pearl millet inbred lines for primary root growth on young plants grown in a paper-based hydroponic system and initiated an association genetics study to identify genomic regions controlling this trait.

2. Material and methods

2.1 Plant material

A panel of pearl millet inbred lines derived from West and Central African landraces (open-pollinated varieties) was used in this study. Seeds were produced in 2014 in Niger. Since pearl millet is naturally outcrossing, the open-pollinated varieties experienced a high degree of inbreeding depression and, as a result, the inbred lines were developed using initial selfing for three generations, followed by two generations of sibling and then a last generation of selfing. This panel has already been phenotyped under low phosphorus conditions and genotyped with diversity array technology (DarT) markers (Gemenet et al., 2015). This genotyping revealed that the panel was weakly structured into 3 groups. The panel contained 345 seed lots belonging to 192 distinct lines. Some biological replicates existed, consisting on seeds coming from different selfed plants belonging to the same line.

2.2 Root phenotyping

Plants were phenotyped for primary root growth with a paper-based hydroponic system, as described in Passot et al. (2016). Seeds were surface-sterilized and pre-germinated in Petri dishes, transferred into pouches 24 hours after germination at a density of 3 seeds per paper and then maintained in a growth room with a 14 hours photoperiod (28°C during day and 24°C during night). Pictures of the root systems were taken 6 days after germination with a D5100 DSLR camera (Nikon) at a resolution of 16 M pixels. The camera was fixed on a holder to maintain the same distance between the lens and each root system. Primary root lengths were measured using RootNav (Pound et al., 2013).

Broad sense heritability was computed with the following formula:

$$H^2 = \frac{\mathrm{Var(line)}}{\mathrm{Var(line)} + \frac{\mathrm{Var(res)}}{n_{\mathrm{plant/line}}}},$$

where

- $n_{\mathrm{plant/line}}$ is the average number of plants measured per line,
- Var(line) is the variance associated with lines,
- Var(res) is the residual variance.

Both variances are parameters of the following linear mixed model:

$$Length = \mu + \alpha_{line} + \varepsilon_{res},$$

where μ is the overall mean length, α_{line} is the random effect attached to the lines with $\alpha_{\mathrm{line}} \sim \mathrm{N}(0, \mathrm{Var(line)})$ and $\varepsilon_{\mathrm{res}}$ is the error term with $\varepsilon_{\mathrm{res}} \sim \mathrm{N}(0, \mathrm{Var(res)})$.

2.3 Plant genotyping

Genomic DNA was extracted from fresh leaves sampled on young plants as described in Mariac et al. (2006). Leaves were frozen in liquid N_2 just after sampling and ground with a Tissue Lyser II (Qiagen). Ground leaves (approximately 0.2 g) were re-suspended in 1 mL extraction buffer (Tris (100 mM), NaCl (1.4 M), EDTA (20 mM), CTAB (2%) and DTT (0.2%), pH = 8) and incubated at 65°C for 3 hours. Samples were centrifugated 1 minute at 8 000 rpm and supernatants were washed (1:1) with phenol-chloroforme-isoamyl acohol (25:24:1). Samples were centrifugated for 10 minutes at 10 000 rpm at 10°C and supernatants were retrieved and incubated with 10 µL RNase A (Qiagen) for 30 minutes at 37°C. A second washing step with phenol-chloroforme-isoamylacohol was then applied. DNA was precipitated with isopropanol (0.6 volume) and sodium acetate (3 M, pH = 5, 1/10 volume) at 4°C for 20 minutes. Samples were centrifugated 10 minutes at 10 000 rpm at 10°C and supernatants were removed. DNA pellet were washed two times with ethanol (70%) and centrifugated 5 minutes at 10000 rpm at 10°C. DNA pellets were re-suspended in 100 µL TE buffer and stored at -20°C. DNA concentration and purity were checked with a Spectrophotometer ND-1000 (Nanodrop). DNA quality was assessed on a 1% agarose gel. An aliquot of 10% of the samples was digested with EcoRI or HindIII (1 unit/reaction; Promega) for 2 hours at 37°C to check DNA accessibility to restriction.

Genotyping was performed by the method genotyping-by-sequencing (GBS) at the Genetic Diversity Facility of Cornell University (Ithaca, USA). For each pearl millet line phenotyped for root trait (see part II.2) two runs were performed on the HiSeq2500 (Illumina). Genomic DNA was cut with ApeK1 restriction enzyme and sequencing was done with single-end reads. The Genetic Diversity Facility of Cornell University provided the fastq, vcf and SAM files as well as the GBS bioinformatics pipeline they used for the analyses (TASSEL commands). To check each step of the GBS analyses and test different parameters of Single Nucleotide Polymorphisms (SNPs) filtering, the creation of the vcf file from the original fasq files was performed a second time using TOGGLE (Monat et al., 2015). The filtering of the SNPs was performed by VCFtools.

3. Results

A total of 853 plants were phenotyped, divided in 3 unequal experiments of 559, 116 and 178 plants each respectively. Due to germination problems, only 136 seed lots, belonging to 108 different lines, were phenotyped. An average of 7.9 plants/line was analyzed. This experiment focused on primary root length at 6 days after germination and this character showed a large genetic variability (**Figure 3-1**). A broad sense heritability of 0.53 was estimated for this trait on this large panel confirming that primary root growth has a strong genetic control.

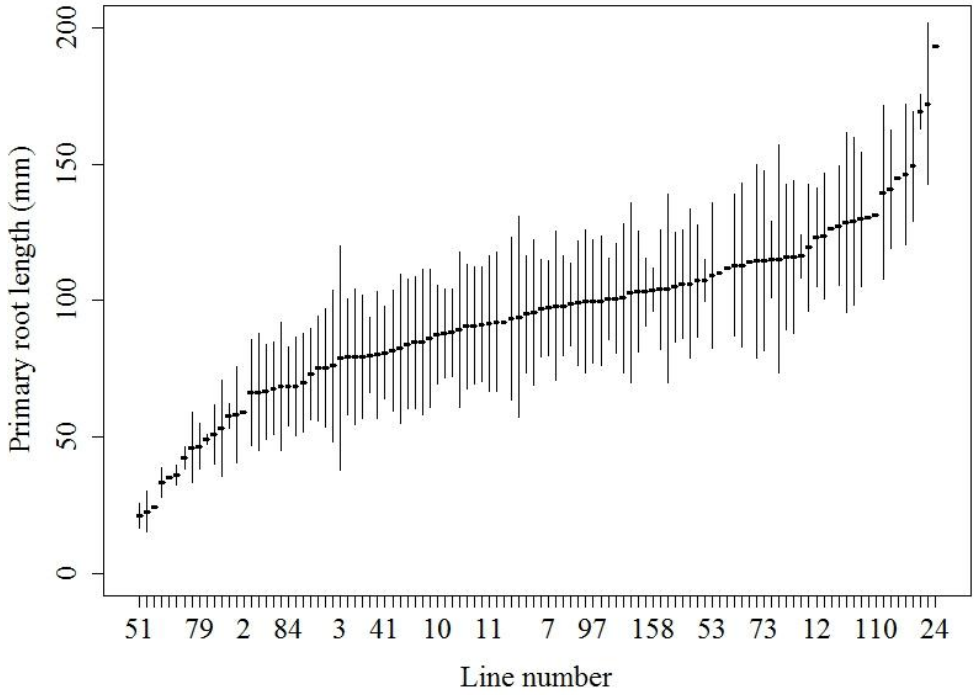

Figure 3-1: Primary root length of the lines of the inbred panel, measured after 6 days of growth. N = mean +/- standard deviation

Primary analyses given by the Genetic Diversity Facility identified 1,677,181 SNPs before filtering, among which 481,897 were present in at least half of the plants. The mean site depth was 2.86. We expect that further filtration steps would lead to approximately 300,000 SNPs.

Analyses of the genetic structure and the genome wide association study will be done respectively with the R packages LEA and GAPIT.

4. Discussion and perspectives

Here we phenotyped a panel of pearl millet inbred lines for primary root length at 6 days. This measurement can be considered as a good proxy for early primary root growth only if this early growth is nearly constant in all lines. Else it may be biased by differences existing in early growth dynamics among the panel. The variability found for this character was large and the individual variability within each line accounted for a significant part of it, as evidenced by the medium value of the broad sense heritability. Variability within line is due to individual differences between seeds. As seeds from the same lot all come from the same plant, this variability is attributed to small environmental differences during seed filling and maturation. In particular, seed position on the mother plant is known to influence seed germination (Gutterman, 2000). This effect may be negligible when studying plants during longer time scale, as seed reserve just play a role during the first few days of growth of the seedling. For very short growth durations, as it was the case here, lower variability within line could be obtained by choosing seeds coming from the same part of the spike. In perennial

grasses, it has been reported that seeds located at the basal part of the spike tend to have better germination rate than seeds located in the middle or the apical part of the spike (González-Rabanal et al., 1994). Pearl millet is usually sown by putting several seeds together in a hole, only the vigorous seedlings being kept after germination. This practice suggests that maximum potential early primary growth rate could be the most interesting trait to select, as only the best performing plants will be kept after germination. Should this experiment be repeated, the protocol may consist in sampling only seeds coming from the basal part of the spike in order to estimate primary root length only for the seeds supposed to have the best germination ability. This technique may also improve average germination rate, which was quite low for some lines and therefore negatively impacted the total amount of plants measured per line.

We also performed genotyping on the same lines in order to be able to conduct genotype/phenotype association studies. Genotyping-by-sequencing is a powerful genotyping technology permitted by the very fast decrease of sequencing cost that occurred during the last ten years thanks to next-generation sequencing technologies (Poland and Rife, 2012). One advantage of this technique for association studies is that sequencing is already done when markers associated to traits of interest are identified. In our case, it will for example permit to identify very quickly sequences homologous to known genes already characterized in other cereals in regions associated with our trait of interest.

A transcriptomic approach will be used to complete the results we expect to find by association study. Two lines with contrasted primary root growth rate in the phenotyping experiment were selected from the inbred panel (lines were also chosen on the basis of the number of plants phenotyped in order to have a strong confidence in the phenotype). Plants will be grown in hydroponics (3 replicates per line) and primary root tips (first cm) will be harvested 7 days after germination. RNA will then be extracted and used to perform a RNAseq experiment. We have now optimized the experimental conditions for plant growth and RNA extraction. This experiment will give us two types of information:

1) what are the genes that are expressed in the root tip (i.e. in the region responsible for root growth through cell division and expansion),

2) what are the genes that are differentially expressed in this region in two contrasted lines. Significantly regulated genes will be confirmed on a larger number of contrasted lines by qPCR.

We will then cross this information with the list of candidate genes in the genomic region(s) associated with primary root growth in the association study. This might help us identify the gene responsible for the quantitative difference.

The inbred panel described here has already been phenotyped for tolerance to low phosphate availability (Gemenet et al., 2015). It would be interesting to confront our results with these ones to find potential relationship between primary root growth and low phosphate tolerance. Drought stress tolerance is currently being assessed for this inbred panel at the ISRA Bambey experimental station (Senegal). Plant performances in the field are measured in well-watered and drought-stressed conditions along with some physiological and agronomical traits. Our phenotyping results will be compared with the measurements done in the field to assess whether primary root growth has an impact on field performance under drought. Plants tolerate drought differently depending on its occurrence time within the growing season

(early, intermediate or late) and, as we expect that early primary root growth mainly impacts early drought tolerance, further experiments simulating a very early drought stress may be performed to refine these predictions. The combined use of phenotyping experiments in laboratory conditions and agronomic trials in the field permit to concomitantly estimate the agronomic value of root traits and to look for genes controlling them (Atkinson et al., 2015). In this respect, further phenotyping experiment, performed on longer time scale, can be used to identify more traits of interest, concerning lateral roots, crown roots, distribution of the root length in the depth profile, etc… The inbred panel is currently tested for its capacity to structure the surrounding soil in rhizosphere by measuring the weight of root adhering soil with a standard protocol. As rhizosphere help the plant to tolerate drought episodes, selecting plants with higher root adhering soil mass is another way to improve pearl millet drought tolerance.

In a longer term, markers significantly associated with root traits beneficial for drought tolerance, identified by association study, will be included in marker assisted selection programs to help breeding new pearl millet varieties with improved root traits.

Discussion and perspectives

The objective of this work was to characterize pearl millet root system development. This root system was poorly known and this newly-acquired knowledge will be useful for breeding new pearl millet varieties with improved root traits. Root system improvement is meant to enhance plant water and nutrient acquisition efficiency and therefore to increase drought and low nutrient stress tolerance, two major limiting factors in West Africa for this important crop.

1. Lateral roots: an unexplored diversity

During this PhD, we developed a novel pipeline to analyze the growth of a large number of lateral roots. This new approach revealed that lateral roots show three growth trends defining three lateral root types in two cultivated cereals, pearl millet and maize. Interestingly, these three growth trends were linked with three anatomical types in pearl millet (but not in maize). A positive link between lateral root diameter and growth duration has been shown on maize, but without grouping of lateral roots (Wu et al., 2016). There is therefore a diversity of lateral roots whose development and function is still poorly explored.

Different lateral root types have been previously described in other cereals based on anatomy (Henry et al., 2016; Varney et al., 1991; Watt et al., 2008). Link between a classification of lateral roots based upon growth profile and anatomical groups was only investigated in rice (Rebouillat et al., 2009), where root growth rates are very contrasted among lateral roots, but assignment to classes was based on expert knowledge. Our work not only confirms the relevance of expert classification but also can be used to objectify the classification and to better characterize the different trends found. Further work could focus on understanding how anatomical structure numbers, that are discrete (number of xylem tracheary elements, in particular), are linked with growth rate profiles, that are continuous-valued time series. The statistical approach designed at this occasion can be used to compare classifications in other conditions, other genotypes or other cereals. Interestingly, the lateral root types described in rice seem quite similar to the ones we found in pearl millet and maize. This might suggest that the existence of these different lateral root types is a shared feature of cereals. Concerning dicots, the model plant *Arabidopsis* only has one lateral root type. That simplicity allows lots of molecular studies on lateral roots in this plant (Malamy and Benfey, 1997). In other plants, specialized lateral root types have been evidenced, especially proteoid roots. These are small lateral roots highly efficient in P acquisition organized in clusters that are produced by Proteaceae under P deficiency (Dinkelaker et al., 1995). Root clusters homologous to proteoid roots also exist in some other dicot families. In trees, a positive relationship has been shown between root growth rate and root apical diameter (Pagès, 1995). Hence some variability has been shown among dicot lateral roots.

This raises interesting and important questions about the origin and the roles of these different lateral root types. This has been little studied but it would be very relevant to identify strategies to improve root system efficiency. In rice, the development of lateral root primordia is similar for both large and small lateral roots, except that, at a very early stage, additional periclinal cell divisions in the endodermal cell layer produce additional ground

tissue cell layers in the large lateral roots (Rebouillat et al., 2009). In maize, many lateral roots stay very short and this growth arrest is attributed to the loss of root apical meristem that differentiates into mature cells at some point (Varney and McCully, 1991). This growth arrest happens in the field but not when plants are grown in nutrient solution, thus indicating a clear effect of the environment on lateral root growth.

The function of these different lateral root types must be understood in order to help finding a compromise between lateral root density, proportion of the different types and local conditions. In rice, lateral roots can be divided into three types: the L types are generally long and coarse and capable of branching into higher-order laterals; M types are long and coarse but without a branch and S types are short, fine and non-branching but usually numerous (Gowda et al., 2011). It is suggested that these three lateral root types fulfill different functions, among which branching is the most visible. In the case of maize, root tips have been observed to break in some lateral roots and this would render lateral root able to transport efficiently water from the soil to the xylem, as water is mainly absorbed via mature parts of the roots (Varney and McCully, 1991). Functions of different lateral root types could be further explored by analyzing potential mutants affecting lateral root type proportions. For example, one can imagine that some roots could exudates particular molecules favoring P acquisition, like proteoid roots existing in dicots (Dinkelaker et al., 1995).

In conclusion, it will be necessary to take into account the existence of a small number of well-defined lateral root types in future work. First, it would be relevant to study the impact of the environment on lateral root types, in terms of proportion and of average behavior of each type. In particular, the availability of water and phosphorus and the temperature of growth may have an impact on lateral roots. The pipeline propose in **Chapter 2** is suitable for such studies. The function and mechanisms of development responsible for the formation of these different root types also need to be studied. Moreover, the existence of different lateral root types could be taken into account for breeding, where root carbon cost is a main concern (Lynch and Ho, 2005). It has been shown that root length heterogeneity is positively linked with foraging performance (Pagès, 2011). Breeding needs in a first place that targeted traits are genetically determined but for now nothing tells us that this is the case for relative proportions of the different lateral root types. These proportions could be set mainly by environmental conditions. This supposition is supported by the very similar proportions found for maize and pearl millet in similar conditions, meaning that proportions could even be conserved among species. Studying genetically diverse accessions will permit to know whether genetics influences lateral root types and in which direction: modification of type proportions, of growth rate profile, of growth duration… Given the high inter-individual heterogeneity, such genetic studies would need either to better control this heterogeneity or to use phenotyping methods with higher throughput than what was put in place during my PhD.

2. Root phenotyping: the new frontier

During this PhD, several phenotyping techniques for root architecture were used, offering different advantages and constraints. Hydroponic phenotyping on blue paper (Atkinson et al., 2015) was used in **Chapter 1** to explore the existing diversity in root architecture and in **Chapter 3** for high throughput phenotyping of primary root length. This set up allowed to phenotype a large number of plants in a reduced space. The limiting factor

for throughput in that case was seed availability and germination rate and amount of human intervention needed to transfer the germinated seeds on pouches on one day. This issue can be skirted by staggering the start of the experiment for seed lots, but this automatically raises the question of homogeneity of environmental conditions. An intrinsic limitation of this system is the artificiality of the growth conditions, that does not offer mechanical resistance to root growth, for example, and limited duration during which plants can grow. Moreover, it was especially susceptible to contaminations.

A rhizotron system was used in **Chapter 1** and **Chapter 2**. It offered more realistic growth conditions, as it opposed mechanical impedance to root system growth and water and nutrients were extracted from a substrate rather than from a nutrient solution. It was used to follow precisely the growth of individual roots, on a daily time scale, and the growth duration was longer than on the blue papers thanks to the bigger dimensions of the growth system. The main drawback of this system is the amount of human workforce it requires and therefore its low throughput. The system size could be increased but daily manual handling imposes some weight restrictions and the rhizotrons already weighted about 6 kg with that size. Robotic handling would solve the weight problem. The other limiting factor is the need for human intervention for semi-automatic tracing of the root systems. Even if growing larger number of plants is practically conceivable, the image analysis task will be a bottleneck for improving throughput. Improvement of the existing image analysis softwares like SmartRoot will be needed to address this issue. Solutions like analyzing only small parts of the root system could also be used should a larger number of plants be required, for example to compare different treatments.

Last, X-ray microcomputed tomography was used in **Chapter 1**. This technique can be used to get a 3D representation of root system growing in soil. It has the advantage of permitting non-destructive observations of root systems grown in 3 dimensions in a real soil. However, the efforts to render growth conditions more realistic have their drawbacks. A compromise has to be found between pot sizes and scanning duration. Higher scanning duration at constant pot size results in better scan definition but imposes lower throughput. The compromise we chose implied medium pot size, in which root systems reached the bottom quite quickly. However, even with medium pots and with the scanning duration we chose, the scan definition was not sufficient to detect all lateral roots and in particular thin ones. This may be improved by a fine contrast adjustment associated with adequate image treatment. There is still no automation, even partial, for root system segmentation from the stack of images generated by the scanner which rendered the image analysis very time consuming and tedious. This also favored a certain amount of subjectivity of the tracing, that depends on the experimenter. Fully manual segmentation also compromises the scaling of this particular experimental setup for high-throughput phenotyping. The development of an algorithm for automatic segmentation of roots from soil scans would be ideal to improve the repeatability of the segmentation and the possibilities to increase throughput (Mairhofer et al., 2012), as long as its use is simple enough and does not require too many expert interventions.

To sum up, we used one phenotyping technique focused on high-throughput, one focused on information precision and one focused on reality of growth conditions. The efforts made on one special point always led to drawbacks on the other ones and these three techniques thus illustrate the necessary compromise between throughput, spatial and temporal

resolution, and relevance of growth conditions. Spatial resolution depends on the image acquisition technique and better resolution usually requires higher image acquisition duration. This was the case with the scanner and the CT-scan. On the other side, temporal resolution depends on the frequency with which images are acquired (daily with rhizotrons, one every other day with blue papers and every 4 to 6 days with the CT-scan). This point depends on the amount of work necessary to acquire the images and to treat them and also on the availability of the image acquisition system (limited availability in time for micro-CT). Improved temporal resolution can be reached by automatically moving the plants toward the image acquisition system or by moving the image acquisition system itself in the growth room, in which case spatial and temporal resolution become tightly linked (Fahlgren et al., 2015b).

Root phenotyping is a very active field of research and many other phenotyping solutions exist for root system. Shovelomics consists in excavating root system of field grown plants and evaluating some defined root traits with a precise technique (Trachsel et al., 2011). Depending on the root traits of interest, this technique can be rendered high throughput and it is the one that offer the most realistic growth conditions. It can be used to screen large population of plants for genetic studies but thus needs a lot of human work. MRI is another solution to phenotype root systems grown in soil (van Dusschoten et al., 2016). It has the same dimension limitation as X-ray CT but skirts the segmentation issue with a different image acquisition technology. Growing root system in transparent medium is a different strategy. It allows 3-dimensional phenotyping of large number of plants and association studies (Topp et al., 2013). Growing root systems in 2 dimensions can also be done in transparent media, such as glass beads (Courtois et al., 2013).

A lot of phenotyping techniques exist, each one proposing its own compromise in terms of throughput and spatial and temporal resolution. Although phenotyping technologies and platforms may be reused or copied, it appears that experimental conditions are usually adapted for every phenotyping experiment in order to fulfill specific requirements and all existing experimental set ups are example among which ideas can be picked up. Phenotyping is a matter of whole pipeline rather than single technology and most phenotyping pipelines have their limiting step. Lots of progresses have been done in automation and image acquisition techniques but analyzing these images and handling large amount of data can reveal limiting. To finish with, good quality datasets are often underexploited. In particular, few experiments end up with real spatio-temporal analyses, although the data collected would suit these analyses, and synthetic traits are often the only ones to be really exploited. Limiting steps of phenotyping platforms shift from plant culture and image acquisition to analysis of large datasets produced and efforts are needed to exploit these dataset at best.

3. Root breeding: how do we turn knowledge on root development to progresses in yield and resilience to stresses?

High throughput phenotyping techniques can be used to screen large number of plants for root traits and find genetic determinant of these traits. We showed the existence of variability in primary root growth and lateral root density in a diversity panel derived from cultivated varieties, which opened the possibility to use this existing variability in root system breeding. An association study was started on a large panel of pearl millet inbred lines from diverse origins to understand the genetic control of primary root elongation and the origin of the

existing diversity. Results will reveal new information on the genetic control of root growth and open the way to marker-assisted selection for root traits in pearl millet.

It is necessary to assess the role of root trait potentially targeted for breeding. A first approach is the use of functional-structural plant models to test hypotheses on the impact of different root traits on water or nutrient capture. The use of these models fastens trait evaluation in different environments and could be used to find optimal traits in certain conditions. Indeed, optimal traits are not always intuitive, for example low crown root number was shown to be beneficial for nitrate uptake in maize (Saengwilai et al., 2014) and low lateral root density is beneficial for drought tolerance (Zhan et al., 2015). For example, favoring phosphate uptake could for more efficient than water uptake if phosphate is the most limiting factor. For pearl millet, two contrasted lines have been phenotyped for root architecture and will be used for parameterization and testing of such model (Adama NDOUR PhD in our team). Beside, a field phenotyping study has been started on pearl millet to compare architectural traits measured in rhizotron and in soil and to adapt existing functional-structural plant models to better represent root system architecture in soil. Among potential options, one would be to select root traits favoring mycorrhization rather than focusing only on direct nutrient uptake by the root system itself. Indeed, mycorrhization was shown to participate in early P uptake (Li et al., 2006) and favoring fungal symbiosis could be a good strategy for pearl millet, as it is usually grown on soils with poor available P. A study on the effect of mycorrhization on root system architecture and drought tolerance has been started on pearl millet in our team.

Another complementary approach is to link the findings of root phenotyping in controlled conditions with field performance on a same panel of diverse lines (Atkinson et al., 2015). For our pearl millet panel, such an experiment is underway in Senegal, at the ISRA Bambey experimental station. It consists in submitting the plants of the panel described in **Chapter 3** to an early drought stress. This was performed during the dry season and the drought stress was applied by holding watering 3 weeks after germination, during 40 days. A first experiment was run in 2015 and a second one is underway. These two experiments will be analyzed to measure the early drought tolerance of our panel in field conditions. This opens the way to look for correlations between the root traits we measured and field performances. Another option is to study a selection of inbred lines with contrasted root traits, previously identified in controlled condition phenotyping.

Root system architecture is known to be very plastic in response to environmental conditions (Rich and Watt, 2013). It is worth asking whether root breeding should be done on fixed traits or should select root system abilities to adapt to the environmental conditions. For example, in the aerial part, tillering is known to participate in pearl millet intermittent drought stress tolerance, as development of tillers is delayed compared to the main shoot and thus can compensate the loss of yield due to a drought-related failure of the main shoot (Vadez et al., 2012). At the root level, transient drought stress has been shown to repress lateral root formation in barley (Babé et al., 2012). Root system architecture of different cereals have been compared, along with their tolerance to drought (Yamauchi et al., 1996). It has been found that species presenting the best drought tolerance had a root system characterized by few but long nodal roots, many of which elongated obliquely in the soil profile, due to a large rooting angle. Under drought condition, the concentration of lateral root development shifted

to the deeper soil layers in these cereals. Pearl millet was in this case. The better drought tolerance of wheat cultivars compared to rice have been suggested to be due to plant plasticity and especially root traits (Kadam et al., 2015). This exemplifies that improved root system plasticity could increase drought tolerance in a given species and would be an interesting trait to target. Plasticity is typically measured by comparing root traits under well-watered and stressed conditions (drought or nutrient scarcity for example) (Kadam et al., 2015; Padilla et al., 2007; Yamauchi et al., 1996), which requires to finely calibrate stress application if we want to insure measurement reproducibility.

4. Orphan cereals: how do we apply knowledge from model plants to these poorly-known crops?

One originality of my PhD was the focus on pearl millet, a little-studied African cereal. Studying pearl millet has an interest by itself as its improvement by breeding is susceptible to increase food security in arid countries but it also had some practical advantages. One of them was the very fast germination time, generally under 24 hours and the absence of need to vernalize seeds, as it is the case in winter wheat for example.

The study of this plant cast light on the way knowledge acquired on model plants can be transposed to non-model crops. Model plants have been selected to focus research efforts on single species (Izawa and Shimamoto, 1996). It is expected that gene controlling root growth, for example, will be found more easily with the help of knowledge on *Arabidopsis*, rice or maize. Moreover, the confrontation of genes found in pearl millet with information available on model plants may be a way to understand the specificities of this species, for example in terms of root growth rate. Although studies at small scales export quite well to non-model plants (Orman-Ligeza et al., 2013), physiological knowledge seems to be more specific to each plant. In particular, abiotic stress tolerance is reported to benefit a lot from the study of grasses rather than model dicots (Tester and Bacic, 2005). Maize is a cereal that is at the same time quite close phylogenetically to pearl millet and that has been subject of many studies, but these two cereals still have a lot of differences. For example, domestication has led to very different morphologies for these two cereals, maize having numerous ears per stem but does not tiller, contrary to pearl millet. Culture conditions of these two cereals are also different. Some similarities have been found for lateral root types and anatomy between pearl millet and other better known cereals but it seemed to be closer to wheat or rice than to maize. Studying poorly explored plants belonging to various branches of the phylogenetic tree of cereals thus reveals unknown commonalities among its members. Model plants seem to be a useful tool for molecular and genetic studies but this can hardly be extended to higher scales, like physiological or field studies.

To conclude, my PhD work provided a precise description of pearl millet root system that was little studied to date. Our data were used for parameterization and testing of functional-structural plant models simulating root growth and water transport. A pipeline was developed for characterization of the lateral root growth rate profiles, including an original statistical model that may be used on other cereals. Finally, results from our association study will reveal new information on the genetic control of root growth and open the way to marker assisted selection for root traits in pearl millet.

References

Aguirrezabal, L. A. N., Deleens, E., and Tardieu, F. (1994). Root elongation rate is accounted for by intercepted PPFD and source-sink relations in field and laboratory-grown sunflower. *Plant, Cell Environ.* 17, 443–450. doi:10.1111/j.1365-3040.1994.tb00313.x.

Andrew, D. J., and Kumar, K. A. (1992). Pearl millet for food, feed, and forage. *Adv. Agron.* 48, 89–139.

Araki, H., Morita, S., Tatsumi, J., Iijima, M., Araki, H., Morita, S., et al. (2002). Physiol-Morphological Analysis on Axile Root Growth in Upland Rice Physiol-Morphological Analysis on Axile Root Growth in Upland Rice. *Plant Prod. Sci.* 5, 286–293. doi:10.1626/pps.5.286.

Atkinson, J. A., Wingen, L. U., Griffiths, M., Pound, M. P., Gaju, O., Foulkes, M. J., et al. (2015). Phenotyping pipeline reveals major seedling root growth QTL in hexaploid wheat. *J. Exp. Bot.* doi:10.1093/jxb/erv006.

Babé, A., Lavigne, T., Séverin, J.-P., Nagel, K. a, Walter, A., Chaumont, F., et al. (2012). Repression of early lateral root initiation events by transient water deficit in barley and maize. *Philos. Trans. R. Soc. Lond. B. Biol. Sci.* 367, 1534–41. doi:10.1098/rstb.2011.0240.

Bai, C., Liang, Y., and Hawkesford, M. J. (2013). Identification of QTLs associated with seedling root traits and their correlation with plant height in wheat. *J. Exp. Bot.* 64, 1745–1753. doi:10.1093/jxb/ert041.

Band, L. R., Wells, D. M., Larrieu, A., Sun, J., Middleton, A. M., French, A. P., et al. (2012). Root gravitropism is regulated by a transient lateral auxin gradient controlled by a tipping-point mechanism. *Proc. Natl. Acad. Sci. U. S. A.* 109, 4668–4673. doi:10.1073/pnas.1201498109.

Baskin, T. I., Peret, B., Balu??ka, F., Benfey, P. N., Bennett, M., Forde, B. G., et al. (2010). Shootward and rootward: Peak terminology for plant polarity. *Trends Plant Sci.* 15, 593–594. doi:10.1016/j.tplants.2010.08.006.

Bationo, A., Kihara, J., Vanlauwe, B., Waswa, B., and Kimetu, J. (2007). Soil organic carbon dynamics, functions and management in West African agro-ecosystems. *Agric. Syst.* 94, 13–25. doi:10.1016/j.agsy.2005.08.011.

Von Behrens, I., Komatsu, M., Zhang, Y., Berendzen, K. W., Niu, X., Sakai, H., et al. (2011). Rootless with undetectable meristem 1 encodes a monocot-specific AUX/IAA protein that controls embryonic seminal and post-embryonic lateral root initiation in maize. *Plant J.* 66, 341–353. doi:10.1111/j.1365-313X.2011.04495.x.

Bennetzen, J. L., Schmutz, J., Wang, H., Percifield, R., Hawkins, J., Pontaroli, A. C., et al. (2012). Reference genome sequence of the model plant Setaria. *Nat. Biotechnol.* 30, 555–61. doi:10.1038/nbt.2196.

Berg, A., De Noblet-Ducoudré, N., Sultan, B., Lengaigne, M., and Guimberteau, M. (2013). Projections of climate change impacts on potential C4 crop productivity over tropical regions. *Agric. For. Meteorol.* 170, 89–102. doi:10.1016/j.agrformet.2011.12.003.

Bidinger, F. R., and Hash, C. T. (2004). "Pearl millet," in *Physiology and Biotechnology Integration for Plant Breeding*, eds. H. T. Nguyen and A. Blum (New York), 225–270.

Bilquez, A. (1974). Amélioration des mils au Sénégal.

Bishopp, A., and Lynch, J. P. (2015). The hidden half of crop yields. *Nat. Plants* 1, 15117.

doi:10.1038/nplants.2015.117.

Bohn, M., Novais, J., Fonseca, R., Tuberosa, R., and Grift, T. E. (2006). Genetic evaluation of root complexity in maize. *Acta Agron. Hungarica* 54, 291–303. doi:10.1556/AAgr.54.2006.3.GENETIC.

Brück, H., Piro, B., Sattelmacher, B., and Payne, W. a. (2003a). Spatial distribution of roots of pearl millet on sandy soils of Niger. *Plant Soil* 256, 149–159.

Brück, H., Sattelmacher, B., and Payne, W. A. (2003b). Varietal differences in shoot and rooting parameters of pearl millet on sandy soils in Niger. *Plant Soil* 251, 175–185.

Brunken, J., Wet, J. de, and Harlan, J. (1977). The morphology and domestication of pearl millet. *Econ. Bot.* 31, 163–174.

Bühlmann, P., and Wyner, A. J. (1999). Variable length markov chains. *Ann. Stat.* 27, 480–513. doi:10.1214/aos/1018031204.

Burton, A. L., Johnson, J. M., Foerster, J. M., Hirsch, C. N., Buell, C. R., Hanlon, M. T., et al. (2014). QTL mapping and phenotypic variation for root architectural traits in maize (Zea mays L.). *Theor. Appl. Genet.* 127, 2293–2311. doi:10.1007/s00122-014-2353-4.

Casero, P. J., Casimiro, I., and Lloret, P. G. (1995). Lateral root initiation by asymmetrical transverse divisions of pericycle cells in four plant species: Raphanus sativus, Helianthus annuus, Zea mays, andDaucus carota. *Protoplasma* 188, 49–58. doi:10.1007/BF01276795.

Castillo, C., Puccio, F., Morales, D., Borie, F., and Sieverding, E. (2012). Early arbuscular mycorrhiza colonization of wheat, barley and oats in Andosols of southern Chile. *J. Soil Sci. Plant Nutr.* 12, 511–524.

Champoux, M. C., Wang, G., Sarkarung, S., Mackill, D. J., O'Toole, J. C., Huang, N., et al. (1995). Locating genes associated with root morphology and drought avoidance in rice via linkage to molecular markers. *Theor. Appl. Genet.* 90, 969–981. doi:10.1007/BF00222910.

Chen, C.-W., Yang, Y.-W., Lur, H.-S., Tsai, Y.-G., and Chang, M.-C. (2005). A Novel Function of Abscisic Acid in the Regulation of Rice (Oryza sativa L.) Root Growth and Development. *Plant Cell Physiol.* 47, pci216. doi:10.1093/pcp/pci216.

Chien, S. H., Henao, J., Christianson, C. B., Bationo, a., and Mokwunye, a. U. (1990). Agronomic Evaluation of Two Unacidulated and Partially Acidulated Phosphate Rocks Indigenous to Niger. *Soil Sci. Soc. Am. J.* 54, 1772. doi:10.2136/sssaj1990.03615995005400060045x.

Chopart, J.-L. (1983). Etude du systeme racinaire du mil (pennisetum typhoides) dans un sol sableux du Sénégal. *Agron. Trop.* XXXVIII, 37–51.

Clark, R. T., Famoso, A. N., Zhao, K., Shaff, J. E., Craft, E. J., Bustamante, C. D., et al. (2013). High-throughput two-dimensional root system phenotyping platform facilitates genetic analysis of root growth and development. *Plant, Cell Environ.* 36, 454–466. doi:10.1111/j.1365-3040.2012.02587.x.

Clotault, J., Thuillet, A.-C., Buiron, M., De Mita, S., Couderc, M., Haussmann, B. I. G., et al. (2012). Evolutionary history of pearl millet (Pennisetum glaucum [L.] R. Br.) and selection on flowering genes since its domestication. *Mol. Biol. Evol.* 29, 1199–212. doi:10.1093/molbev/msr287.

Comas, L. H., Becker, S. R., Cruz, V. M. V, Byrne, P. F., and Dierig, D. a (2013). Root traits contributing to plant productivity under drought. *Front. Plant Sci.* 4, 442. doi:10.3389/fpls.2013.00442.

Coudert, Y., Dievart, A., Droc, G., and Gantet, P. (2013). ASL/LBD phylogeny suggests that genetic mechanisms of root initiation downstream of auxin are distinct in lycophytes and euphyllophytes. *Mol. Biol. Evol.* 30, 569–572. doi:10.1093/molbev/mss250.

Courtois, B., Audebert, A., Dardou, A., Roques, S., Ghneim-Herrera, T., Droc, G., et al. (2013). Genome-wide association mapping of root traits in a japonica rice panel. *PLoS One* 8, 1–18. doi:10.1371/journal.pone.0078037.

Coutts, M. P. (1987). Developmental processes in tree root systems. *Can. J. For. Res.* 17, 761–767.

Csiszár, I., and Talata, Z. (2006). Context tree estimation for not necessarily finite memory processes, Via BIC and MDL. *IEEE Trans. Inf. Theory* 52, 1007–1016. doi:10.1109/TIT.2005.864431.

Debi, B. R., Taketa, S., and Ichii, M. (2005). Cytokinin inhibits lateral root initiation but stimulates lateral root elongation in rice (Oryza sativa). *J. Plant Physiol.* 162, 507–515. doi:10.1016/j.jplph.2004.08.007.

Devos, K. M., Pittaway, T. S., Reynolds, A., and Gale, M. D. (2000). Comparative mapping reveals a complex relationship between the pearl millet genome and those of foxtail millet and rice. *Theor. Appl. Genet.* 100, 190–198. doi:10.1007/s001220050026.

Dhondt, S., Wuyts, N., and Inzé, D. (2013). Cell to whole-plant phenotyping: The best is yet to come. *Trends Plant Sci.* 18, 1360–1385. doi:10.1016/j.tplants.2013.04.008.

Dinkelaker, B., Hengeler, C., and Marschner, H. (1995). Distribution and function of proteoid roots and other root clusters. *Acta Bot.* 108, 169–276. doi:10.1111/j.1438-8677.1995.tb00850.x.

Doussan, C., Jouniaux, L., and Thony, J. L. (2002). Variations of self-potential and unsaturated water flow with time in sandy loam and clay loam soils. *J. Hydrol.* 267, 173–185. doi:10.1016/S0022-1694(02)00148-8.

Drew, M. C. (1975). Comparison of the effects of a localized supply of phosphate, nitrate, ammonium and potassium on the growth of the seminal root sytem, and the shoot, in barley. 75, 479–490.

van Dusschoten, D., Metzner, R., Kochs, J., Postma, J. A., Pflugfelder, D., Buehler, J., et al. (2016). Quantitative 3D analysis of plant roots growing in soil using magnetic resonance imaging. *Plant Physiol.* 170, pp.01388.2015. doi:10.1104/pp.15.01388.

Edwards, E. J. (2012). Rapid report New grass phylogeny resolves deep evolutionary relationships and discovers C 4 origins. 304–312.

Eldin, M. (1993). "Analyse de l'effet des déficits hydriques sur la récolte du mil au Niger : conséquences agronomiques," in *Le mil en Afrique, diversité genetique et agro-physiologique: Potentialites et contraintes pour l'amelioriation et la culture.*, ed. S. Hamon (Paris), 149–160. Available at: http://www.documentation.ird.fr/hor/fdi:38958.

Fahlgren, N., Feldman, M., Gehan, M. A., Wilson, M. S., Shyu, C., Bryant, D. W., et al. (2015a). A versatile phenotyping system and analytics platform reveals diverse temporal responses to water availability in Setaria. *Mol. Plant* 8, 1520–1535. doi:10.1016/j.molp.2015.06.005.

Fahlgren, N., Gehan, M. a, and Baxter, I. (2015b). Lights, camera, action: high-throughput plant phenotyping is ready for a close-up. *Curr. Opin. Plant Biol.* 24, 93–99. doi:10.1016/j.pbi.2015.02.006.

FAO (Food and Agriculture Organization of the United Nation) (2014). FAOSTAT database. Available at: http://faostat3.fao.org/browse/Q/*/E.

FAO (Food and Agriculture Organization of the United Nation), FIDA (Fond international de développement agricole), and PAM (Programme Alimentaire Mondial) (2015). L'état de l'insécurité alimentaire dans le monde 2015. Objectifs internationaux 2015 de réduction de la faim: des progrès inégaux. Rome.

Forde, B. G. (2009). Is it good noise? The role of developmental instability in the shaping of a root system. *J. Exp. Bot.* 60, 3989–4002. doi:10.1093/jxb/erp265.

Freixes, S., Thibaud, M. C., Tardieu, F., and Muller, B. (2002). Root elongation and branching is related to local hexose concentration in arabidopsis thaliana seedlings. *Plant, Cell Environ.* 25, 1357–1366. doi:10.1046/j.1365-3040.2002.00912.x.

Gamuyao, R., Chin, J. H., Pariasca-Tanaka, J., Pesaresi, P., Catausan, S., Dalid, C., et al. (2012). The protein kinase Pstol1 from traditional rice confers tolerance of phosphorus deficiency. *Nature* 488, 535–539. doi:10.1038/nature11346.

Gemenet, D. C., Leiser, W. L., Zangre, R. G., Angarawai, I. I., Sanogo, M. D., Sy, O., et al. (2015). Association analysis of low-phosphorus tolerance in West African pearl millet using DArT markers. *Mol. Breed.* 35, 171. doi:10.1007/s11032-015-0361-y.

González-Rabanal, F., Casal, M., and Trabaud, L. (1994). Effects of high temperatures, ash and seed position in the inflorescence on the germination of three Spanish grasses. *J. Veg. Sci.* 5, 289–294. doi:10.2307/3235851.

Gowda, V. R. P., Henry, A., Yamauchi, A., Shashidhar, H. E., and Serraj, R. (2011). Root biology and genetic improvement for drought avoidance in rice. *F. Crop. Res.* 122, 1–13. doi:10.1016/j.fcr.2011.03.001.

Guédon, Y. (2003). Estimating Hidden Semi-Markov Chains From Discrete Sequences. *J. Comput. Graph. Stat.* 12, 604–639. doi:10.1198/1061860032030.

Guédon, Y. (2005). Hidden hybrid Markov / semi-Markov chains. *Comput. Stat. Data Anal.* 49, 663–688. doi:10.1016/j.csda.2004.05.033.

Guédon, Y. (2007). Exploring the state sequence space for hidden Markov and semi-Markov chains. *Comput. Stat. Data Anal.* 51, 2379–2409. doi:10.1016/j.csda.2006.03.015.

Guigaz, M. (2002). *Memento de l'Agronome*. Quae. , eds. CIRAD-GRET and Ministère des Affaires Etrangères.

Gurney, A. L., Slate, J., Press, M. C., and Scholes, J. D. (2006). A novel form of resistance in rice to the angiosperm parasite Striga hermonthica. *New Phytol.* 169, 199–208. doi:10.1111/j.1469-8137.2005.01560.x.

Gutterman, Y. (2000). "Maternal Effects on Seeds During Development," in *Seeds: The Ecology of Regeneration in Plant Communities (2nd edition)* (Wallingford: CABI Publishing), 59–84. doi:10.1079/9780851994321.0059.

Henry, S., Divol, F., Bettembourg, M., Bureau, C., Guiderdoni, E., Périn, C., et al. (2016). Immunoprofiling of Rice Root Cortex Reveals Two Cortical Subdomains. *Front. Plant Sci.* 6, 1–9. doi:10.3389/fpls.2015.01139.

Herder, G. Den, Van Isterdael, G., Beeckman, T., and De Smet, I. (2010). The roots of a new green revolution. *Trends Plant Sci.* 15, 600–607. doi:10.1016/j.tplants.2010.08.009.

Hetz, W., Hochholdinger, F., Schwall, M., and Feix, G. (1996). Isolation and characterization of rtcs, a maize mutant deficient in the formation of nodal roots. *Plant J.* 10, 845–857. doi:10.1046/j.1365-313X.1996.10050845.x.

Hoagland, D. R., and Arnon, D. I. (1950). The Water-Culture Method for Growing Plants without Soil. *Calif. Agric. Exp. Stn. Circ.* 347.

Hochholdinger, F., and Feix, G. (2002). "Genetic Analysis of Maize Root Development," in

Plant Roots: the Hidden Half, eds. A. Eshel and T. Beeckman (CRC Press), 239–248.

Hochholdinger, F., Park, W. J., Sauer, M., and Woll, K. (2004). From weeds to crops: Genetic analysis of root development in cereals. *Trends Plant Sci.* 9, 42–48. doi:10.1016/j.tplants.2003.11.003.

Hochholdinger, F., and Tuberosa, R. (2009). Genetic and genomic dissection of maize root development and architecture. *Curr. Opin. Plant Biol.* 12, 172–177. doi:10.1016/j.pbi.2008.12.002.

Hodge, A. (2004). The plastic plant: root responses to heterogeneous supplies of nutrients. *New Phytol.* 162, 9–24. doi:10.1111/j.1469-8137.2004.01015.x.

Ichii, M., and Ishikawa, M. (1997). Genetic analysis of newly induced Short-root mutants in Rice (Oryza sativa L.). *Breed. Sci.* 47, 121–125. Available at: http://www.ncbi.nlm.nih.gov/pubmed/8720163.

ICRISAT (2013). EXPLOREit @ ICRISAT. Available at: http://exploreit.icrisat.org/page/pearl_millet/680 [Accessed June 15, 2016].

Inukai, Y., Miwa, M., Nagato, Y., Kitano, H., and Yamauchi, A. (2001a). Characterization of Rice Mutants Deficient in the Formation of Crown Roots. *Breed. Sci.* 51, 123–129. doi:10.1270/jsbbs.51.123.

Inukai, Y., Miwa, M., Nagato, Y., Kitano, H., and Yamauchi, A. (2001b). RRLI, RRL2 and CRL2 loci regulating root elongation in rice. *Breed. Sci.* 51, 231–239. doi:10.1270/jsbbs.51.231.

Inukai, Y., Sakamoto, T., Ueguchi-Tanaka, M., Shibata, Y., Gomi, K., Umemura, I., et al. (2005). Crown rootless1, which is essential for crown root formation in rice, is a target of an AUXIN RESPONSE FACTOR in auxin signaling. *Plant Cell* 17, 1387–1396. doi:10.1105/tpc.105.030981.

Iyer-Pascuzzi, A. S., Symonova, O., Mileyko, Y., Hao, Y., Belcher, H., Harer, J., et al. (2010). Imaging and analysis platform for automatic phenotyping and trait ranking of plant root systems. *Plant Physiol.* 152, 1148–1157. doi:10.1104/pp.109.150748.

Izawa, T., and Shimamoto, K. (1996). Becoming a model plant: The importance of rice to plant science. *Trends Plant Sci.* 1, 95–99. doi:10.1016/S1360-1385(96)80041-0.

Jain, M., Kaur, N., Garg, R., Thakur, J. K., Tyagi, A. K., and Khurana, J. P. (2006). Structure and expression analysis of early auxin-responsive Aux/IAA gene family in rice (Oryza sativa). *Funct. Integr. Genomics* 6, 47–59. doi:10.1007/s10142-005-0005-0.

Jansen, L., Hollunder, J., Roberts, I., Forestan, C., Fonteyne, P., Van Quickenborne, C., et al. (2013). Comparative transcriptomics as a tool for the identification of root branching genes in maize. *Plant Biotechnol. J.* 11, 1092–1102. doi:10.1111/pbi.12104.

Javot, H., Lauvergeat, V., Santoni, V., Martin-Laurent, F., Güçlü, J., Vinh, J., et al. (2003). Role of a Single Aquaporin Isoform in Root Water Uptake. *Plant Cell* 15, 509–522. doi:10.1105/tpc.008888.

Jayne, B., and Quigley, M. (2014). Influence of arbuscular mycorrhiza on growth and reproductive response of plants under water deficit: a meta-analysis. *Mycorrhiza* 24, 109–19. doi:10.1007/s00572-013-0515-x.

Jordan, M. O., Harada, J., Bruchou, C., and Yamazaki, K. (1993). Maize nodal root ramification: Absence of dormant primordia, root classification using histological parameters and consequences on sap conduction. *Plant Soil* 153, 125–143. doi:10.1007/BF00010551.

Kadam, N. N., Yin, X., Bindraban, P. S., Struik, P. C., and Jagadish, K. S. V (2015). Does

Morphological and Anatomical Plasticity during the Vegetative Stage Make Wheat More Tolerant of Water Deficit Stress Than Rice? *Plant Physiol.* 167, 1389–401. doi:10.1104/pp.114.253328.

Kato, Y., Abe, J., Kamoshita, A., and Yamagishi, J. (2006). Genotypic variation in root growth angle in rice (Oryza sativa L.) and its association with deep root development in upland fields with different water regimes. *Plant Soil* 287, 117–129. doi:10.1007/s11104-006-9008-4.

Kitomi, Y., Inahashi, H., Takehisa, H., Sato, Y., and Inukai, Y. (2012). OsIAA13-mediated auxin signaling is involved in lateral root initiation in rice. *Plant Sci.* 190, 116–122. doi:10.1016/j.plantsci.2012.04.005.

Kitomi, Y., Ito, H., Hobo, T., Aya, K., Kitano, H., and Inukai, Y. (2011). The auxin responsive AP2/ERF transcription factor CROWN ROOTLESS5 is involved in crown root initiation in rice through the induction of OsRR1, a type-A response regulator of cytokinin signaling. *Plant J.* 67, 472–484. doi:10.1111/j.1365-313X.2011.04610.x.

Kitomi, Y., Ogawa, A., Kitano, H., and Inukai, Y. (2008). CRL4 regulates crown root formation through auxin transport in rice. *Plant Root* 2, 19–28. doi:10.3117/plantroot.2.19.

Kountche, B. A., Hash, C. T., Dodo, H., Laoualy, O., Sanogo, M. D., Timbeli, A., et al. (2013). Development of a pearl millet Striga-resistant genepool: Response to five cycles of recurrent selection under Striga-infested field conditions in West Africa. *F. Crop. Res.* 154, 82–90. doi:10.1016/j.fcr.2013.07.008.

Kuijken, R. C. P., van Eeuwijk, F. a, Marcelis, L. F. M., and Bouwmeester, H. J. (2015). Root phenotyping: from component trait in the lab to breeding. *J. Exp. Bot.* 66, 5389–401. doi:10.1093/jxb/erv239.

Lagerwerff, J. V., Ogata, G., and E., E. H. (1961). Control of osmotic pressure of culture solutions with polyethylene glycol. *Science (80-.).* 133, 1486–1487. doi:http://dx.doi.org/10.1126/science.133.3463.1486.

Lartaud, M., Perin, C., Courtois, B., Thomas, E., Henry, S., Bettembourg, M., et al. (2014). PHIV-RootCell: a supervised image analysis tool for rice root anatomical parameter quantification. *Front. Plant Sci.* 5, 790. doi:10.3389/fpls.2014.00790.

Lavenus, J., Goh, T., Roberts, I., Guyomarc'h, S., Lucas, M., De Smet, I., et al. (2013). Lateral root development in Arabidopsis: Fifty shades of auxin. *Trends Plant Sci.* 18, 1360–1385. doi:10.1016/j.tplants.2013.04.006.

Lecompte, F., Pagès, L., and Ozier-Lafontaine, H. (2005). Patterns of variability in the diameter of lateral roots in the banana root system. *New Phytol.* 167, 841–850. doi:10.1111/j.1469-8137.2005.01457.x.

Li, H., Smith, S. E., Holloway, R. E., Zhu, Y., and Smith, F. A. (2006). Arbuscular mycorrhizal fungi contribute to phosphorus uptake by wheat grown in a phosphorus-fixing soil even in the absence of positive growth responses. *New Phytol.* 172, 536–543. doi:10.1111/j.1469-8137.2006.01846.x.

Li, H., Wang, H., and Yin, Y. (2012). Interdecadal variation of the West African summer monsoon during 1979-2010 and associated variability. *Clim. Dyn.* 39, 2883–2894. doi:10.1007/s00382-012-1426-9.

Li, J., Zhao, Y., Chu, H., Wang, L., Fu, Y., Liu, P., et al. (2015). SHOEBOX Modulates Root Meristem Size in Rice through Dose-Dependent Effects of Gibberellins on Cell Elongation and Proliferation. *PLoS Genet.* 11, 1–21. doi:10.1371/journal.pgen.1005464.

Lièvre, M., Granier, C., and Guédon, Y. (2016). Identifying developmental phases in the

Arabidopsis thaliana rosette using integrative segmentation models. *New Phytol.* doi:10.1111/nph.13861.

Liu, S., Wang, J., Wang, L., Wang, X., Xue, Y., Wu, P., et al. (2009). Adventitious root formation in rice requires OsGNOM1 and is mediated by the OsPINs family. *Cell Res.* 19, 1110–1119. doi:10.1038/cr.2009.70.

Lobet, G., Pagès, L., and Draye, X. (2011). A novel image-analysis toolbox enabling quantitative analysis of root system architecture. *Plant Physiol.* 157, 29–39. doi:10.1104/pp.111.179895.

Lynch, J. P. (2011). Root Phenes for Enhanced Soil Exploration and Phosphorus Acquisition: Tools for Future Crops. *Plant Physiol.* 156, 1041–1049. doi:10.1104/pp.111.175414.

Lynch, J. P., Chimungu, J. G., and Brown, K. M. (2014). Root anatomical phenes associated with water acquisition from drying soil: Targets for crop improvement. *J. Exp. Bot.* 65, 6155–6166. doi:10.1093/jxb/eru162.

Lynch, J. P., and Ho, M. D. (2005). Rhizoeconomics: Carbon costs of phosphorus acquisition. *Plant Soil* 269, 45–56. doi:10.1007/s11104-004-1096-4.

MacLeod, R. D. (1990). Lateral root primordium inception in Zea mays L. *Environ. Exp. Bot.* 30, 225–234. doi:10.1016/0098-8472(90)90068-F.

Mairhofer, S., Zappala, S., Tracy, S. R., Sturrock, C., Bennett, M., Mooney, S. J., et al. (2012). RooTrak: Automated Recovery of Three-Dimensional Plant Root Architecture in Soil from X-Ray Microcomputed Tomography Images Using Visual Tracking. *Plant Physiol.* 158, 561–569. doi:10.1104/pp.111.186221.

Maiti, R. K., and Bidinger, F. R. (1981). Growth and development of the pearl millet plant. *ICRISAT Res. Bull.*

Malamy, J. E. (2005). Intrinsic and environmental response pathways that regulate root system architecture. *Plant, Cell Environ.* 28, 67–77. doi:10.1111/j.1365-3040.2005.01306.x.

Malamy, J. E., and Benfey, P. N. (1997). Organization and cell differentiation in lateral roots of Arabidopsis thaliana. *Development* 124, 33–44. doi:VL - 124.

Manning, K., Pelling, R., Higham, T., Schwenniger, J.-L., and Fuller, D. Q. (2011). 4500-Year old domesticated pearl millet (Pennisetum glaucum) from the Tilemsi Valley, Mali: new insights into an alternative cereal domestication pathway. *J. Archaeol. Sci.* 38, 312–322. doi:10.1016/j.jas.2010.09.007.

Mariac, C., Luong, V., Kapran, I., Mamadou, A., Sagnard, F., Deu, M., et al. (2006). Diversity of wild and cultivated pearl millet accessions (Pennisetum glaucum [L.] R. Br.) in Niger assessed by microsatellite markers. *Theor. Appl. Genet.* 114, 49–58. doi:10.1007/s00122-006-0409-9.

Meijón, M., Satbhai, S. B., Tsuchimatsu, T., and Busch, W. (2014). Genome-wide association study using cellular traits identifies a new regulator of root development in Arabidopsis. *Nat. Genet.* 46, 77–81. doi:10.1038/ng.2824.

Monat, C., Tranchant-Dubreuil, C., Kougbeadjo, A., Farcy, C., Ortega-Abboud, E., Amanzougarene, S., et al. (2015). TOGGLE: toolbox for generic NGS analyses. *BMC Bioinformatics* 16, 374. doi:10.1186/s12859-015-0795-6.

Muller, B., Stosser, M., and Tardieu, F. (1998). Spatial distributions of tssue expansion and cell division rattes are related to irradiance and to sugar content in the growing zone of maize roots. *Plant. Cell Environ.* 21, 149–158.

National Research Council (1997). *Lost Crops of Africa*.

Neufeld, H. S., Durall, D. M., Rich, P. M., and Tingey, D. T. (1989). A rootbox for quantitative observations on intact entire root systems. *Plant Soil* 117, 295–298.

Orman-Ligeza, B., Parizot, B., Gantet, P. P., Beeckman, T., Bennett, M. J., and Draye, X. (2013). Post-embryonic root organogenesis in cereals: branching out from model plants. *Trends Plant Sci.* 18, 459–67. doi:10.1016/j.tplants.2013.04.010.

Oumar, I., Mariac, C., Pham, J.-L., and Vigouroux, Y. (2008). Phylogeny and origin of pearl millet (Pennisetum glaucum [L.] R. Br) as revealed by microsatellite loci. *Theor. Appl. Genet.* 117, 489–97. doi:10.1007/s00122-008-0793-4.

Padilla, F. M., Miranda, J. D. D., and Pugnaire, F. I. (2007). Early root growth plasticity in seedlings of three Mediterranean woody species. *Plant Soil* 296, 103–113. doi:10.1007/s11104-007-9294-5.

Pagès, L. (1995). Growth patterns of the lateral roots of young oak (Quercus robur) tree seedlings Relationship with apical diameter. *New Phytol.* 130, 503–509. doi:doi: 10.1111/j.1469-8137.1995.tb04327.x.

Pagès, L. (2011). Links between root developmental traits and foraging performance. *Plant. Cell Environ.* 34, 1749–60. doi:10.1111/j.1365-3040.2011.02371.x.

Pahlavanian, A. M., and Silk, W. K. (1988). Effect of Temperature on Spatial and Temporal Aspects of Growth in the Primary Maize Root. *Plant Physiol.* 87, 529–532.

Passot, S., Gnacko, F., Moukouanga, D., Lucas, M., Guyomarc'h, S., Moreno Ortega, B., et al. (2016). Characterization of Pearl Millet Root Architecture and Anatomy Reveals Three Types of Lateral Roots. *Front. Plant Sci.* 7, 1–11. doi:10.3389/fpls.2016.00829.

Paterson, A. H., Bowers, J. E., Bruggmann, R., Dubchak, I., Grimwood, J., Gundlach, H., et al. (2009). The Sorghum bicolor genome and the diversification of grasses. *Nature* 457, 551–556. doi:10.1038/nature07723.

Payne, W. A., Lascano, R. J., Hossner, L. R., Wendt, C. W., and Onken, A. B. (1991). Pearl millet growth as affected by phosphorus and water. *Agron. J.* 83, 942–948.

Plant Ontology Available at: http://www.plantontology.org/.

Poland, J. a, and Rife, T. W. (2012). Genotyping-by-Sequencing for Plant Breeding and Genetics. *Plant Genome J.* 5, 92–102. doi:10.3835/plantgenome2012.05.0005.

Poncet, V., Lamy, F., Enjalbert, J., Joly, H., Sarr, A., and Robert, T. (1998). Genetic analysis of the domestication syndrome in pearl millet (Pennisetum glaucum L ., Poaceae): inheritance of the major characters. 81, 648–658.

Pritchard, J., Tomos, A. D., and Wyn Jones, R. G. (1987). Control of Wheat Root Elongation Growth. *J. Exp. Bot.* 38, 948–959.

R Development Core Team (2008). *R: A language and environment for statistical computing*. R Foundation for Statistical Computing, Vienna, Austria Available at: http://www.r-project.org.

Rebouillat, J., Dievart, A., Verdeil, J. L., Escoute, J., Giese, G., Breitler, J. C., et al. (2009). Molecular genetics of rice root development. *Rice* 2, 15–34. doi:10.1007/s12284-008-9016-5.

Rich, S. M., and Watt, M. (2013). Soil conditions and cereal root system architecture: review and considerations for linking Darwin and Weaver. *J. Exp. Bot.* 64, 1193–1208. doi:10.1093/jxb/ert043.

Ron, D., Singer, Y., and Tishby, N. (1997). The power of amnesia: Learning probabilistic automata with variable memory length. *Mach. Learn.* 25, 117–149. doi:10.1007/BF00114008.

Rostamza, M., Richards, R. a., and Watt, M. (2013). Response of millet and sorghum to a varying water supply around the primary and nodal roots. *Ann. Bot.* 112, 439–446. doi:10.1093/aob/mct099.

Saengwilai, P., Tian, X., and Lynch, J. P. (2014). Low crown root number enhances nitrogen acquisition from low-nitrogen soils in maize. *Plant Physiol.* 166, 581–9. doi:10.1104/pp.113.232603.

Saïdou, A. A., Mariac, C., Luong, V., Pham, J. L., Bezançon, G., and Vigouroux, Y. (2009). Association studies identify natural variation at PHYC linked to flowering time and morphological variation in pearl millet. *Genetics* 182, 899–910. doi:10.1534/genetics.109.102756.

Salehin, M., Bagchi, R., and Estelle, M. (2015). SCFTIR1/AFB-based auxin perception: mechanism and role in plant growth and development. *Plant Cell* 27, 9–19. doi:10.1105/tpc.114.133744.

Scheres, B., Wolkenfelt, H., Willemsen, V., Terlouw, M., Lawson, E., Dean, C., et al. (1994). Embryonic origin of the Arabidopsis primary root and root meristem initials. *Development* 2487, 2475–2487. doi:10.1038/36856.

Schmidt, J. E., Bowles, T. M., and Gaudin, A. C. M. (2016). Using Ancient Traits to Convert Soil Health into Crop Yield: Impact of Selection on Maize Root and Rhizosphere Function. *Front. Plant Sci.* 7, 373. doi:10.3389/fpls.2016.00373.

Schneider, C. a, Rasband, W. S., and Eliceiri, K. W. (2012). NIH Image to ImageJ: 25 years of image analysis. *Nat. Methods* 9, 671–675. doi:10.1038/nmeth.2089.

Scott-Wendt, J., Chase, R. G., and Hossner, L. R. (1988). Soil Chemical Variability in Sandy Ustalfs in Semiarid Niger, West Africa. *Soil Sci.* 145, 414. Available at: http://content.wkhealth.com/linkback/openurl?sid=WKPTLP:landingpage&an=00010694-198806000-00002.

Seago, J. L., and Fernando, D. D. (2013). Anatomical aspects of angiosperm root evolution. *Ann. Bot.* 112, 223–38. doi:10.1093/aob/mcs266.

Souci, S. W., Fachmann, W., and Kraut, H. (2000). *Food composition and nutrition tables*. 6th editio. Medpharm Scientific Publishers Stuttgart.

Steele, K. A., Price, A. H., Shashidhar, H. E., and Witcombe, J. R. (2006). Marker-assisted selection to introgress rice QTLs controlling root traits into an Indian upland rice variety. *Theor. Appl. Genet.* 112, 208–221. doi:10.1007/s00122-005-0110-4.

Sultan, B., and Gaetani, M. (2016). Agriculture in West Africa in the Twenty-first Century: climate change and impacts scenarios, and potential for adaptation. *Front. Plant Sci.* Under revi.

Takahashi, F., Sato-Nara, K., Kobayashi, K., Suzuki, M., and Suzuki, H. (2003). Sugar-induced adventitious roots in Arabidopsis seedlings. *J. Plant Res.* 116, 83–91. doi:10.1007/s10265-002-0074-2.

Takehisa, H., Sato, Y., Igarashi, M., Abiko, T., Antonio, B. A., Kamatsuki, K., et al. (2012). Genome-wide transcriptome dissection of the rice root system: Implications for developmental and physiological functions. *Plant J.* 69, 126–140. doi:10.1111/j.1365-313X.2011.04777.x.

Taramino, G., Sauer, M., Stauffer, J. L., Multani, D., Niu, X., Sakai, H., et al. (2007). The maize (Zea mays L.) RTCS gene encodes a LOB domain protein that is a key regulator of embryonic seminal and post-embryonic shoot-borne root initiation. *Plant J.* 50, 649–659. doi:10.1111/j.1365-313X.2007.03075.x.

Tester, M., and Bacic, A. (2005). Abiotic Stress Tolerances in Grasses Form Model Plants To Crop Plants. *J. Plant Pathol.* 137, 791–793. doi:10.1104/pp.104.900138.Plant.

Thaler, P., and Pagès, L. (1996). Root apical diameter and root elongation rate of rubber seedlings (Hevea brasiliensis) show parallel responses to photoassimilate availability. *Physiol. Plant.* 97, 365–371.

Tolivia, D., and Tolivia, J. (1987). Fasga : a new polychromatic method for simultaneous and differential staining of plant tissues. *J. Microsc.* 148, 113–117.

Topp, C. N., Iyer-Pascuzzi, A. S., Anderson, J. T., Lee, C.-R., Zurek, P. R., Symonova, O., et al. (2013). 3D phenotyping and quantitative trait locus mapping identify core regions of the rice genome controlling root architecture. *Proc. Natl. Acad. Sci. U. S. A.* 110, E1695–704. doi:10.1073/pnas.1304354110.

Trachsel, S., Kaeppler, S. M., Brown, K. M., and Lynch, J. P. (2011). Shovelomics: High throughput phenotyping of maize (Zea mays L.) root architecture in the field. *Plant Soil* 341, 75–87. doi:10.1007/s11104-010-0623-8.

Uga, Y., Sugimoto, K., Ogawa, S., Rane, J., Ishitani, M., Hara, N., et al. (2013). Control of root system architecture by DEEPER ROOTING 1 increases rice yield under drought conditions. *Nat. Genet.* 45, 1097–102. doi:10.1038/ng.2725.

United Nations Statistics Division (2016). UNData. Available at: http://data.un.org/Data.aspx?q=population&d=PopDiv&f=variableID%3a12.

Vadez, V., Hash, T., Bidinger, F. R., and Kholova, J. (2012). Phenotyping pearl millet for adaptation to drought. *Front. Physiol.* 3 OCT, 386. doi:10.3389/fphys.2012.00386.

Varney, G., Canny, M., Wang, X., and McCully, M. (1991). The branch roots of Zea. I. First Order Branches, Their Number, Sizes and Division into classes. *Ann. Bot.* 67, 357–364.

Varney, G. T., and McCully, M. E. (1991). The branch roots of Zea. II. Developmental loss of the apical meristem in field-grown roots. *New Phytol.* 118, 535–546. doi:10.1111/j.1469-8137.1991.tb00993.x.

Vierheilig, H., Coughlan, A. P., Wyss, U. R. S., and Recherche, C. De (1998). Ink and Vinegar, a Simple Staining Technique for Arbuscular-Mycorrhizal Fungi. *Appl. Environ. Microbiol.* 64, 5004–5007.

Waines, J. G., and Ehdaie, B. (2007). Domestication and crop physiology: Roots of green-revolution wheat. *Ann. Bot.* 100, 991–998. doi:10.1093/aob/mcm180.

Wang, J. R., Hu, H., Wang, G. H., Li, J., Chen, J. Y., and Wu, P. (2009). Expression of PIN genes in rice (Oryza sativa L.): Tissue specificity and regulation by hormones. *Mol. Plant* 2, 823–831. doi:10.1093/mp/ssp023.

Watt, M., Magee, L. J., and McCully, M. E. (2008). Types, structure and potential for axial water flow in the deepest roots of field-grown cereals. *New Phytol.* 178, 135–146. doi:10.1111/j.1469-8137.2007.02358.x.

Woll, K., Borsuk, L. a, Stransky, H., Nettleton, D., Schnable, P. S., and Hochholdinger, F. (2005). Isolation, characterization, and pericycle-specific transcriptome analyses of the novel maize lateral and seminal root initiation mutant rum1. *Plant Physiol.* 139, 1255–1267. doi:10.1104/pp.105.067330.

Wu, Q., Pagès, L., and Wu, J. (2016). Relationships between root diameter, root length and root branching along lateral roots in adult, field-grown maize. *Ann. Bot.*, mcv185. doi:10.1093/aob/mcv185.

Xu, L., Henke, M., Zhu, J., Kurth, W., and Buck-Sorlin, G. (2011). A functional structural model of rice linking quantitative genetic information with morphological development

and physiological processes. *Ann. Bot.* 107, 817–828. doi:10.1093/aob/mcq264.

Yamauchi, A., Jr, J., and Kono, Y. (1996). Root system structure and its relation to stress tolerance. in *Roots and Nitrogen in Cropping Systems of the Semi-Arid Tropics*, 211–233.

Yao, S. G., Mushika, J., Taketa, S., and Ichii, M. (2004). The short-root mutation srt5 defines a sugar-mediated root growth in rice (Oryza sativa L.). *Plant Sci.* 167, 49–54. doi:10.1016/j.plantsci.2004.02.025.

Yao, S. G., Taketa, S., and Ichii, M. (2002). A novel short-root gene that affects specifically early root development in rice (Oryza sativa L.). *Plant Sci.* 163, 207–215. doi:10.1016/S0168-9452(02)00084-5.

Yao, S. G., Taketa, S., and Ichii, M. (2003). Isolation and characterization of an abscisic acid-insensitive mutation that affects specifically primary root elongation in rice (Oryza sativa L.). *Plant Sci.* 164, 971–978. doi:10.1016/S0168-9452(03)00081-5.

York, L. M., Silberbush, M., and Lynch, J. P. (2016). Spatiotemporal variation of nitrate uptake kinetics within the maize (Zea mays) root system is associated with greater nitrate uptake and interactions with root system architectural phenes. *J. Exp. Bot.* 7. doi:10.1093/jxb/erw133.

Zegada-Lizarazu, W., and Iijima, M. (2005). Deep Root Water Uptake Ability and Water Use Efficiency of Pearl Millet in Comparison to Other Millet Species. *Plant Prod. Sci.* 8, 454–460.

Zhan, A., Schneider, H., and Lynch, J. P. (2015). Reduced Lateral Root Branching Density Improves Drought Tolerance in Maize. *Plant Physiol.* 168, 1603–15. doi:10.1104/pp.15.00187.

Zhao, Y., Cheng, S., Song, Y., Huang, Y., Zhou, S., Liu, X., et al. (2015). The Interaction between Rice ERF3 and WOX11 Promotes Crown Root Development by Regulating Gene Expression Involved in Cytokinin Signaling. *Plant Cell* 27, tpc.15.00227. doi:10.1105/tpc.15.00227.

Zhao, Y., Hu, Y., Dai, M., Huang, L., and Zhou, D.-X. (2009). The WUSCHEL-Related Homeobox Gene WOX11 Is Required to Activate Shoot-Borne Crown Root Development in Rice. *Plant Cell Online* 21, 736–748. doi:10.1105/tpc.108.061655.

Zhu, J., Brown, K. M., and Lynch, J. P. (2010). Root cortical aerenchyma improves the drought tolerance of maize (Zea mays L.). *Plant. Cell Environ.* 33, 740–9. doi:10.1111/j.1365-3040.2009.02099.x.

Zhu, Z. X., Liu, Y., Liu, S. J., Mao, C. Z., Wu, Y. R., and Wu, P. (2012). A gain-of-function mutation in OsIAA11 affects lateral root development in rice. *Mol. Plant* 5, 154–161. doi:10.1093/mp/ssr074.

Appendix

Supplementary Figure 1-1: Stele diameter of primary root (A) crown root (B) and type 3 lateral root (C) measured at different distances to the root apex

Supplementary Figure 1-2: Seed weight of each line against average primary root length after 6 DAG, measured in pouches.

Appendix 1-1: Python script to compute volume explored by the root system in 3D

Appendix 2-1: Definition of semi-Markov switching linear models and associated statistical methods

Appendix 2-2: Empirical selection of the number of classes of lateral roots.

Appendix 2-3: Algorithm for correcting growth rate profiles

Appendix 2-4: Definition of stationary variable-order Markov chains and associated statistical methods

Supplementary result 2-1: Link between interval length and lateral root type proportions

Supplementary figure 2-1: Four-state semi-Markov switching linear model estimated on the basis of maize lateral root growth rate series: (a) Growth duration distributions; (b) Graph of transitions. The possible transitions between states are represented by arcs with the attached probabilities noted nearby when < 1. The arcs entering in states indicate initial states and the attached initial probabilities are noted nearby. (c) Linear trend models estimated for each state.

Supplementary figure 2-2: Ranked posterior probabilities of the optimal assignment of each lateral root growth rate series to a group: (a) pearl millet; (b) maize. Limits (dotted lines) between unambiguously and ambiguously explained lateral root growth rate series are positioned on the basis of a curve shape criterion.

Supplementary figure 2-3: Pearl millet: daily median growth rate (and associated mean absolute deviation −m.a.d.−) for (a) 2 groups, (b) 3 groups and (c) 4 groups.

Supplementary figure 2-4: Cumulative distribution functions of the length of growth rate profiles assigned to each group: (a) pearl millet; (b) maize.

Table S2-1: Pearl millet: Overlaps (i.e. 1 – sup norm distance) between growth rate distributions corresponding to consecutive lateral root categories (α-β for 2 categories, A-B and B-C for 3 categories and a-b, b-c, and c-d for 4 categories) extracted from the optimal assignment of each lateral root growth rate profiles using the estimated 3-, 4- and 5-state semi-Markov switching linear models.

Table S2-2: Maize: Overlaps (i.e. 1 – sup norm distance) between growth rate distributions corresponding to consecutive lateral root categories (α-β for 2 categories, A-B and B-C for 3 categories and a-b, b-c, and c-d for 4 categories) extracted from the optimal assignment of each lateral root growth rate profiles using the estimated 3-, 4- and 5-state semi-Markov switching linear models.

Table S2-3: Maize: Overlaps (i.e. 1 – sup norm distance) between growth rate distributions and apical diameter distributions corresponding to consecutive lateral root categories (A-B and B-C) extracted from the optimal assignment of each lateral root growth rate profiles using the estimated 4-state semi-Markov switching linear model.

Table S2-4: Length of the interval between successive lateral roots in pearl millet, classified according to the types of the two lateral roots delimiting the interval.

Table S2-5: Length of the interval between successive lateral roots in pearl millet, classified according to the types of the two lateral roots delimiting the interval.

Résumé substantiel en français

Supplementary Figure 1-1: Stele diameter of primary root (A) crown root (B) and type 3 lateral root (C) measured at different distances to the root apex

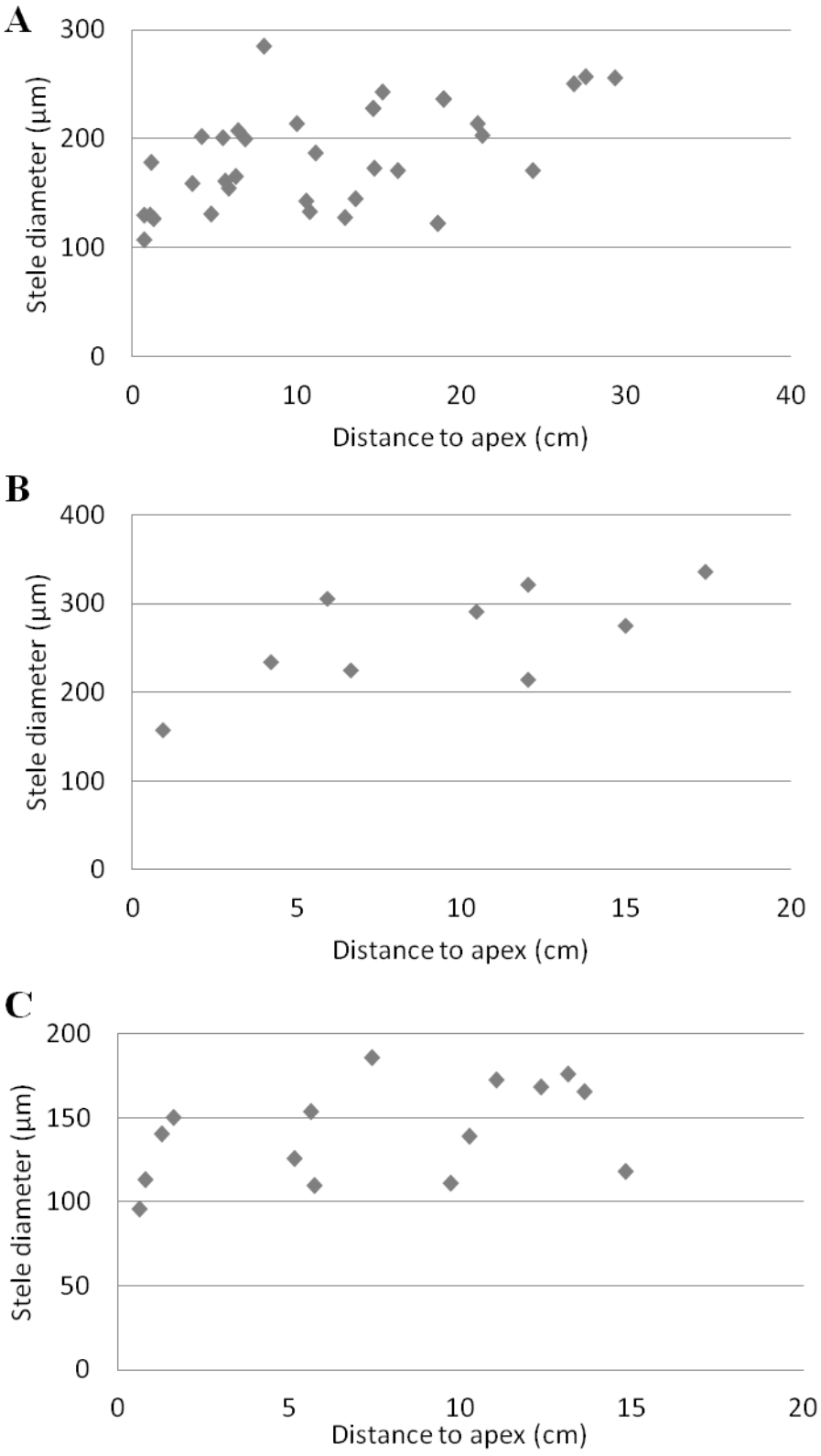

Supplementary Figure 1-2: Seed weight of each line against average primary root length after 6 DAG, measured in pouches.

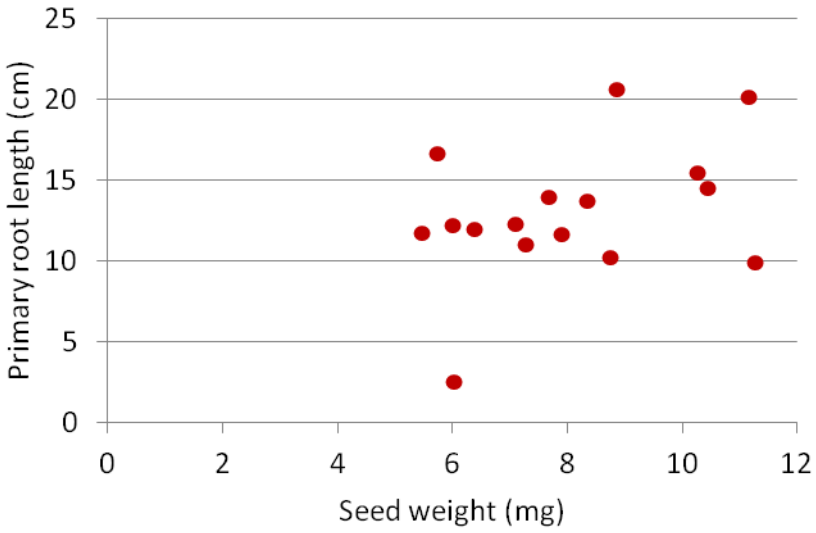

Appendix 1-1: Python function to compute volume explored by the root system in 3D

This function takes in arguments the image stack representing the root system in 3D, the distance at which to compute the explored volume and the image resolution. It returns the total volume comprised within a set distance of any point of the root system.

```
def volume_at_distance(img, distance, resolution, zslices = [ None]):
     print 'Compute volume at distance'
     distancevoxel = distance / resolution
     voxelvolume   = resolution ** 3
     maxdepth = img.shape[2]

     imgatdistance =  (0 < img) & (img < distancevoxel)

     res = []
     for zslice in zslices:
         if zslice is None:
            res.append(float(voxelvolume * np.sum(imgatdistance)))
         else:
            pzslice = (zslice[0]/resolution if not zslice[0] is None else
0, min(maxdepth,zslice[1]/resolution) if not zslice[1] is None else
maxdepth)
                 res.append(float(voxelvolume *
np.sum(imgatdistance[:,:,pzslice[0]:pzslice[1]])))

return res
```

Appendix 2-1: Definition of semi-Markov switching linear models and associated statistical methods

Semi-Markov chains

Let $\{S_t\}$ be a semi-Markov chain with finite-state space $\{0,\ldots,J-1\}$. A *J*-state semi-Markov chain $\{S_t\}$ is defined by the following parameters:

- initial probabilities $\pi_j = P(S_1 = j)$ with $\sum_j \pi_j = 1$;
- transition probabilities
  - nonabsorbing state *i*: for each $j \neq i, p_{ij} = P(S_t = j \mid S_t \neq i, S_{t-1} = i)$ with $\sum_{j \neq i} p_{ij} = 1$ and $p_{ii} = 0$ by convention,
  - absorbing state *i*: $p_{ii} = P(S_t = i \mid S_{t-1} = i) = 1$ and for each $j \neq i, p_{ij} = 0$.

An explicit occupancy distribution is attached to each nonabsorbing state:

$$d_j(u) = P(S_{t+u+1} \neq j, S_{t+u-v} = j, v = 0,\ldots,u-2 \mid S_{t+1} = j, S_t \neq j), \quad u = 1,2,\ldots$$

Since $t = 1$ is assumed to correspond to a state entering, the following relation is verified:

$$P(S_t \neq j, S_{t-v} = j, v = 1,\ldots,t) = d_j(t)\pi_j.$$

We define as possible parametric state occupancy distributions binomial distributions, Poisson distributions and negative binomial distributions with an additional shift parameter *d* ($d \geq 1$) which defines the minimum sojourn time in a given state.

The binomial distribution with parameters *d*, *n* and *p* ($q = 1-p$), B(*d*, *n*, *p*) where $0 \leq p \leq 1$, is defined by

$$d_j(u) = \binom{n-d}{u-d} p^{u-d} q^{n-u}, \qquad u = d, d+1,\ldots,n.$$

The Poisson distribution with parameters *d* and λ, P(*d*, λ), where λ is a real number ($\lambda > 0$), is defined by:

$$d_j(u) = \frac{e^{-\lambda}\lambda^{u-d}}{(u-d)!}, \qquad u = d, d+1,\ldots$$

The negative binomial distribution with parameters *d*, *r* and *p*, NB(*d*, *r*, *p*), where *r* is a real number ($r > 0$) and $0 < p \leq 1$, is defined by:

$$d_j(u) = \binom{u-d+r-1}{r-1} p^r q^{u-d}, \qquad u = d, d+1,\ldots$$

Semi-Markov switching linear models

A semi-Markov switching model can be viewed as a pair of stochastic processes $\{S_t, X_t\}$ where the "output" process $\{X_t\}$ is related to the "state" process $\{S_t\}$, which is a

finite-state semi-Markov chain, by a probabilistic function or mapping denoted by *f* (hence $X_t = f(S_t)$). Since the mapping *f* is such that a given output may be observed in different states, the state process $\{S_t\}$ is not observable directly but only indirectly through the output process $\{X_t\}$. This output process $\{X_t\}$ is related to the semi-Markov chain $\{S_t\}$ by the observation (or emission) models. The output process at time *t* depends only on the underlying semi-Markov chain at time *t*.

The output process $\{X_t\}$ is related to the state process $\{S_t\}$, by a linear trend model

$$X_t = \alpha_j + \beta_j t + \varepsilon_j, \qquad \varepsilon_j \sim \mathrm{N}(0, \sigma_j^2).$$

The maximum likelihood estimation of the parameters of a semi-Markov switching linear model requires an iterative optimization technique, which is an application of the EM algorithm. Once a semi-Markov switching model has been estimated, the most probable state series $\mathbf{s}^*$ with its associated posterior probability $P(\mathbf{S} = \mathbf{s}^* \mid \mathbf{X} = \mathbf{x})$ can be computed for each observed series **x** using the so-called Viterbi algorithm (Guédon, 2003). In our application context, the most probable state series can be interpreted as the optimal segmentation of the corresponding observed series into at most two sub-series corresponding to a given growth phase either censored or followed by a growth arrest; see Guédon (2003, 2005, 2007) for the statistical methods for hidden semi-Markov chains that directly apply to semi-Markov switching linear models.

Appendix 2-2: Empirical selection of the number of classes of lateral roots

The empirical selection of the number of lateral root classes combines the three following criteria:

1. Posterior probabilities of the optimal assignment of each lateral root growth rate profile to a growth state (followed or not by the growth arrest state at a given age) i.e. weight of the optimal assignment among all the possible assignments of a given growth rate profile. Ambiguous assignments can be explained by two types of alternative assignments that can be combined: (i) assignment to an alternative growth state, (ii) alternative assignment corresponding to a shift (usually a 1-day shift) of the transition from the optimal growth state to the growth arrest state. The posterior probabilities of the optimal assignments are expected to decrease with the increase of the number of growth states.
2. Comparison between location and dispersion measures of growth rate profiles for each lateral root class deduced from the optimal assignment of each lateral root growth rate profile. Because the empirical growth rate distributions for the less vigorous roots at high ages were semi-continuous and highly right-skewed combining zero values for arrested roots with continuous positive values for growing roots, we chose to use robust measures of location and dispersion (i.e. median and mean absolute deviation from the median). We in particular focused on the relative dispersion of growth rate distributions for the most vigorous root class. Relative dispersions are indeed irrelevant in the case of median at zero or close to zero corresponding to a high proportion of arrested roots.
3. Overlap between growth rate profiles for consecutive lateral root classes deduced from the optimal assignment of each lateral root growth rate profile. Since the growth rate profiles were highly divergent at the beginning of growth, we focused on the overlap from age 3. The high overlap in the case of a high proportion of arrested roots in the two classes being compared (less vigorous roots at the highest ages) should indeed not be considered for the selection of the number of root classes.

To assess the separability of growth rate profiles for each lateral root class, we used the sup-norm distances between the growth rate distributions at a given age for consecutive classes (i.e. A and B or B and C in the case of 3 classes):

$$\sup_x \left|F(x) - G(x)\right| = 1 - \int \min\left\{f(x), g(x)\right\} dx.$$

This distance, which is the maximum absolute difference between the two cumulative distribution functions $F(x)$ and $G(x)$, is also one minus the overlap between the two distributions in our case of non-crossing cumulative distribution functions. This distance is between 0 (full overlap, i.e. identical distributions) and 1 (no overlap). In the case of crossing cumulative distribution functions (which was rather infrequent in our context), this distance generalizes to

$$\sum_j \sup_{x \in [\tau_j, \tau_{j+1}]} \left|F(x) - G(x)\right| = 1 - \int \min\left\{f(x), g(x)\right\} dx.$$

where sup norm distances computed over each interval $[\tau_j, \tau_{j+1}]$ between two consecutive crossings of cumulative distribution functions are summed.

As expected, the proportion of ambiguously assigned lateral root increased with the number of growth states (i.e. of lateral root classes). For pearl millet, approximately 5% of lateral roots were ambiguously assigned in the case of 2 classes, 19% in the case of 3 classes and 29% in the case of 4 classes; see **SupFigure 2-2a**., For maize, approximately 9% of lateral roots were ambiguously assigned in the case of 2 classes, 22% in the case of 3 classes and 33% in the case of 4 classes; see **SupFigure 2-2b**. These proportions indeed favor the most parsimonious models but stay reasonably low even for 4-class models confirming the rather strong clustering structure. It should be noted that these posterior probabilities do not represent, in the case of uncensored growth rate profiles, the different growth phase durations in the optimal growth state but only the optimal growth phase duration. They thus provide a more stringent criterion than the posterior probabilities of the optimal assignment of each lateral root growth rate profile to a growth state.

The high dispersion measure with respect to the location measure at the highest ages for the most vigorous lateral roots makes the 2-class models rather irrelevant regarding the definition of growth rate profile classes. This is especially marked for pearl millet comparing daily median growth rate and associated mean absolute deviation of the most vigorous lateral root class between 2 and 3 classes (**SupFigure 2-3 a and b**). This is less marked for maize where the most vigorous lateral root class likely combines lateral roots whose growth rate started to decrease with lateral roots whose growth rate continued to increase at the highest ages.

In the case of 3 classes, the overlap between growth rate profiles of classes A and B stays roughly constant from age 3 onward while the overlap between growth rate profiles of classes B and C progressively increases because of the increasing masses of zero corresponding to arrested roots for these two classes; see **Tables S2-1 and S2-2**. The situation was very different in the case of 4 classes were the overlap between growth rate profiles was high from age 3 for the two classes of the less vigorous lateral roots. These two classes were thus not well separated in terms of growth rate profiles. Combining these three criteria, we selected for both species 3 lateral root classes that correspond to the best compromise between the proportion of ambiguously assigned lateral roots, the relative dispersion of growth rate profiles for the most vigorous root class and the overlap between growth rate profiles for consecutive classes.

Appendix 2-3: Algorithm for correcting growth rate profiles

Identification of putatively erroneous growth rate

The correction algorithm was based on the observation of growth rate profiles and was decomposed in two steps: the labeling of each day with a qualifier and the correction of the growth rate profile according to the qualifiers. The qualifiers were assigned according to the following rules:

- "stopped" if growth rate ≤ 0.1 mm.day^{-1};
- "growing" if growth rate > 0.1 mm.day^{-1};
- "zombie" if day is labeled "growing" and the previous day is labeled "stopped";
- "stopping" if day is labeled "growing" and the subsequent day is labeled "stopped";
- "rough stopping" if day is labeled "stopping" and growth rate is higher than a threshold representing an improbable growth rate for a root the day preceding it arrest. This threshold was fixed at 10 mm.day^{-1}.

Correction strategy of growth rate profiles

The roots containing problematic labels ("zombie" or "rough stopping") were visually examined to identify possible common sources of error in image analysis. A frequent case within the zombie category was alternative stopped and zombie states with low growth rate (< 2 mm.day^{-1}). We assumed that this pattern probably arose from slight alignment defaults in SmartRoot tracings for roots that have stopped their growth and we forced the corresponding growth rates to zero. The other frequent source of zombies was the lack of manual elongation at a single day. The result was a zero growth followed by an overestimated growth rate. In these cases, we either corrected the data directly in the SmartRoot tracing if possible, or applied a local smoothing filter on the zombie growth rate, and its two immediate neighbors. All other zombies remaining after these corrections were truncated.

Rough stops were mostly due to the root system becoming progressively denser, therefore increasing the probability for a fast-growing root to encounter another root, hampering correct monitoring of root growth. The roots containing a rough stopping were either examined and corrected individually in the case of pearl millet, where the low number of plants allowed to visually check all the images, or truncated after the last high growth rate in the case of maize.

The intermediate case, where zombie growth rate was comprised between 2 and 10 mm.day^{-1}, were dealt manually in the case of pearl millet and removed from the dataset in the case of maize.

The pearl millet dataset was initially composed of 1256 lateral roots, 9% containing a growth rate classified as zombie and 5% classified as rough stopping. The maize dataset was initially composed of 3896 lateral roots, 18% containing a growth rate classified as zombie and 4% classified as rough stopping.

Appendix 2-4: Definition of stationary variable-order Markov chains and associated statistical methods

Stationary variable-order Markov chains

In the following, we first introduce high-order Markov chains before defining variable-order Markov chains. In the case of a *r*th-order Markov chain $\{S_t; t = 0,1,\ldots\}$, the conditional distribution of S_t given $S_0,\ldots,S_{t-1}$ depends only on the values of $S_{t-r},\ldots,S_{t-1}$ but not further on $S_0,\ldots,S_{t-r-1}$,

$$P(S_t = s_t \mid S_{t-1} = s_{t-1},\ldots,S_0 = s_0) = P(S_t = s_t \mid S_{t-1} = s_{t-1},\ldots,S_{t-r} = s_{t-r})$$

In our context, the random variables represent the lateral root types and can take the three possible values A, B and C. These possible values correspond to the Markov chain states. A *J*-state *r*th-order Markov chain has $J^r(J-1)$ independent transition probabilities if all the transitions are possible. Therefore, the number of free parameters of a Markov chain increases exponentially with the order. Let the transition probabilities of a second-order Markov chain be given by

$$p_{hij} = P(S_t = j \mid S_{t-1} = i, S_{t-2} = h) \quad \text{with} \sum_j p_{hij} = 1.$$

These transition probabilities can be arranged as a $J^2 \times J$ matrix where the row $(p_{hi0},\ldots,p_{hiJ-1})$ corresponds to the transition distribution attached to the [state *h*, state *i*] memory. If for a given state *i* and for all pairs of states (h,h') with $h \neq h'$, $p_{h'ij} = p_{hij}$ for each state *j*, i.e. once S_{t-1} is known, S_{t-2} conveys no further information about S_t, the *J* memories of length 2 [state *h*, state *i*] with $h = 0,\ldots,J-1$ can be grouped together and replaced by the single [state *i*] memory of length 1 with associated transition distribution $(p_{i0},\ldots,p_{iJ-1})$. This illustrates the principle used to build a variable-order Markov chain where the order (or memory length) is variable and depends on the "context" within the sequence. The memories of a Markov chain can be arranged as a memory tree such that each vertex (i.e. element of a tree graph) is either a terminal vertex or has exactly *J* "offspring" vertices. A transition distribution is associated with each terminal vertex of this memory tree.

A stationary Markov chain starts from its stationary distribution and will continue to have that distribution at all subsequent time points. In the case of a variable-order Markov chain, the stationary distribution − which is the implicit initial distribution− is defined on the possible memories.

Selection of the memories of a stationary variable-order Markov chain

The order of a Markov chain can be estimated using the Bayesian information criterion (BIC). For each possible order *r*, the following quantity is computed

$$\mathrm{BIC}(r) = 2\log(L_r) - d_r \log n \quad \text{(S1)},$$

where L_r is the likelihood of the *r*th-order estimated Markov chain for the observed sequences, d_r is the number of free parameters of the *r*th-order estimated Markov chain and *n*

is the cumulative length of the observed series. The principle of this penalized likelihood criterion consists in making a trade-off between an adequate fitting of the model to the data (given by the first term in (S1)) and a reasonable number of parameters to be estimated (controlled by the second term in (S1), the penalty term). In practice, it is infeasible to compute a BIC value for each possible variable-order Markov chain of maximum order $r \leq R$ since the number of hypothetical memory trees is very large. An initial maximal memory tree is thus built combining criteria relative to the maximum order (3 or 4 in our case) and to the minimum count of memory occurrences in the observed series. This memory tree is then pruned using a two-pass algorithm which is an adaptation of the Context-tree maximizing algorithm (Csiszár and Talata, 2006): a first dynamic programming pass starting from the terminal vertices and progressing towards the root vertex for computing the maximum BIC value attached to each sub-tree rooted in a given vertex, is followed by a second tracking pass starting from the root vertex and progressing towards the terminal vertices for building the memory tree.

Supplementary result 2-1: Link between interval length and lateral root type proportions

We tested whether the interval lengths and the proportion of lateral roots types were related, based on the two plant classifications. As the number of plants were small (8 for pearl millet, 13 for maize), we put in parallel the two groupings but could not perform statistical comparison. The following results are therefore only descriptive and should be interpreted with caution. For pearl millet, two groups could be distinguished:

- the first group was formed of 3 plants, belonging to interval group a or ab, and to proportion group a or ab. It corresponded to a large interval and a low proportion of type A lateral roots.

- the second group was formed of 4 plants, belonging to interval group b and to proportion group b or c. It corresponded to a small inter-root interval and higher proportion of type A and type B lateral roots compared to the first group.

- one plant (10.9) did not fit in this grouping, as it belonged to group b for interval and to group ab for proportion.

This link suggested that more vigorous plants could present a higher lateral root density and proportionally more type A lateral roots.

For maize, no clear similarities between groups were visible.

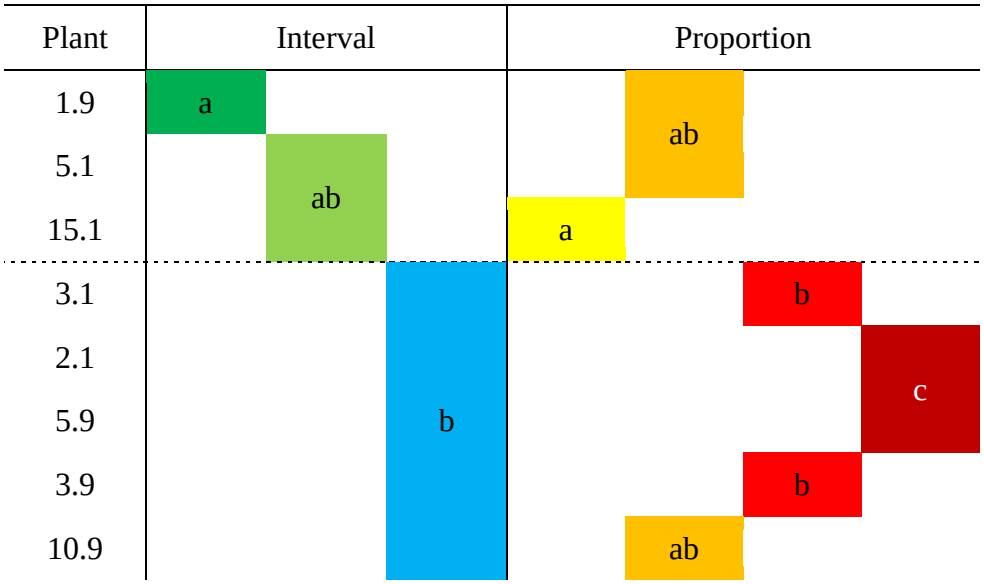

Table: Comparison of the individual plant classifications based on interval lengths and on lateral root type proportions in pearl millet.

Supplementary figure 2-1: Four-state semi-Markov switching linear model estimated on the basis of maize lateral root growth rate series: (a) Growth duration distributions; (b) Graph of transitions. The possible transitions between states are represented by arcs with the attached probabilities noted nearby when < 1. The arcs entering in states indicate initial states and the attached initial probabilities are noted nearby. (c) Linear trend models estimated for each state.

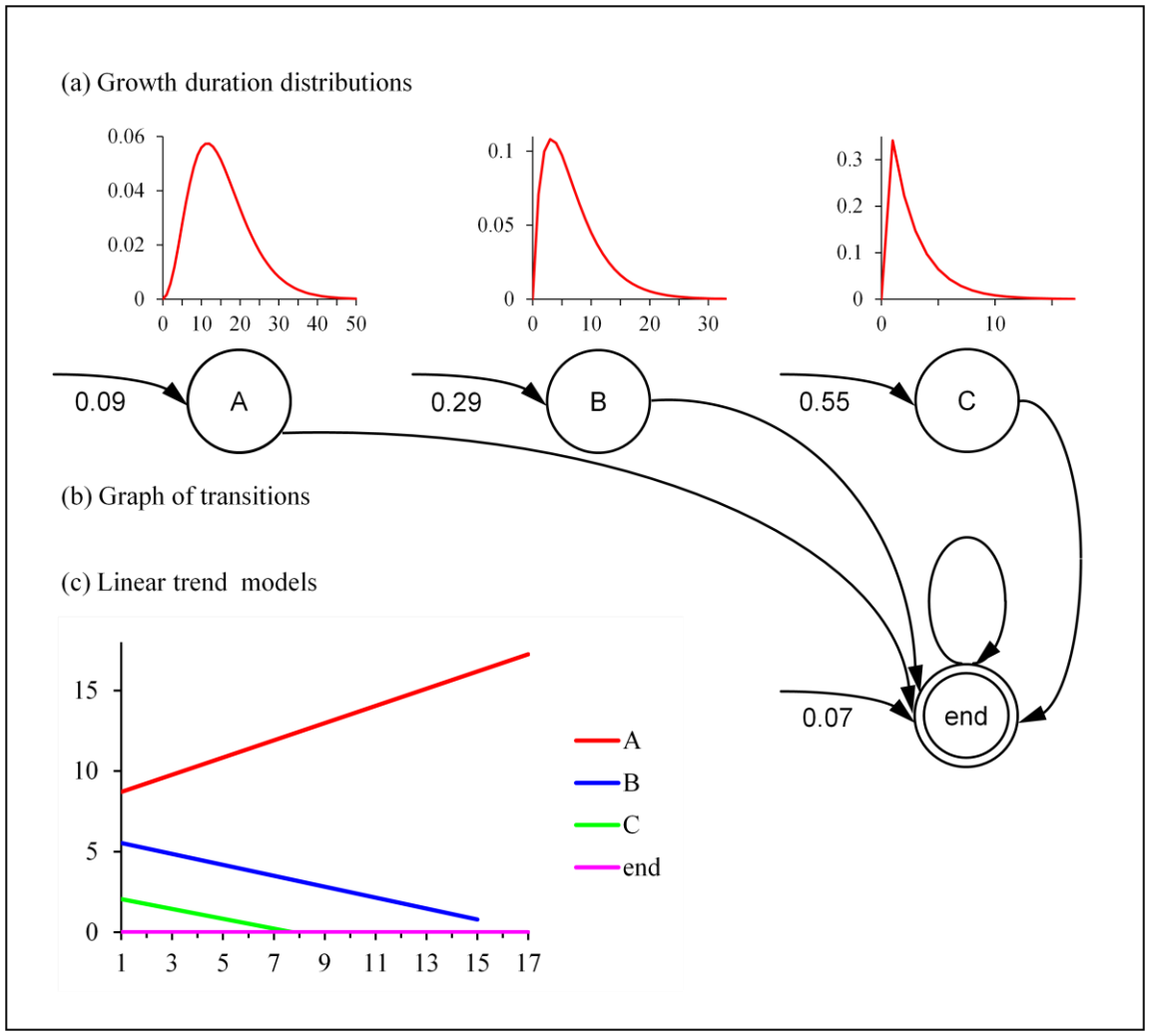

Supplementary figure 2-2: Ranked posterior probabilities of the optimal assignment of each lateral root growth rate series to a group: (a) pearl millet; (b) maize. Limits (dotted lines) between unambiguously and ambiguously explained lateral root growth rate series are positioned on the basis of a curve shape criterion.

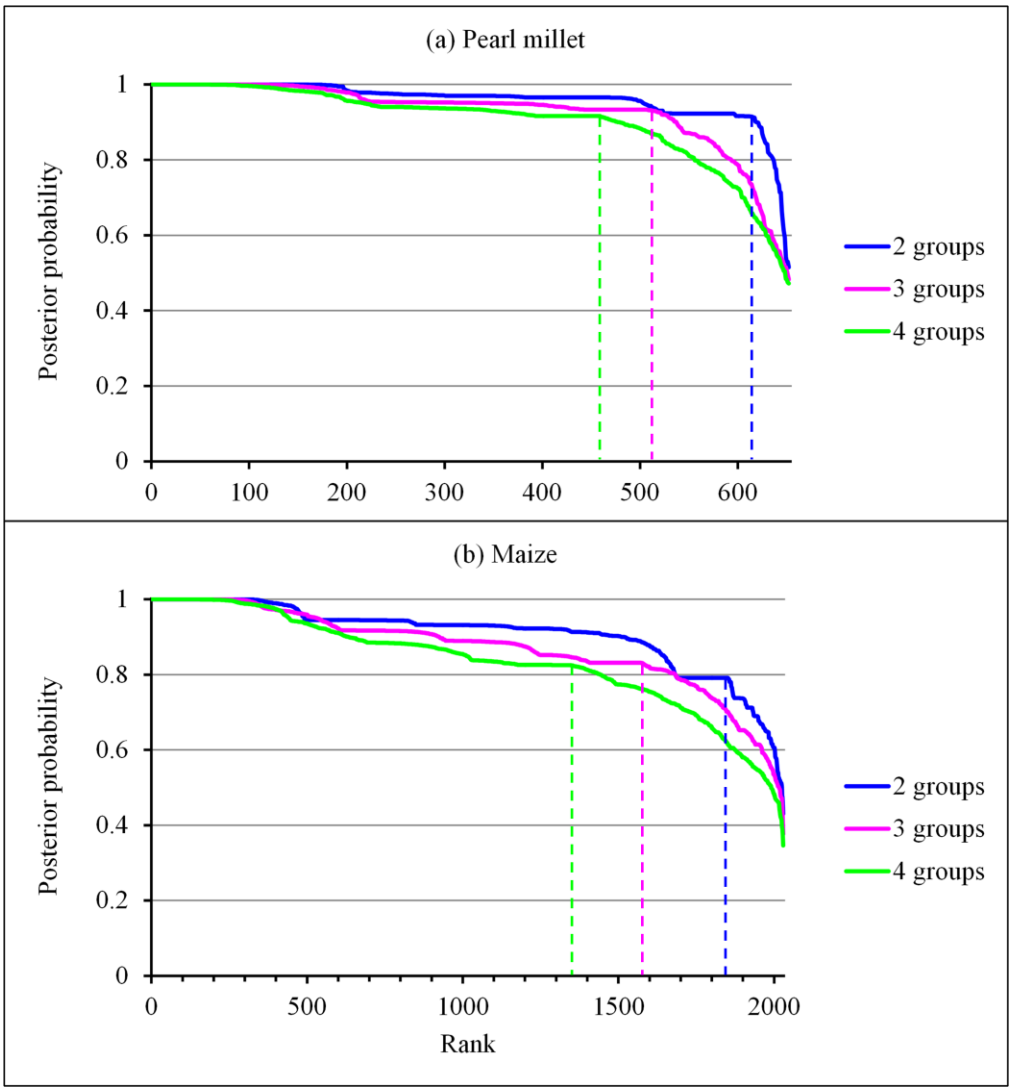

Supplementary figure 2-3: Pearl millet: daily median growth rate (and associated mean absolute deviation −m.a.d.−) for (a) 2 groups, (b) 3 groups and (c) 4 groups.

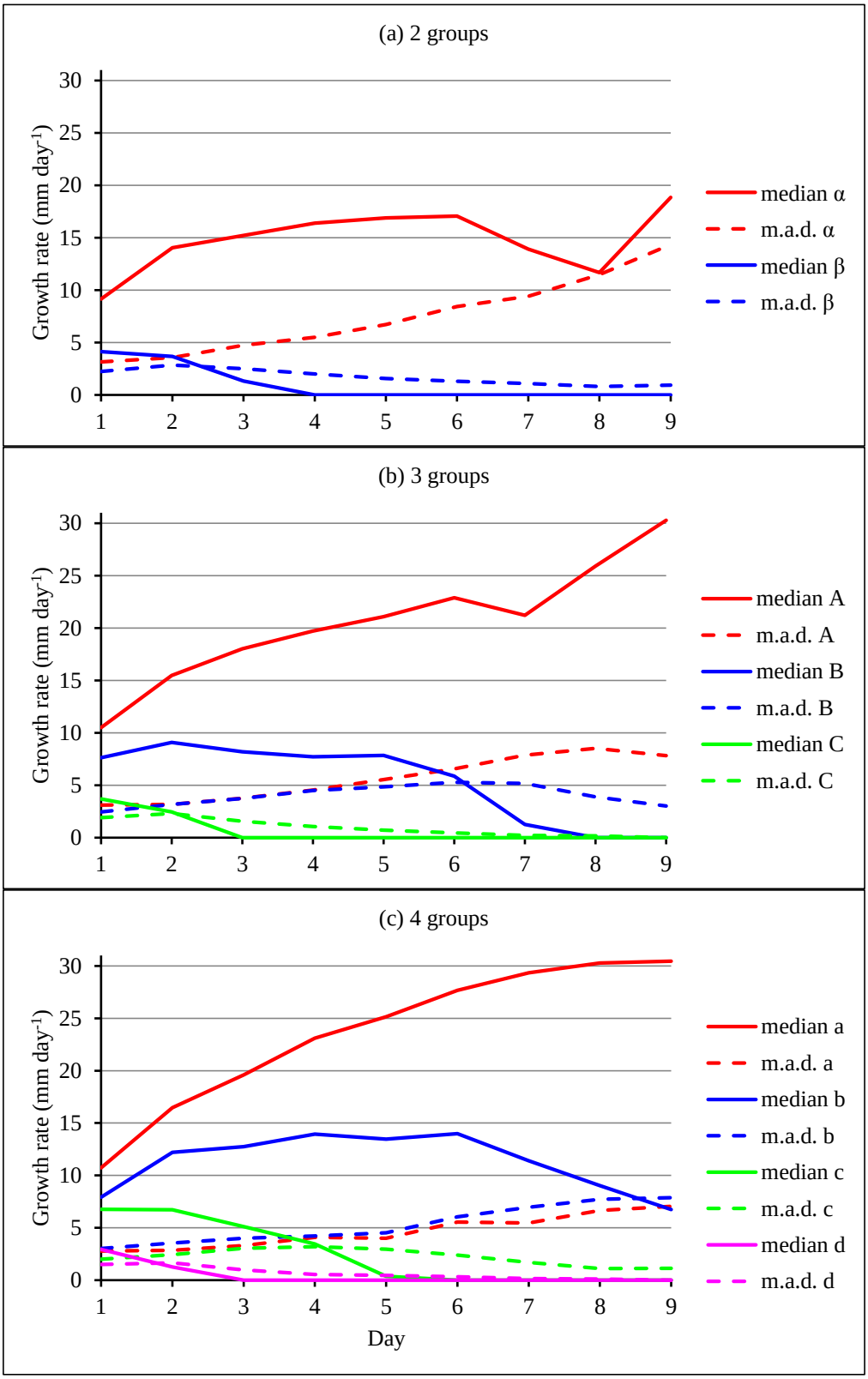

Supplementary figure 2-4: Cumulative distribution functions of the length of growth rate profiles assigned to each group: (a) pearl millet; (b) maize.

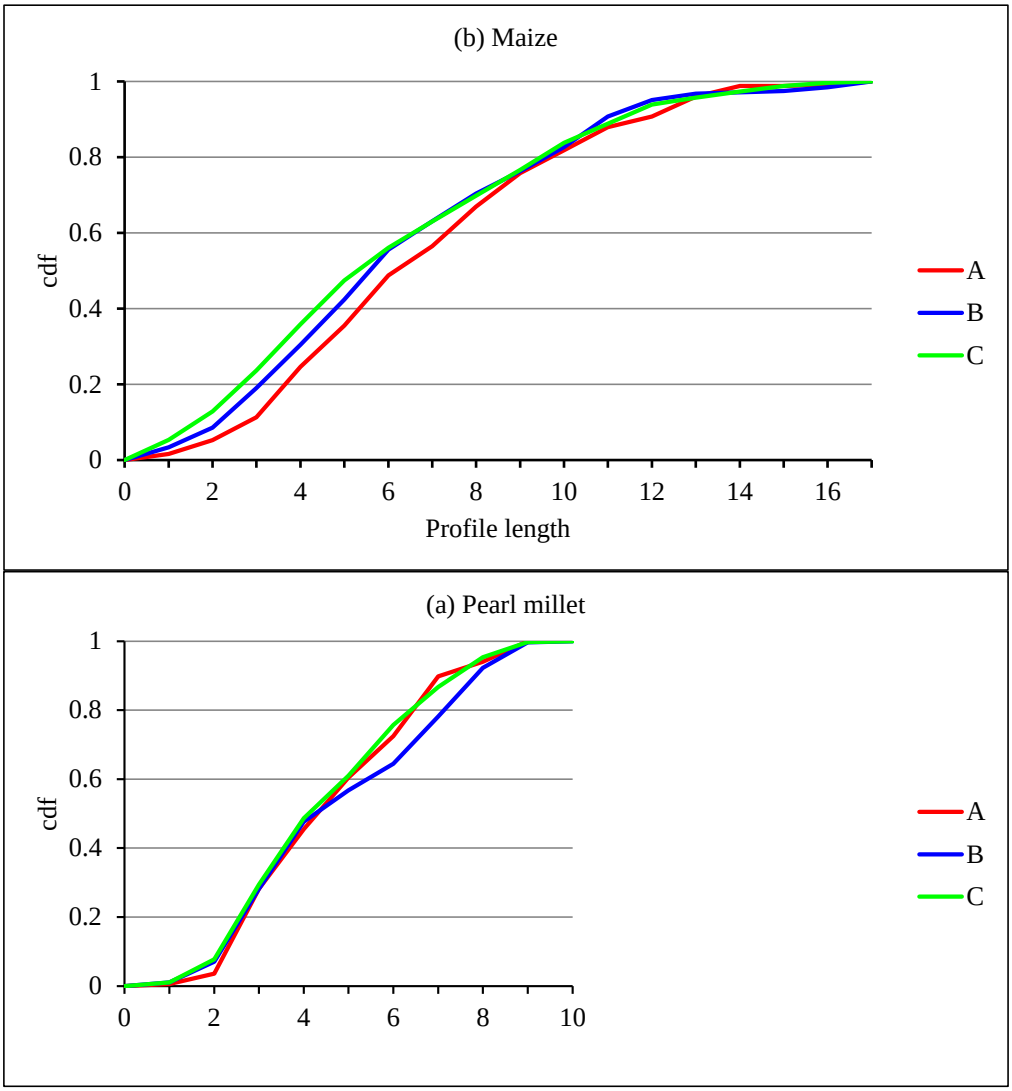

Table S2-1: Pearl millet: Overlaps (i.e. 1 – sup norm distance) between growth rate distributions corresponding to consecutive lateral root classes (α-β for 2 classes, A-B and B-C for 3 classes and a-b, b-c, and c-d for 4 classes) extracted from the optimal assignment of each lateral root growth rate profiles using the estimated 3-, 4- and 5-state semi-Markov switching linear models.

	2 classes	3 classes		4 classes		
Age	α-β	A-B	B-C	a-b	b-c	c-d
1	0.47	0.55	0.53	0.53	0.67	0.4
2	0.22	0.38	0.32	0.5	0.39	0.27
3	0.16	0.27	0.3	0.37	0.31	0.5
4	0.15	0.23	0.34	0.28	0.25	0.51
5	0.17	0.2	0.39	0.09	0.31	0.65
6	0.25	0.18	0.45	0.19	0.37	0.72
7	0.34	0.28	0.54	0.17	0.45	0.79

Table S2-2: Maize: Overlaps (i.e. 1 – sup norm distance) between growth rate distributions corresponding to consecutive lateral root classes (α-β for 2 classes, A-B and B-C for 3 classes and a-b, b-c and c-d for 4 classes) extracted from the optimal assignment of each lateral root growth rate profiles using the estimated 3-, 4- and 5-state semi-Markov switching linear models.

	2 classes	3 classes		4 classes		
Age	α-β	A-B	B-C	a-b	b-c	c-d
1	0.29	0.61	0.27	0.78	0.44	0.21
2	0.17	0.46	0.22	0.65	0.3	0.31
3	0.17	0.25	0.32	0.34	0.28	0.47
4	0.24	0.23	0.4	0.25	0.37	0.57
5	0.32	0.19	0.5	0.22	0.48	0.65
6	0.38	0.23	0.55	0.19	0.53	0.7
7	0.4	0.24	0.59	0.16	0.55	0.78
8	0.43	0.25	0.64	0.14	0.57	0.83
9	0.46	0.31	0.71	0.13	0.57	0.9
10	0.48	0.3	0.8	0.14	0.61	0.94
11	0.5	0.29	0.85	0.17	0.65	0.96

Table S2-3: Maize: Overlaps (i.e. 1 – sup norm distance) between growth rate distributions and apical diameter distributions corresponding to lateral root classes (A-B, B-C and A-C only for apical diameters) extracted from the optimal assignment of each lateral root growth rate profiles using the estimated 4-state semi-Markov switching linear model.

	Growth rate		Apical diameter		
Age	A-B	B-C	A-B	A-C	B-C
1	0.61	0.27	0.65	0.48	0.79
2	0.46	0.22	0.62	0.48	0.85
3	0.25	0.32	0.49	0.45	0.89
4	0.23	0.4	0.47	0.42	0.87
5	0.19	0.5	0.47	0.43	0.77
6	0.23	0.55	0.41	0.37	0.84
7	0.24	0.59	0.38	0.38	0.86
8	0.25	0.64	0.34	0.4	0.84
9	0.31	0.71	0.35	0.39	0.78
10	0.3	0.8	0.33	0.37	0.8
11	0.29	0.85	0.39	0.33	0.62

Table S2-4: Length of the interval between successive lateral roots in pearl millet, classified according to the types of the two lateral roots delimiting the interval. No significant differences between the means were found (ANOVA, p = 0.52).

Lateral root types	A-A	A-B	A-C	B-A	B-B	B-C	C-A	C-B	C-C
Sample size	23	37	105	48	76	172	93	182	510
Mean (cm)	0.26	0.23	0.21	0.26	0.22	0.20	0.22	0.19	0.22
Standard deviation (cm)	0.22	0.17	0.31	0.52	0.23	0.17	0.19	0.16	0.19

Table S2-5: Length of the interval between successive lateral roots in maize, classified according to the types of the two lateral roots delimiting the interval. No significant differences between the means were found (ANOVA, p = 0.39).

Lateral root types	A-A	A-B	A-C	B-A	B-B	B-C	C-A	C-B	C-C
Sample size	44	67	138	59	269	502	143	491	1324
Mean (cm)	0.17	0.19	0.14	0.15	0.15	0.16	0.15	0.16	0.17
Standard deviation (cm)	0.19	0.20	0.12	0.11	0.15	0.16	0.11	0.12	0.16

Résumé substantiel en français

Ce résumé comprend une introduction générale et présente les objectifs de la thèse. Il reprend ensuite les principaux résultats présentés dans le corps de la thèse et se termine par une discussion et une conclusion générales.

Introduction générale

La sécurité alimentaire est un défi majeur pour la recherche agronomique du 21ème siècle. Selon l'Organisation des Nations unies pour l'alimentation et l'agriculture, 795 millions de personnes étaient en situation de sous-nutrition en 2015, dont 780 millions dans les pays en développement. Bien que la faim ait régressé dans certaines régions du monde, l'Afrique subsaharienne reste la région avec la plus forte prévalence de malnutrition, avec près de 25% de personnes touchées. Il apparaît nécessaire d'augmenter la production alimentaire à destination des paysans pauvres d'Afrique sub-saharienne dans le contexte des changements globaux, qui posent de nouvelles menaces pour l'agriculture. Le mil est la 6ème céréale cultivée dans le monde avec plus de 33 millions d'hectares récoltés en 2013 et c'est une culture d'importance majeure dans les régions arides et semi-arides comme le Sahel. Le mil est la céréale qui occupe la plus grande surface cultivée en Afrique de l'Ouest, avec plus de 13 millions d'hectares en 2013. Cependant, il est seulement quatrième en termes de production totale. Le mil est particulièrement tolérant aux conditions environnementales difficiles (température élevée, pluviométrie faible, sols peu fertiles) et est ainsi cultivé préférentiellement dans les zones où d'autres céréales échoueraient. Au contraire, dès que les conditions de culture s'améliorent (possibilités d'irrigation par exemple), le mil est abandonné au profit de cultures plus exigeantes (sorgho, maïs). Le mil est donc de préférence cultivé dans les régions arides où la fertilité est faible, où il est souvent la seule céréale viable. L'augmentation des rendements dans ces régions produirait une amélioration substantielle de la sécurité alimentaire mais les pratiques agronomiques sont souvent contraintes et le déploiement de l'irrigation ou l'utilisation accrue d'engrais sont difficiles dans certaines régions. Les efforts de recherche doivent donc se concentrer sur la sélection et l'amélioration variétale afin de produire des variétés plus productives dans les conditions de culture habituelles du mil. Le mil a un bon profil nutritionnel parmi les céréales et cet avantage doit être conservé et si possible amélioré chez les nouvelles variétés créées. Les stratégies de sélection chez le mil ont principalement ciblé des caractères physiologiques ou architecturaux observés sur la partie aérienne tels que le rendement en grains, la taille de la plante ou la résistance aux bioagresseurs. Une idée originale serait de cibler les caractères racinaires pour l'amélioration variétale. Le système racinaire est l'interface entre la plante et le sol et constitue la porte d'entrée de l'eau et des nutriments pour la plante. Dans certaines plantes cultivées, la sélection a conduit à une réduction de la taille du système racinaire. En effet, depuis la domestication des céréales, les agriculteurs se sont concentrés sur la maximisation du rendement en grains. Au cours de la Révolution Verte, la poursuite de cet objectif s'est traduite par l'augmentation de l'indice de récolte et la sélection de variétés adaptées aux

apports d'engrais. Cependant, cette stratégie nécessite le recours aux à des engrais souvent trop coûteux pour les paysans pauvres et les cultures spécifiquement africaines telles que le mil ont été peu concernées par cette phase d'amélioration. L'amélioration du système racinaire peut conduire à la production de variétés avec une meilleure efficacité d'absorption de l'eau et des minéraux. Cette option est particulièrement pertinente pour les plantes cultivées sur des sols pauvres et sous un climat aride étant donné que l'augmentation du rendement ne peut être obtenue par l'irrigation ou par une augmentation significative des apports de fertilisant.

Objectifs de la thèse

Le manque d'eau et la faible disponibilité en nutriments sont les principaux facteurs limitant la production du mil, notamment en Afrique. L'architecture du système racinaire étant un élément crucial pour l'acquisition de ces éléments, l'amélioration variétale axée sur l'adaptation du système racinaire est une stratégie prometteuse pour améliorer la tolérance du mil à la sécheresse et la faible fertilité des sols. Cependant, peu d'informations sont disponibles sur le développement et le fonctionnement du système racinaire du mil. La dynamique générale de son développement a été décrite mais il existe de la variabilité au sein des variétés de mil cultivée et celle-ci a été peu explorée. En outre, les études existantes ont considéré principalement le système racinaire dans son ensemble, sans séparer la racine primaire, les racines coronaires et les racines latérales, alors que leurs fonctions sont différentes. De plus, ces études ont eu majoritairement recours à des méthodes destructrices pour étudier le système racinaire. Les techniques de phénotypage modernes permettent désormais d'étudier le système racinaire de façon non destructive et ainsi d'avoir des mesures plus précises de caractères temporels associés au développement des racines.

Dans ce contexte, le premier objectif de mon travail était de produire une description précise du système racinaire du mil. Nous avons donc procédé à une description morphologique générale du développement précoce du système racinaire, obtenu des données quantitatives sur sa dynamique de développement, et décrit l'anatomie des différents types de racine. Nous avons également évalué la diversité existante au sein d'un panel diversifié de lignées de mil. Ces résultats sont présentés dans le C**hapitre 1**.

Nos données mettent en évidence l'existence d'une variabilité dans les profils de croissance des racines latérales. Nous avons donc conçu un pipeline pour mesurer efficacement les profils de croissance d'un grand nombre de racines latérales et utilisé un modèle statistique pour classer ces racines en fonction de leurs profils de croissance. Cette classification a été utilisée pour caractériser la variabilité existante et la condenser. Cette réduction de la complexité temporelle a permis d'analyser la relation entre le comportement de croissance des racines latérales et d'autres caractères, en particulier anatomiques. Elle a également permis de décrire la répartition de ces différents types de racines latérales le long de la racine primaire et d'évaluer l'influence locale des types de racines sur les racines latérales voisines. Ces résultats sont détaillés dans le **Chapitre 2**. Ce travail a été mené en

parallèle sur deux espèces, le mil et le maïs, ce qui a permis de mettre en évidence les ressemblances et les spécificités de ces deux espèces.

Le contrôle génétique du développement racinaire du mil est encore mal connu. Nous avons initié une étude de génétique d'association pour identifier des gènes contrôlant la croissance de la racine primaire. Un large panel de diversité a été phénotypé pour la vitesse de croissance de la racine primaire et chaque accession a été génotypée par séquençage. Le **Chapitre 3** présente la méthodologie utilisée et les résultats obtenus après le phénotypage et le génotypage.

Ce résumé en français détaille les principaux résultats présentés dans les différents chapitres, sans reprendre la description des méthodes expérimentales et les discussions détaillées de ces résultats.

Chapitre 1 : Description générale du système racinaire du mil

Ce chapitre est composé de deux parties. La première partie reprend les résultats d'un article scientifique qui a été publié dans le journal Frontiers in Plant Sciences. L'objectif général de cette étude était de fournir une description morphologique et anatomique du système racinaire du mil, en particulier dans les premiers stades de développement. Une nouvelle nomenclature pour la désignation des racines du mil était également nécessaire car les noms existants étaient en contradiction avec ceux proposés par Plant Ontology, qui est la référence la plus largement partagée pour nommer des éléments végétaux. Ce document fournit une description dynamique de l'architecture racinaire du mil dans les stades précoces ainsi qu'une description anatomique des différents types de racines. Il révèle l'existence de trois types de racines latérales anatomiquement distincts. Il met également en évidence l'existence d'une grande diversité dans la croissance précoce de la racine primaires et dans la densité des racines latérales au sein d'un échantillon de lignées de mil issu d'un panel de diversité de mil servant ainsi de démonstration de faisabilité de futures analyses génétiques. La deuxième partie décrit la comparaison de la mise en place de l'architecture racinaire chez deux lignées de mil avec des traits racinaires contrastés, identifiées au cours du phénotypage à haut débit.

La première racine qui émerge de la graine, d'abord appelée radicule, est ensuite nommée racine primaire. Un petit segment, le mésocotyle, relie la graine et la base de la tige. Plus tard, les racines coronaires émergent de la base de la tige. Les ramifications qui apparaissent sur les racines primaires ou coronaires sont appelées racines latérales. Les racines latérales peuvent elles-aussi se ramifier. La mise en place précoce de l'architecture racinaire a été étudiée sur des plantes cultivées en rhizotrons pendant 11 jours. La racine primaire émerge 12 à 24 heures après réhydratation de la graine. La vitesse de croissance de cette racine primaire augmente pendant les 6 premiers jours de croissance pour atteindre un maximum de 9,1 cm/jour. Après cette date, la vitesse de croissance ralentit légèrement mais reste autours de 7 cm/jour après 11 jours. La longueur moyenne de la racine primaire après 11 jours de croissance est de 66,3 cm. Les racines coronaires et latérales commencent à émerger

après 6 jours de croissance, lorsque la vitesse de croissance de la racine primaire atteint son maximum, respectivement de la base de la tige et de la racine primaire. Le nombre total de racines coronaires étaient en moyenne de deux par plante à la fin de l'expérience, ce qui est attribué à la faible durée du suivi. La vitesse moyenne de croissance de ces racines à l'émergence était de 3,7 cm. Le rythme d'apparition des racines latérales augmente rapidement entre 6 et 8 jours de croissance, puis plus faiblement jusqu'à 11 jours. Les vitesses de croissance des racines latérales étaient hétérogènes, atteignant jusqu'à 3 cm/jour.

Le développement précoce du système racinaire a également été analysé en 3 dimensions dans un sol grâce à la tomographie à rayons X. Les plantes ont été cultivées dans des petites colonnes de sol (5 cm de diamètre x 12 cm de haut) et scannées après 4, 8, 14 et 18 jours de croissance. La dynamique de mise en place observée grâce à la tomographie a confirmé celle mesurée en rhizotron, appuyant l'hypothèse que les rhizotrons fournissent une évaluation réaliste du développement de l'architecture des racines dans des conditions naturelles.

L'anatomie des différentes racines a été observée sur des coupes histologiques. La racine primaire possède un grand vaisseau métaxylème situé au centre de la stèle. Le cortex est formé de 3 à 5 couches de cellules. La présence d'aérenchymes a été observée dans les parties matures de la racine. Les racines coronaires sont plus épaisses que les racines primaires avec une stèle significativement plus grande et possèdent 2 à 5 (3 dans la plupart des cas) gros vaisseaux de métaxylème centraux, séparés par des cellules de parenchyme. Ces racines possèdent également 3 à 5 couches de cellules corticales et des aérenchymes. L'observation en autofluorescence a mis en évidence une lignification progressive de l'apex à la base des racines ainsi que la présence d'un cadre de Caspary en fer à cheval au niveau de l'endoderme. Une coloration au FASGA a permis de dénombrer 6 pôles du xylème en alternance avec 6 pôles de phloème dans la racine primaire, tandis que les racines coronaires contiennent 12 à 16 pôles de xylème. Les parties matures des racines de la couronne présentent un sclérenchyme, entouré d'un hypoderme et d'un rhizoderme. Des sections longitudinales (5 μm) à travers le méristème de la racine primaire ont révélé une organisation en méristème fermée avec des files de cellules convergeant vers un petit groupe de cellules dont l'emplacement et la taille sont compatibles avec celles d'un centre quiescent. Les racines coronaires ont montré une organisation similaire du méristème, avec une plus grande stèle.

Des coupes transversales effectuées sur des racines latérales provenant de racines primaires ou coronaires ont révélé l'existence d'organisations distinctes. Les racines latérales ont pu être classées en trois types en fonction de leur anatomie. Les racines latérales de type 1 très fines (68-140 μm de diamètre) présentent 2 pôles protoxylème (organisation diarche). Elles présentent un endoderme, 2 couches de cellules corticales et un épiderme mais pas de sclérenchyme ni d'aérenchyme. Les racines latérales de type 2 ont un diamètre moyen (235-291 μm), un petit vaisseau de métaxylème central (16 μm de diamètre en moyenne) et 3 couches de cellules corticales. Comme les racines latérales de type 1, elles ne présentent pas de sclérenchyme ou ni d'aérenchyme. Enfin, les racines latérales de type 3 ont un grand diamètre, similaire à celui des racines primaires (328-440 μm) et la même organisation que

les racines primaires, indépendamment de la racine à partir de laquelle ils émergent (ie primaire ou coronaire). Nous avons évalué la diversité d'architectures racinaires existant au sein d'un échantillon de lignées de mil issu d'un panel de diversité d'un panel de lignées fixées. Cette étude a révélé l'existence d'une grande variabilité dans la vitesse de croissance des racines primaires et la densité des racines latérales le long de la racine primaire. L'héritabilité large sens était égale à 0,72 pour la longueur des racines primaires et à 0,34 pour la densité des racines latérales.

Au cours d'expériences complémentaires, nous avons comparé en rhizotrons les vitesses de développement racinaire de deux lignées identifiées comme contrastées lors de l'étude de diversité. Malgré des valeurs absolues distinctes, les vitesses de croissance des racines primaires suivaient la même dynamique pour les deux lignées, avec un maximum à 6 jours de croissance suivie d'un plateau. En revanche, les taux d'émergence des racines latérales montraient des profils différents pour les deux lignées. Ce taux augmentait pendant toute la durée de l'expérience chez une lignée tandis qu'il augmentait jusqu'à 8 jours de croissance chez l'autre, avant de diminuer jusqu'à la fin de l'expérience. Les taux d'émergence absolus étaient également différents. Les nombres de racines coronaires étaient semblables chez les deux lignées. Globalement, les valeurs observées en rhizotrons étaient en cohérences avec celles observées lors du phénotypage du panel, donc dans des conditions différentes.

Chapitre 2 : L'analyse spatio-temporelle du développement précoce du système racinaire chez deux céréales, le mil et le maïs, révèle l'existence de trois types de racines latérales et un patron de ramification aléatoire le long de la racine primaire

Pour analyser plus finement la dynamique de développement des racines latérales, nous avons effectué un suivi plus précis de la croissance des racines latérales de 8 plantes de mil pendant 15 jours dans des rhizotrons. Cette expérience a également été réalisée sur des plantes de maïs dans des conditions similaires, ce qui a permis d'étudier les similarités et les différences entre ces deux espèces. Nous avons décomposé l'analyse de ces données spatio-temporelles en deux étapes, temporelle puis spatiale. Nous avons d'abord analysé les profils de vitesse de croissance des racines latérales à l'aide de modèles statistiques dédiés à ce type de données longitudinales, caractérisé par la faible longueur des profils et un niveau de censure élevé, dû au fait que de nombreuses racines latérales étaient encore en croissance à la fin du suivi. Une des sorties de ces analyses longitudinales a été le classement des racines latérales en trois types. Les longueurs d'intervalle entre les racines latérales successives et la succession des types de racines latérales le long de la racine primaire ont ensuite été analysées. Pour cette étape, les racines latérales ont été regroupées en fonction de leurs profiles de croissance.

Le jeu de données était composé des profils de croissance de 1254 et 3050 racines latérales de 8 plantes de mil et 13 plantes de maïs, respectivement. Ces racines latérales ont été suivies jusqu'à 10 et 17 jours respectivement après émergence des racines primaires.

L'analyse exploratoire de ces profils de croissance a mis en évidence une organisation longitudinale forte avec des taux de croissance augmentant ou diminuant avec l'âge de la racine latérale. Les profils de croissance étaient visiblement divergents par rapport à l'origine et la dispersion des taux de croissance augmentait avec l'âge des racines latérales. Par conséquent, les racines latérales pouvaient être grossièrement classées en fonction de leurs profils de croissance. Cela soulevait la question d'une structuration de ces données longitudinales plus forte qu'un simple classement des profils de croissance. Nous avons donc choisi d'approfondir l'analyse par une approche de classification basée sur un modèle pour ces données longitudinales. Cela a soulevé deux types de difficultés: les longueurs de profils étaient limitées (jusqu'à 10 taux de croissance successifs pour le mil et 17 pour le maïs) et le niveau de censure était élevé, avec une forte proportion de racines latérales encore en croissance à la fin de l'expérience. Nous avons donc conçu un modèle statistique pour classer les profils de croissance en utilisant seulement les profils d'une durée de 5 jours ou plus (correspondant à 652 racines latérales pour le mil et 2029 pour le maïs), en fonction des hypothèses suivantes:

- un profil de taux de croissance est modélisé par une phase de croissance unique, censurée ou suivie d'un arrêt de croissance,
- les variations de taux de croissance au sein d'une phase de croissance sont modélisées par une tendance linéaire. Cette hypothèse paramétrique forte était une conséquence de la faible longueur des profils de croissance. Par conséquent, ces tendances linéaires doivent être considérées comme des modèles instrumentaux pour le regroupement des profils de croissance plutôt que des représentations fidèles de chaque profil de taux de croissance.

Le modèle statistique proposé est composé d'états de croissance, chacun correspondant à un type de profil de vitesses de croissance des racines latérales. Une distribution représentant la durée de la phase de croissance (en jours) et un modèle linéaire représentant la variation du taux de croissance au cours de la phase de croissance ont été associées à chacun de ces états de croissance. Les états de croissance ont été systématiquement suivis d'un état d'arrêt de croissance. Le modèle global est un modèle linéaire à transitions semi-markoviennes (SMSLM). Ce type de modèle statistique intégratif permet d'estimer systématiquement les distributions de durée de la phase de croissance en combinant les phases de croissance complètes et censurées. Nous avons ensuite eu à définir le nombre d'états de croissance, c'est à dire le nombre de types de racines latérales. En raison de la structure spécifique du modèle, où chaque état peut être visité au plus une fois, les critères de sélection de modèles habituels ne sont pas applicables. Nous avons donc dû concevoir une méthode de sélection de modèle empirique pour sélectionner le nombre d'états de croissance. Nous avons sélectionné pour les deux espèces 3 types de racines latérales, ce qui correspond au meilleur compromis entre (i) la proportion de racines latérales assignées de façon ambiguë, (ii) la dispersion relative des profils de croissance pour le type de racine le plus vigoureux et (iii) le chevauchement entre profils de croissance pour les types voisins.

Les distributions de durée de la phase de croissance estimées étaient très similaires pour les deux espèces pour chaque type (A, B ou C), avec des durées moyennes de croissance de 17,3 et 15,2 jours pour le type A, 7,6 et 6,8 jours pour le type B et 3,2 et 3,0 jours pour

Type C pour le mil et le maïs, respectivement, et des écarts-types égaux à 7,6 et 7,7 pour le type A, 4,6 et 5,0 pour le type B, et 2,6 et 2,4 pour le type C. Le niveau de censure est défini comme la proportion de phases de croissance incomplètement observées pour un type donné de racines latérales. Le niveau de censure a été calculé pour chaque état de croissance comme sous-produit de l'estimation de la distribution de la durée de la phase de croissance correspondante dans les SMSLM et prend en compte toutes les affectations possibles des profils de croissance de longueur ≥ 5. Nous avons obtenu 96% de censure pour l'état A, 54% pour l'état B et 14% pour l'état C dans le cas du mil et 80% pour l'état A, 36% pour l'état B et 10% pour l'état C dans le cas du maïs. Le niveau de censure plus élevé pour le mil par rapport au maïs est une conséquence de la longueur plus courte des profils de croissance pour le mil, car les distributions de durée de la phase de croissance sont similaires pour les deux espèces.

Les profils de croissance médians ont été calculés à partir des profils de longueur ≥ 5, qui ont été utilisés pour la construction des SMSLMs, et des profils de longueur < 5, qui ont été attribués a posteriori à des classes en utilisant le SMSLM. Chez les deux espèces, les taux de croissance quotidiens médians étaient divergents entre les trois types de racines latérales. Les profils de croissance médians pour le type B et le type C devenaient nuls après 7-8 et 3-4 jours respectivement, tandis que le taux de croissance médian du type A restait positif et ne diminuait pas chez les deux espèces. La principale différence entre les deux espèces, en dehors des différents taux de croissance absolus, concernait les racines latérales de type B, où le taux de croissance médian restait presque constant jusqu'au jour 5 chez le mil alors qu'il commençait à diminuer juste après émergence chez le maïs, et les racines de type A, où le taux de croissance médian a continué d'augmenter chez le mil alors qu'il se stabilise après quelques jours chez le maïs.

Nous avons exploré les liens existant entre la cinétique de croissance des racines latérales et leur anatomie sur un échantillon de 35 racines de mil et 15 racines de maïs ayant des profils de croissance contrastés. Les racines latérales ont été affectées à l'une des 3 classes définies précédemment en fonction de leur profil de croissance. Nous avons mesuré 2 traits anatomiques identifiés comme contrastés entre les racines dans le chapitre 1, le diamètre de la stèle et le diamètre du vaisseau central. Pour le mil, la classification ABC des profils de croissance se reflétait dans le classement des deux diamètres mesurés, bien qu'il y ait un certain chevauchement entre les classes. En revanche, aucune tendance claire n'a pu être détectée chez le maïs, en raison notamment du faible nombre (1) de racines de type A. Ces résultats suggèrent une corrélation entre les traits anatomiques et le profil de croissance pour les racines latérales chez le mil mais pas chez le maïs. La petite taille de l'échantillon pour les racines de maïs pourrait expliquer l'absence de relation observable.

Nous avons analysé la répartition des types de racines latérales (A, B et C) le long de la racine primaire afin de déterminer si elle était aléatoire ou structurée. Nous avons d'abord évalué l'impact du type de racine sur la longueur de l'intervalle entre une racine latérale et sa plus proche voisine dans la direction de l’apex racinaire. Aucune différence n'a été trouvée dans la longueur de l'intervalle moyen pour les trois types de racines chez les deux espèces (ANOVA, p-value = 0,83 et 0,7 pour le mil et le maïs, respectivement). Le même type

d'analyse a été effectué en séparant les intervalles en 9 groupes, en fonction des types des deux racines latérales délimitant l'intervalle et à nouveau, aucun effet des types de racines latérales sur les longueurs d'intervalle n'a été trouvé. Par conséquent, nos résultats indiquent qu'il n'y a pas d'influence des types de racines sur des longueurs d'intervalle entre deux racines latérales successives.

Nous avons ensuite évalué si la séquence des types de racines latérales était aléatoire ou structurée d'une certaine manière. Nous avons d'abord calculé la fonction d'autocorrélation de Spearman pour ces séquences. La valeur de la fonction était dans l'intervalle de confiance correspondant à l'hypothèse d'une répartition aléatoire pour la plupart des plantes, ce qui indique que la distribution des différents types de racines latérales le long de la racine primaire était stationnaire et ne suggérait aucune dépendance marquée entre les types de racines latérales successifs. Nous avons analysé la structure de ramification de la racine primaire en utilisant une approche de modélisation statistique. Nous avons modélisé les dépendances potentielles entre les types de racines latérales successives décrites du collet vers l'apex de la racine. Des chaînes de Markov d'ordre variable à trois états ont été construites, chaque état correspondant à un type de racines latérales. Les ordres des chaînes de Markov ont été sélectionnés pour la séquence de ramification de chaque racine primaire et pour chaque espèce. Pour toutes les plantes et pour les deux espèces, une chaîne de Markov d'ordre zéro a été sélectionnée. Ceci a confirmé que le type de racine latérale est indépendant du type des racines latérales précédentes. Par conséquent, les résultats indiquent qu'il n'y a aucune influence de la dynamique de croissance des racines latérales sur la distance à la racine latérale suivante ou sur son profile de croissance. Les différentes plantes de mil et de maïs étudiées présentaient des différences dans les longueurs moyennes d'intervalles entre racines latérales successives ainsi que dans les proportions relatives des 3 types de racines latérales. Malgré cela, le motif de ramification, aléatoire et stationnaire, était nettement conservé dans toutes les plantes.

Chapitre 3: Recherche de gènes contrôlant la croissance de la racine primaire chez le mil

Ce chapitre présente des résultats préliminaires qui devront être approfondis et complétés. Nous avons caractérisé une grande collection de lignées de mil fixées pour la croissance de la racine primaire et entamé une étude de génétique d'association pour identifier les régions génomiques contrôlant ce trait. La mesure de la croissance de la racine primaire a été faite sur de jeunes plantes cultivées dans un système de culture hydroponique sur papier. Un total de 853 plantes ont été phénotypées, divisées en 3 expériences de 559, 116 et 178 plantes. En raison de problèmes de germination, seuls 136 lots de graines, appartenant à 108 lignes différentes, ont été phénotypés. Une moyenne de 7,9 plantes/lignée a été analysée. Cette expérience a porté sur la longueur de la racine primaire 6 jours après germination et ce caractère a montré une grande variabilité génétique. Une héritabilité au sens large de 0,53 a été estimée pour ce caractère sur cette collection, confirmant que la croissance de la racine primaire a un contrôle génétique fort. Les lignées étudiées ont été génotypées par séquençage

par la plateforme Genetic Diversity Facility de l'Université de Cornell. Les premières analyses ont identifié 1.677.181 SNP avant filtrage, parmi lesquels 481.897 étaient présents dans au moins la moitié des plantes. La profondeur de séquençage moyenne par site était de 2,86. Nous attendons un nombre final d'environ 300.000 SNPs après les autres étapes de filtrage. Les analyses de la structure génétique de la population et l'analyse d'association se feront respectivement avec les packages R LEA et GAPIT.

Discussion

L'objectif de ce travail de thèse était de caractériser le développement du système racinaire du mil. Ce système racinaire était mal connu et cette connaissance nouvellement acquise sera utile pour sélectionner de nouvelles variétés de mil avec des caractéristiques racinaires améliorées. Cette amélioration du système racinaire vise à accroitre l'efficacité d'acquisition d'eau et des nutriments par la plante et donc à augmenter sa tolérance à la sécheresse et à la faible disponibilité en nutriments, deux facteurs importants qui limitent la production de cette culture en Afrique de l'Ouest.

Ce travail de thèse a mis en évidence l'existence d'une grande variabilité dans les profils de croissance des racines latérales. Ces racines ont pu être classées en trois types à l'aide d'un modèle statistique et ces types cinétiques étaient fortement liés avec des traits anatomiques des racines. Une classification des racines latérales en types anatomiques distincts a été proposée chez plusieurs céréales (blé, orge, riz…) et une variabilité dans les taux de croissance de ces racines a également été observée chez différents végétaux, mais le lien entre ces caractères cinétiques et anatomiques était rarement fait. Des fonctions différentes pour ces types racinaires ont été suggérées (ramification, absorption d'eau…) mais de plus amples recherches sont nécessaires pour préciser ces fonctions. De plus, les facteurs influençant la formation de ces différents types, génétiques ou environnementaux, devront être compris. La compréhension des fonctions respectives des différents types racinaires pourrait permettre d'intégrer leur existence dans les programmes de sélection racinaire.

Plusieurs techniques de phénotypage racinaire ont été utilisées au cours de ma thèse : la croissance sur papier de germination imbibé de solution nutritive, la croissance en rhizotron et la croissance en sol associée à la tomographie. Chaque technique présente des avantages et des inconvénients en termes de débit, de durée de croissance, de précision du suivi et de représentativité des conditions de croissance par rapport aux conditions de culture habituelles. Les différents modes de culture des plantes sont associés à des techniques d'acquisition d'image adaptées. Nous avons utilisé des techniques de phénotypage variées mais il en existe d'autres, qui répondent différemment à ces contraintes. Par exemple, l'excavation de systèmes racinaires de plantes cultivées au champ permet d'avoir un aperçu des racines de plantes cultivées dans des conditions proches des conditions habituelles de croissance, au prix d'une grande quantité de travail humain. Le MRI est une autre solution d'acquisition d'images racinaires en sol, ressemblant à la tomographie mais qui facilite la segmentation des racines par rapport au sol. Certaines équipes utilisent des milieux transparents reproduisant les

propriétés du sol pour faire pousser des plantes à phénotyper. Chaque technique possède des avantages et des inconvénients, le choix s'effectuant en fonction des objectifs scientifiques de chaque campagne de phénotypage. Le phénotypage ne recouvre pas seulement le mode de culture mais tout le processus, de la germination des graines à l'analyse de données, en passant par l'acquisition des images. L'analyse de grands jeux de données spatio-temporelles, dont l'acquisition est permise par les techniques de phénotypage actuelle, doit également être considérée comme faisant partie du processus, afin d'exploiter au mieux les données récoltées au cours des expériences.

Les modèles de plante structure-fonction permettent de simuler le fonctionnement des plantes en fonction des valeurs de certains traits d'intérêt et permettent ainsi de comprendre le rôle des traits racinaires qui peuvent être la cible de programmes d'amélioration. De tels modèles ont permis d'identifier des architectures racinaires optimales sous certaines contraintes (sécheresse, faible disponibilité en azote ou en phosphore) chez le maïs, par exemple. Un modèle de ce type est en cours de développement chez le mil, à l'aide des données de phénotypage racinaire récoltés lors de ma thèse. Des expérimentations en champ sont également en cours sur la collection de lignées phénotypées dans le chapitre 3 et doivent permettre de trouver les corrélations existant entre les traits racinaires mesurés au laboratoire et les performances agronomiques des plantes en condition contrôle ou soumises à un stress hydrique. L'adaptation à la sécheresse peut être liée à certains traits racinaires mais aussi à la capacité des plantes à une certaine plasticité face aux conditions environnementales. Les évaluations agronomiques effectuées dans des conditions contrastées permettent d'avoir un aperçu de cette plasticité.

Conclusion générale

Pour conclure, mon travail de thèse a fourni une description précise du système racinaire du mil, qui avait été très peu étudié à ce jour. Les données acquises lors des expériences de phénotypage ont été utilisées pour le paramétrage et l'essai de modèles de plantes structure-fonction simulant la croissance des racines et le transport de l'eau. Un pipeline a été développé pour la caractérisation des profils de croissance les racines latérales. Il comprend un modèle statistique original qui pourra être utilisé sur d'autres céréales. Enfin, les résultats de l'étude d'association devraient révéler de nouvelles informations sur le contrôle génétique de la croissance racinaire et ouvrir la voie à la sélection assistée par marqueurs pour les traits racinaires chez le mil.